



저작자표시-비영리-변경금지 2.0 대한민국

이용자는 아래의 조건을 따르는 경우에 한하여 자유롭게

- 이 저작물을 복제, 배포, 전송, 전시, 공연 및 방송할 수 있습니다.

다음과 같은 조건을 따라야 합니다:



저작자표시. 귀하는 원저작자를 표시하여야 합니다.



비영리. 귀하는 이 저작물을 영리 목적으로 이용할 수 없습니다.



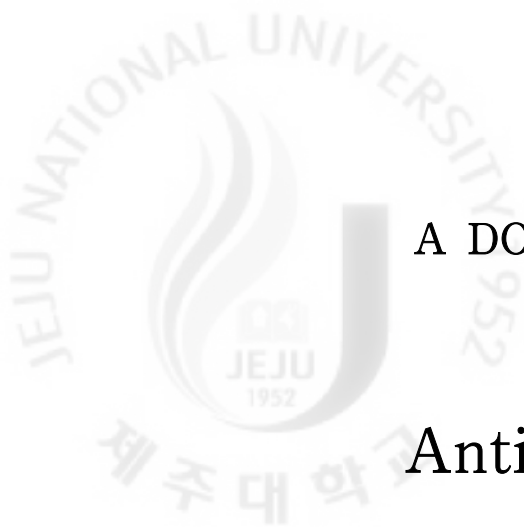
변경금지. 귀하는 이 저작물을 개작, 변형 또는 가공할 수 없습니다.

- 귀하는, 이 저작물의 재이용이나 배포의 경우, 이 저작물에 적용된 이용허락조건을 명확하게 나타내어야 합니다.
- 저작권자로부터 별도의 허가를 받으면 이러한 조건들은 적용되지 않습니다.

저작권법에 따른 이용자의 권리는 위의 내용에 의하여 영향을 받지 않습니다.

이것은 [이용허락규약\(Legal Code\)](#)을 이해하기 쉽게 요약한 것입니다.

[Disclaimer](#)



A DOCTORAL DISSERTATION

Anti-obesity Effects of  
*Petalonia binghamiae*, *Citrus sunki*,  
and *Sasa quepaertensis*

Seong-Il Kang

Department of Life Science

Graduate School

Jeju National University

February, 2012



미역쇠, 진굴 및 제주조릿대의 항비만  
효과에 관한 연구

지도교수 김 세 재

강 성 일

이 논문을 이학 박사학위 논문으로 제출함

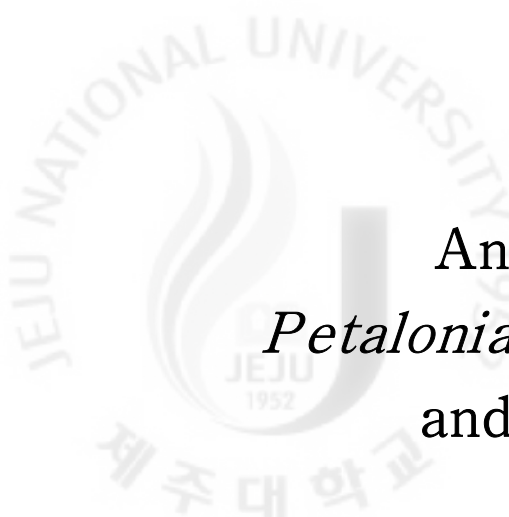
2012년 2월

강성일의 이학 박사학위 논문을 인준함

심사위원장 \_\_\_\_\_ ①  
위 원 \_\_\_\_\_ ①  
위 원 \_\_\_\_\_ ①  
위 원 \_\_\_\_\_ ①  
위 원 \_\_\_\_\_ ①

제주대학교 대학원

2012년 2월



Anti-obesity Effects of  
*Petalonia binghamiae*, *Citrus sunki*,  
and *Sasa quepaertensis*

Seong-Il Kang  
(Supervised by professor Se-Jae Kim)

A dissertation submitted in partial fulfillment of the requirement for  
the degree of Doctor of Science

February, 2012

This dissertation has been examined and approved by

.....  
Chairperson of the Committee  
.....  
.....  
.....  
.....

.....  
Date

Department of Life Science  
GRADUATE SCHOOL  
JEJU NATIONAL UNIVERSITY



# BACKGROUND

Obesity is a leading cause of morbidity and mortality worldwide [World Health Organization, 2002] and is known to arise from an imbalance between energy intake and expenditure. Obesity is a medical condition in which excess body fat has accumulated to the extent that it may have an adverse effect on health, leading to reduced life expectancy and/or increased health problems [Haslam and James, 2005]. It is most commonly caused by a combination of excessive food energy intake, lack of physical activity, and genetic susceptibility, although a few cases are caused primarily by genes, endocrine disorders, medications or psychiatric illness. Obesity is a leading preventable cause of death worldwide, with increasing prevalence in adults and children, and authorities view it as one of the most serious public health problems of the 21st century [Barnes et al., 2007].

Adipose tissue is vital for maintaining metabolic homeostasis, and as an endocrine organ, it secretes various adipokines. Studies on adipose tissue biology have improved our understanding of the mechanisms linking metabolic disorders with altered adipocyte function [Fruhbeck, 2008]. Also, Adipocytes have an important role in energy homeostasis. Adipose tissue stores energy in the form of lipid and releases fatty acids in response to nutritional signals or energy insufficiency [Spiegelman and Flier, 1996]. Further, adipocytes have endocrine functions by secreting hormones and factors that regulate physiological functions, such as immune response, insulin sensitivity and food intake [Fruhbeck et al., 2001; Gregoire, 2001]. Excessive fat accumulation in the body and white adipose tissue causes obesity and results in an increased risk of many serious diseases, including type II diabetes, hypertension and heart disease [Kopelman, 2000]. Therefore, prevention and treatment of obesity are relevant to health promotion.

Dieting and physical exercise are the mainstays of treatment for obesity. Moreover, it is important to improve diet quality by reducing the consumption of energy-dense foods such as those high in fat and sugars, and by increasing the intake of dietary fiber. High-fat feeding has commonly been used to induce visceral obesity in rodent animal models [Hansen et al., 1997] because the pathogenesis of obesity is similar to that found in humans [Katagiri et al., 2007]. Preventive or therapeutic strategies to control most of human obesity should target these abnormalities. Anti-obesity foods and food ingredients may avert the condition, possibly leading to the prevention of lifestyle-related diseases, if they can effectively reduce visceral fat mass [Saito et al., 2005].

Triglycerids (TG) stored in white adipose tissue is the major energy reserve in mammals. Excess TG accumulation in adipose tissue results in obesity. TG is synthesized and stored in cytosolic lipid droplets during times of energy excess, and is mobilized from lipid droplets, via lipolysis, during times of energy need to generate fatty acids. Whereas, TG synthesis occurs in other organs, such as the liver for VLDL production, lipolysis for the provision of fatty acids as an energy source for other organs is a unique function of adipocytes. Increasing lipolysis in adipocytes may be a potentially useful therapeutic target for treating obesity. However, chronically high levels of fatty acids in the blood, typically observed in obesity, are correlated with many detrimental metabolic consequences such as insulin resistance [Ahmadian et al., 2010]. Therefore, lipolysis and fatty acid oxidation are important mechanisms involved in reducing body fat. At the cellular level, obesity is caused by an increase in the number and size of adipocytes derived from fibroblastic preadipocytes in adipose tissue [Spiegelman and Flier, 1996]. Thus, experimental evidence suggests that some metabolic disorders may be treatable or preventable through the inhibition of adipogenesis and the modulation of adipocyte function [Fruhbeck, 2008].

Currently available drugs for the treatment of obesity have undesirable side effects, there is high demand for a safe but therapeutically potent anti-obesity drug. A number of plants, plant extracts, and phytochemicals have anti-obesity properties or have direct effects on adipose tissue, and have thus been used as dietary supplements [Rayalam et al., 2008]. As a result, interest in exploring the applications of medicinally beneficial plants has increased [Kessler et al., 2001].

This study was performed to find available anti-obesity materials from plants which were inhabited in Jeju Island. Initially, about 300 plant extracts were screened for the potential that inhibited the differentiation of 3T3-L1 preadipocytes. Among them, three plant species [*Petalonia binghamiae* (J. Agaradh) Vinogradova, *Citrus sunki* Hort. ex Tanaka, *Sasa quepaertensis* Nakai) were selected for further study. This study reported the anti-obesity effects of the extracts from thalli extracts of *P. binghamiae*, peel extracts of immature *C. sunki*, and leaf extracts of *S. quepaertensis*. Also, the anti-obesity effects of fucoxanthin which was isolated from *P. binghamiae*, and sinensetin which was isolated from *C. sunki* were represented.

**Keywords:** *Petalonia binghamiae*, *Citrus sunki*, *Sasa quepaertensis*, Fucoxanthin, Sinensetin, 3T3-L1 cell, High-fat-diet (HFD)-induced obesity, Lipolysis,  $\beta$ -oxidation, Anti-obesity



# ABSTRACT

## Part 1. Anti-obesity effect of brown algae *Petalonia binghamiae* and fucoxanthin derived from it

In this study, we reported that anti-obesity effects of *Petalonia binghamiae* extracts and fucoxanthin isolated from *P. binghamiae*.

Firstly, the anti-obesity properties of the enzymatic digestion extract (PBEE) in high-fat-diet (HFD)-induced obese rats were investigated. PBEE inhibits preadipocyte differentiation and adipogenesis in a dose-dependent manner. In differentiating 3T3-L1 preadipocytes, it decreased the expression of peroxisome proliferator activated receptor (PPAR)  $\gamma$ , CCAAT/enhancer binding proteins (C/EBP)  $\alpha$ , and fatty-acid-binding protein aP2. It also inhibited the mitotic clonal expansion process of adipocyte differentiation, and it inhibited insulin-stimulated uptake of glucose into mature 3T3-L1 adipocytes by reducing phosphorylation of insulin receptor substrate (IRS). In rats with high-fat-diet (HFD)-induced obesity, PBEE exhibited potent anti-obesity effects. In this animal model, increases in body weight and fat storage were suppressed by the addition of PBEE to the drinking water at 500 mg/L for 30 days. PBEE supplementation reduced serum levels of glutamic pyruvic transaminases (GPT) and glutamic oxaloacetic transaminases (GOT) and increased the serum level of high density lipoprotein (HDL)-cholesterol. Moreover, it significantly decreased the accumulation of lipid droplets in liver tissue, suggesting a protective effect against HFD-induced hepatic steatosis.

Secondly, the anti-obesity properties of the ethanolic extract of *P. binghamiae* (PBE) in HFD-induced obese mice were investigated. The PBE (150 mg/kg/day) administration decreased body weight gain, adipose tissue



weight, and serum triglyceride. It also reduced serum levels of glutamic pyruvic transaminases and glutamic oxaloacetic transaminases, as well as the accumulation of fatty droplets in liver tissue, suggesting a protective effect against HFD-induced hepatic steatosis. Importantly, PBE administration restored the HFD-induced decrease of the phosphorylation of AMP-activated protein kinase (AMPK) and acetyl-CoA carboxylase (ACC) in the epididymal adipose tissue. Consistent with *in vivo* data, PBE increased AMPK and ACC phosphorylation, while it decreased the expression SREBP1c in mature 3T3-L1 adipocytes. These results suggest that PBE exert the anti-obesity properties via promoting  $\beta$ -oxidation and reducing lipogenesis.

Thirdly, I investigated the effects of fucoxanthin, derived from the edible brown seaweed *P. binghamiae*, on adipogenesis during the three differentiations targets of 3T3-L1 preadipocytes. Progression of 3T3-L1 preadipocyte differentiation is divided into early (days 0-2, D0-D2), intermediate (days 2-4, D2-D4), and late stages (day 4 onwards, D4-). When fucoxanthin was applied during the early stage of differentiation (D0-D2), it promoted 3T3-L1 adipocyte differentiation, as evidenced by increased triglyceride accumulation. At the molecular level, fucoxanthin increased protein expression of PPAR  $\gamma$ , C/EBP $\alpha$ , sterol regulatory element binding protein 1c (SREBP1c), and aP2, and adiponectin mRNA expression, in a dose-dependent manner. However, it reduced the expression of PPAR $\gamma$ , C/EBP $\alpha$ , and SREBP1c during the intermediate (D2-D4) and late stages (D4-D7) of differentiation. It also inhibited the glucose uptake in mature 3T3-L1 adipocytes by reducing the phosphorylation of insulin receptor substrate (IRS). Moreover, fucoxanthin increased the phosphorylation of LKB1, AMPK, and ACC in mature 3T3-L1 adipocytes. These results suggest that fucoxanthin exerts differing effects on 3T3-L1 cells of different differentiation stages. Moreover, fucoxanthin inhibits glucose uptake and enhances fatty acid  $\beta$ -oxidation in mature adipocytes.

Taken together, our findings suggested that anti-obesity effects of *Petalonia binghamiae* in HFD-induced obesity animal might attributed partly to fucoxanthin.

## Part 2. Anti-obesity effect of the immature *Citrus sunki* peel and sinensetin derived from it

The peel of *Citrus sunki* Hort. ex Tanaka has been widely used in traditional Asian medicine for the treatment of many diseases, including indigestion and bronchial asthma. In this study, we reported the anti-obesity effects of immature *C. sunki* extract (CSE) and sinensetin isolated from immature *C. sunki* peel.

Firstly, the anti-obesity activity of CSE using HFD-induced obese C57BL/6 mice and mature 3T3-L1 adipocytes were investigated. In the animal study, body weight gain, adipose tissue weight, serum total cholesterol, and triglyceride in the CSE (150 mg/kg/day)-administered group decreased significantly compared to the HFD group. Also, CSE supplementation reduced serum levels of glutamic pyruvic transaminases, glutamic oxaloacetic transaminases, and lactate dehydrogenase. Moreover, it decreased the accumulation of fatty droplets in liver tissue, suggesting a protective effect against HFD-induced hepatic steatosis. Dietary supplementation with CSE reversed the HFD-induced decrease in the phosphorylation levels of AMPK and ACC, which are related to fatty acid  $\beta$ -oxidation, in the epididymal adipose tissue. Also, CSE increased AMPK and ACC phosphorylation in mature 3T3-L1 adipocytes. CSE also enhanced lipolysis by phosphorylation of PKA and HSL in mature 3T3-L1 adipocytes. These results suggested that

CSE had an anti-obesity effect via elevated lipolysis and fatty acid  $\beta$ -oxidation in adipose tissue.

Secondly, sinensetin is a rare polymethoxylated flavone (PMF) found in certain citrus fruits. I investigated the effects of sinensetin isolated from PMF-rich *Citrus sunki* peel on lipid metabolism in 3T3-L1 cells. Sinensetin promoted adipogenesis in 3T3-L1 preadipocytes growing in incomplete differentiation medium, which did not contain 3-isobutyl-1-methylxanthine (IBMX). It also up-regulated the expression of the adipogenic transcription factors PPAR $\gamma$ , C/EBP $\alpha$  and  $\beta$ , and fatty-acid-binding protein aP2. The activation of cAMP-responsive element binding protein (CREB), which play important roles in C/EBP $\beta$  expression and extracellular signal-regulated kinase (ERK), which plays important roles in C/EBP $\beta$  activation, was also potentiated by sinensetin. Sinensetin enhanced the phosphorylation of protein kinase A (PKA) and hormone sensitive lipase (HSL), indicating its lipolytic effects via cAMP-mediated signaling pathway. Also, sinensetin down regulated the expression of sterol regulatory element-binding protein 1c (SREBP1c). It also inhibited glucose uptake in a dose-dependent manner, and decreased the phosphorylation of IRS and Akt. Furthermore, sinensetin increased phosphorylation of AMPK and ACC, which is related to fatty acid  $\beta$ -oxidation. Its also up regulated mRNA expression of carnitine palmitoyltransferase-1a, suggesting that sinensetin enhanced fatty acid  $\beta$ -oxidation through AMPK pathway.

Taken together, our findings demonstrated that anti-obesity effects of *Citrus sunki* in HFD-induced obesity animal might attributed partly to sinensetin.

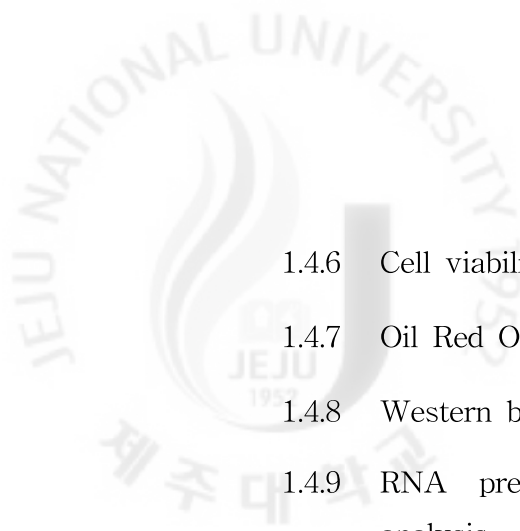
### Part 3. Anti-obesity effect of *Sasa queipaertensis* leaf

The leaves of several *Sasa* species have been shown to exert a number of pharmacological effects, such as anti-oxidant and anti-tumor effects, apoptosis, and improvement of insulin resistance activities. In this study, we explored the anti-obesity activity of *Sasa queipaertensis* leaf extract (SQE) in HFD-induced obese C57BL/6 mice and mature 3T3-L1 adipocytes. The administration of SQE (150 mg/kg/day) with a HFD for 70 days significantly decreased body weight gain, adipose tissue weight, and serum total cholesterol and triglyceride levels in comparison with the HFD group. SQE reduced serum levels of glutamic oxaloacetic transaminase, glutamic pyruvic transaminase, and lactate dehydrogenase and the accumulation of fatty droplets in liver tissue, suggesting a protective effect against HFD-induced hepatic steatosis. SQE also restored the HFD-induced decreases in the phosphorylation of AMPK and ACC protein levels, which are related to fatty acid  $\beta$ -oxidation, in epididymal adipose tissue. In addition, SQE induced AMPK and ACC phosphorylation in mature 3T3-L1 adipocytes. This study reported, for the first time, that SQE might have an anti-obesity effect in a rodent model of HFD-induced obesity through the activation of the AMPK pathway in adipose tissue and the reduction of fatty droplet accumulation in liver tissue.



# CONTENTS

B A C K G R O U N D	-----	1
A B S T R A C T	-----	4
C O N T E N T S	-----	9
LIST OF ABBREVIATIONS	-----	16
P A R T 1	-----	19
Anti-obesity effect of brown algae <i>Petalonia binghamiae</i> and fucoxanthin derived from it		
1.1 LIST OF TABLES	-----	20
1.2. LIST OF FIGURES	-----	21
1.3 INTRODUCTION	-----	25
1.4 MATERIALS AND METHODS	-----	30
1.4.1 Reagents	-----	30
1.4.2 Preparation of a water-soluble extract of <i>Petalonia binghamiae</i> (PBEE)	-----	30
1.4.3 Preparation of <i>Petalonia binghamiae</i> ethanol extract (PBE)	-----	31
1.4.4 Preparation of fucoxanthin from <i>Petalonia binghamiae</i>	----	31
1.4.5 Cell culture and differentiation	-----	34
1.4.5.1 Differentiation I	-----	34
1.4.5.2 Differentiation II	-----	34



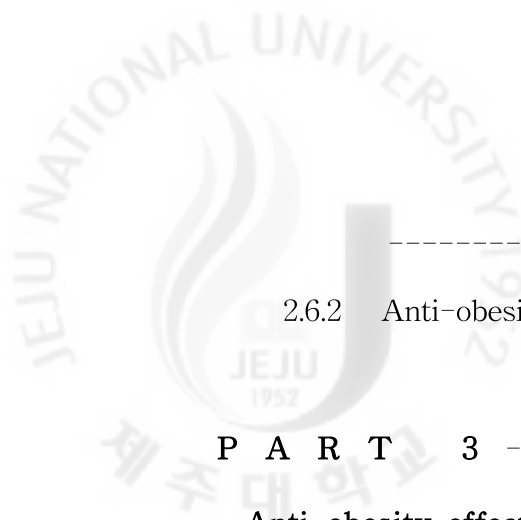
1.4.6	Cell viability and cytotoxicity	-----	34
1.4.7	Oil Red O staining and cell quantification	-----	35
1.4.8	Western blot analysis	-----	35
1.4.9	RNA preparation and quantitative real-time RT-PCR analysis	-----	36
1.4.10	Flow cytometric analysis of the cell cycle	-----	37
1.4.11	Lipolysis assay	-----	37
1.4.12	Glucose uptake activity assay	-----	38
1.4.13	Animals	-----	38
1.4.14	Measurement of body weight, epididymal adipose tissue weight, and food and water intake	-----	40
1.4.15	Biochemical analysis	-----	40
1.4.16	Histology	-----	41
1.4.17	Statistical analysis	-----	42
<b>1.5</b>	<b>RESULTS</b>	-----	<b>43</b>
1.5.1	Anti-obesity effect of <i>Petalonia binghamiae</i> enzymatic extract (PBEE)	-----	43
1.5.1.1	<i>PBEE inhibits 3T3-L1 adipocyte differentiation by modulating the expression of key transcriptional regulators</i>	-----	43
1.5.1.2	<i>PBEE blocks cell cycle progression in 3T3-L1 cells</i>	---	48
1.5.1.3	<i>PBEE inhibits glucose uptake by 3T3-L1 adipocytes</i>	--	50
1.5.1.4	<i>PBEE prevents high-fat-diet (HFD)-induced obesity</i>	--	53
1.5.1.5	<i>PBEE dramatically decreases signs of liver pathology</i>	--	55

1.5.2	Anti-obesity effect of <i>Petalonia binghamiae</i> ethanolic extract (PBE)	58
1.5.2.1	<i>PBE ameliorated high-fat-diet (HFD)-induced obesity</i>	58
1.5.2.2	<i>PBE reduced damage of liver in high-fat-diet (HFD)-induced obese mice</i>	66
1.5.2.3	<i>PBE reduced the expression of SREBP1c and activated the AMPK pathway in mature 3T3-L1 adipocytes</i>	69
1.5.3	Anti-obesity effect of Fucoxanthin derived from PBE	74
1.5.3.1	<i>Fucoxanthin enhances 3T3-L1 adipocyte differentiation at an early stage</i>	74
1.5.3.2	<i>Fucoxanthin inhibits adipocyte differentiation at intermediate and late stages</i>	79
1.5.3.3	<i>Fucoxanthin inhibits glucose uptake in mature 3T3-L1 adipocytes</i>	82
1.5.3.4	<i>Fucoxanthin activated the AMPK pathway in mature 3T3-L1 adipocytes</i>	87
<b>1.6</b>	<b>DISCUSSEION</b>	<b>90</b>
1.6.1	Anti-obesity effect of <i>Petalonia binghamiae</i> enzymetic extract (PBEE)	90
1.6.2	Anti-obesity effect of <i>Petalonia binghamiae</i> ethanolic extract (PBE)	94
1.6.3	Anti-obesity effect of Fucoxanthin derived from PBE	97
<b>P A R T</b>	<b>2</b>	<b>100</b>
	<b>Anti-obesity effect of the immature <i>Citrus sunki</i> peel and sinensetin derived from it</b>	

2.1	LIST OF TABLES	-----	101
2.2.	LIST OF FIGURES	-----	102
2.3	INTRODUCTION	-----	106
2.4	MATERIALS AND METHODS	-----	110
2.4.1	Reagents	-----	110
2.4.2	Preparation of immature <i>Citrus sunki</i> peel extract (CSE)	-----	111
2.4.3	Animals	-----	115
2.4.4	Measurement of body weight, food intake, liver weight epididymal adipose tissue weight, and perirenal adipose tissue weight	-----	115
2.4.5	Biochemical analysis	-----	115
2.4.6	Histology	-----	116
2.4.7	Cell culture and differentiation	-----	116
2.4.7.1	<i>Differentiation I</i>	-----	116
2.4.7.2	<i>Differentiation II</i>	-----	117
2.4.8	Cell viability and cytotoxicity	-----	117
2.4.9	Oil Red O staining and cell quantification	-----	118
2.4.10	Western blot analysis	-----	118
2.4.11	RNA preparation and quantitative real-time RT-PCR analysis	-----	119
2.4.12	Lipolysis assay	-----	120
2.4.13	Glucose uptake activity assay	-----	120
2.4.14	Measurement of cellular cAMP levels	-----	121



2.4.15	Statistical analysis	-----	121
<b>2.5</b>	<b>RESULTS</b>	-----	<b>122</b>
2.5.1	Anti-obesity effect of <i>Citrus sunki</i> ethanolic extract (CSE)	-----	122
2.5.1.1	CSE improved high-fat-diet (HFD)-induced obesity	---	122
2.5.1.2	CSE reduced damage of liver in high-fat-diet (HFD)-induced obese mice	-----	127
2.5.1.3	CSE restored AMPK phosphorylation and adiponectin expression in epididymal adipose tissue	-----	131
2.5.1.4	CSE activated the AMPK pathway in mature 3T3-L1 adipocyte	-----	134
2.5.1.5	CSE activated the PKA pathway in mature 3T3-L1 adipocyte	-----	139
2.5.2	Anti-obesity effect of Sinensetin derived from CSE	-----	142
2.5.2.1	Sinensetin enhances adipogenesis in 3T3-L1 preadipocyte in the absence of IBMX	-----	142
2.5.2.2	Sinensetin activates 3T3-L1 adipocyte differentiation signal at an early stage	-----	146
2.5.2.3	Sinensetin stimulates lipolysis in mature 3T3-L1 adipocytes	-----	152
2.5.2.4	Sinensetin inhibits glucose uptake and lipogenesis in mature 3T3-L1 adipocyte	-----	156
2.5.2.5	Sinensetin activated the fatty acid $\beta$ -oxidation in mature 3T3-L1 adipocyte	-----	161
<b>2.6</b>	<b>DISCUSSEION</b>	-----	<b>165</b>
2.6.1	Anti-obesity effect of <i>Citrus sunki</i> ethanolic extract (CSE)		



-----	165
2.6.2 Anti-obesity effect of Sinensetin derived from CSE -----	169
<b>P A R T 3 -----</b>	<b>174</b>
<b>Anti-obesity effect of the <i>Sasa quelpaertensis</i> leaf</b>	
<b>3.1 LIST OF TABLES -----</b>	<b>175</b>
<b>3.2. LIST OF FIGURES -----</b>	<b>176</b>
<b>3.3 INTRODUCTION -----</b>	<b>178</b>
<b>3.4 MATERIALS AND METHODS -----</b>	<b>180</b>
3.4.1 Reagents -----	180
3.4.2 Preparation of <i>Sasa quelpaertensis</i> extract (SQE) and HPLC analysis -----	180
3.4.3 Animals -----	184
3.4.4 Measurement of body weight, food intake, liver weight epididymal adipose tissue weight, and perirenal adipose tissue weight -----	184
3.4.5 Biochemical analysis -----	184
3.4.6 Histology -----	185
3.4.7 Cell culture and differentiation -----	185
3.4.8 Cell viability and cytotoxicity -----	186
3.4.9 Western blot analysis -----	187
3.4.10 RNA preparation and quantitative real-time RT-PCR analysis -----	187
3.4.11 Statistical analysis -----	188



<b>3.5 RESULTS</b>	189
3.5.1 Anti-obesity effect of <i>Sasa quepaertensis</i> aqueous extract (SQE)	189
3.5.1.1 SQE improved high-fat-diet (HFD)-induced obesity	189
3.5.1.2 SQE reduced damage of liver in high-fat-diet (HFD)-induced obese mice	195
3.5.1.3 SQE restored AMPK phosphorylation and adiponectin expression in epididymal adipose tissue	198
3.5.1.4 SQE activated the AMPK pathway in mature 3T3-L1 adipocyte	201
<b>3.6 DISCUSSEION</b>	205
3.6.1 Anti-obesity effect of <i>Sasa quepaertensis</i> aqueous extract (SQE)	205
<b>C O N C L U S I O N</b>	208
<b>R E F E R E N C E S</b>	210
<b>배 경 / 요 약</b>	224

# LIST OF ABBREVIATIONS

<b>ACC</b>	Acetyl-CoA carboxylase
<b>Akt</b>	PKB, protein kinase B
<b>AMP</b>	Adenosine monophosphate
<b>AMPK</b>	AMP activated protein kinase
<b>ANOVA</b>	Analysis of variance
<b>ATP</b>	Adenosine triphosphate
<b>BCS</b>	Bovine calf serum
<b>BSA</b>	Bovine serum albumin
<b>cAMP</b>	Cyclic adenosine monophosphate
<b>cDNA</b>	Complementary deoxyribonucleic acid
<b>C/EBP</b>	CCAAT/enhancer binding protein
<b>CMC</b>	Carboxymethyl cellulose
<b>CPT-1a</b>	Carnitine palmitoyltransferase-1a
<b>CREB</b>	cAMP-responsive element binding protein
<b>CSE</b>	Ethanol extract of <i>Citrus sunki</i>
<b>DMEM</b>	Dulbecco's modified Eagle's minimum essential medium
<b>DMSO</b>	Dimethyl sulfoxide
<b>DNA</b>	Deoxyribonucleic acid
<b>ERK</b>	Extracellular signal regulated kinase
<b>FACS</b>	Fluorescence activated cell sorting
<b>FBS</b>	Fetal bovine serum
<b>g</b>	gram (s)
<b>GOT</b>	Glutamic oxaloacetic transaminase
<b>GPT</b>	Glutamic pyruvic transaminase

<b>h</b>	Hour
<b>HDL</b>	High-density lipoprotein
<b>H&amp;E</b>	Hematoxylin and eosin
<b>HFD</b>	High fat diet
<b>HPLC</b>	High performance liquid chromatography
<b>HSL</b>	Hormone sensitive lipase
<b>IBMX</b>	3-isobutyl-1-methylxanthine
<b>IRS</b>	Insulin receptor substrate
<b>kDa</b>	Kilo dalton
<b>kg</b>	kilogram (s)
<b>KRH</b>	Krebs-Ringer-Heps
<b>L</b>	liter (s)
<b>LDH</b>	Lactate dehydrogenase
<b>LKB</b>	Tumor suppressor protein
<b>MBq</b>	Megabecquerel
<b>min</b>	Minute (s)
<b>mg</b>	Milligram (s)
<b>mL</b>	Milliliter (s)
<b>mm</b>	Millimeter
<b>mM</b>	Millimole (s)
<b>mRNA</b>	Messenger ribonucleic acid
<b>MTT</b>	3-(4,5-dimethylthiazol-2-yl)-2,5-diphenyl tetrazolium bromide
<b>nm</b>	nanometer
<b>OD</b>	Optical density
<b>PBE</b>	Ethanollic extract of <i>Petalonia binghamiae</i>
<b>PBEE</b>	Enzymatic extract of <i>Petalonia binghamiae</i>
<b>PBS</b>	Phosphate buffered saline
<b>PDA</b>	Photodiode array

<b>PI3-K</b>	Phosphatidylinositol 3-kinase
<b>PKA</b>	Protein kinas A
<b>PMSF</b>	Phenylmethylsulfonyl fluoride
<b>PPAR</b>	Peroxidase proliferator activated receptor
<b>PS</b>	Penicillin-streptomycin
<b>RNA</b>	Ribonucleic acid
<b>ROS</b>	Reactive oxygen species
<b>RSD</b>	Relative standard deviation
<b>RT-PCR</b>	Reverse transcriptase polymerase chain reaction
<b>SDS</b>	Sodium dodecyl sulfate
<b>SQE</b>	Water soluble extract of <i>Sasa quepaertensis</i>
<b>SREBP1c</b>	Sterol-regulatory element binding protein
<b>T-CHO</b>	Total cholesterol
<b>TG</b>	Triglyceride
<b>TNF-<math>\alpha</math></b>	Tumor necrosis factor alpha
<b>S.D.</b>	Standard deviation
<b>S.E.</b>	Standard error
<b><math>\alpha</math></b>	Alpha
<b><math>\beta</math></b>	Beta
<b><math>\gamma</math></b>	Gamma
<b><math>\mu\text{g}</math></b>	Microgram (s)
<b><math>\mu\text{L}</math></b>	Microliter (s)
<b><math>\mu\text{M}</math></b>	Micromole (s)
<b><math>\times \text{g}</math></b>	Gravity



# PART 1

Anti-obesity effect of brown algae *Petalonia binghamiae* and fucoxanthin derived from it

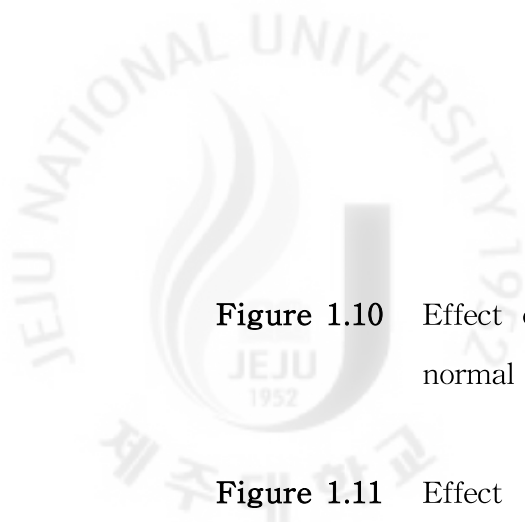
## 1.1. LIST OF TABLES

<b>Table 1.1</b>	Effects of supplementing PBEE on body weight gain, food and water consumption, energy intake, and white adipose weight in high-fat-dien (HFD)-induced experimental group for 30 days -----	<b>54</b>
<b>Table 1.2</b>	Effects of supplementing PBEE on serum profiles in high-fat-diet (HFD)-induced experimental group for 30 days -----	<b>56</b>
<b>Table 1.3</b>	Effects of PBE supplementation on body weight gain in high-fat-diet (HFD)-induced obese experimental group after 70 days -----	<b>60</b>
<b>Table 1.4</b>	Effects of PBE supplementation on epididymal adipose tissue weight and perirenal adipose tissue weight in high-fat-diet (HFD)-induced obese experimental group after 70 days -----	<b>63</b>
<b>Table 1.5</b>	Effects of PBE supplementation on food intake and serum levels of TG in high-fat-diet (HFD)-induced obese experimental group after 70 days -----	<b>64</b>
<b>Table 1.6</b>	Effects of PBE supplementation on serum levels of GPT and GOT and liver weight in high-fat-diet (HFD)-induced obese experimental group after 70 days -----	<b>67</b>

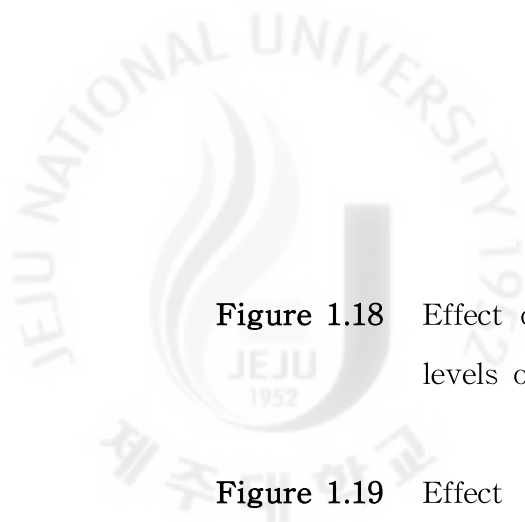


## 1.2. LIST OF FIGURES

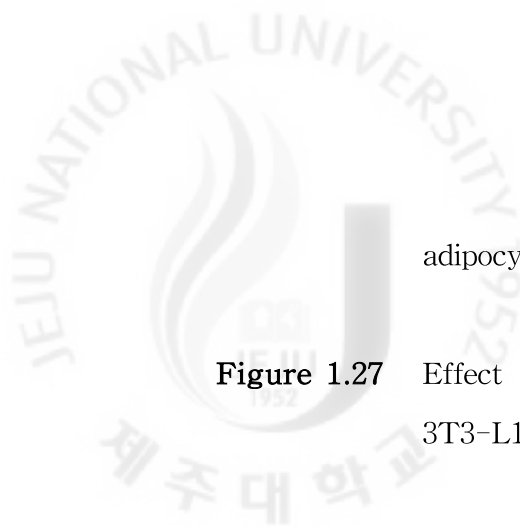
<b>Figure 1.1</b>	Picture of wild <i>Petalonia binghamiae</i> -----	29
<b>Figure 1.2</b>	HPLC chromatograms of <i>Petalonia binghamiae</i> extracts obtained by PDA detector system -----	33
<b>Figure 1.3</b>	Effect of PBEE on the lipid accumulation in 3T3-L1 cells -----	45
<b>Figure 1.4</b>	Effect of PBEE on the differentiation of adipocytes in 3T3-L1 preadipocytes -----	46
<b>Figure 1.5</b>	Effect of PBEE on expression of phospho-ERK and SREBP1c in differentiating 3T3-L1 cells -----	47
<b>Figure 1.6</b>	Effect of PBEE on arrest of differentiation-induced 3T3-L1 preadipocytes at G <sub>1</sub> -----	49
<b>Figure 1.7</b>	Effect of PBEE on glucose uptake in mature 3T3-L1 adipocytes -----	51
<b>Figure 1.8</b>	Effect of PBEE on expression of phospho-IRS in mature 3T3-L1 adipocytes -----	52
<b>Figure 1.9</b>	Effect of PBEE on fatty droplet accumulation in livers of high-fat-diet (HFD)-fed rats -----	57



<b>Figure 1.10</b>	Effect of PBE on body weight changes in mice fed a normal diet (ND), high-fat-diet (HFD), or HFD+PBE --	59
<b>Figure 1.11</b>	Effect of PBE on adiponectin mRNA expression in epididymal adipose tissue of mice fed a normal diet (ND), high-fat-diet (HFD), or HFD+PBE -----	61
<b>Figure 1.12</b>	Effect of PBE on fatty droplets in epididymal adipose tissue of mice fed a normal diet (ND), high-fat-diet (HFD), or HFD+PBE -----	62
<b>Figure 1.13</b>	Effect of PBE on protein expression in epididymal adipose tissue of mice fed a normal diet (ND), high-fat-diet (HFD), or HFD+PBE -----	65
<b>Figure 1.14</b>	Effect of PBE on fatty droplets in the livers of mice fed a normal diet (ND), high-fat-diet (HFD), or HFD+PBE -----	68
<b>Figure 1.15</b>	Effect of PBE on viability and cytotoxicity of mature 3T3-L1 adipocytes -----	70
<b>Figure 1.16</b>	Effect of various PBE concentration on expression of SREBP1c in mature 3T3-L1 adipocytes -----	71
<b>Figure 1.17</b>	Effect of various PBE concentration on phosphorylation of AMPK and ACC in mature 3T3-L1 adipocytes -----	72



<b>Figure 1.18</b>	Effect of various PBE concentration on gene expression levels of CPT-1a in mature 3T3-L1 adipocytes -----	<b>73</b>
<b>Figure 1.19</b>	Effect of fucoxanthin on viability and cytotoxicity of 3T3-L1 preadipocytes -----	<b>75</b>
<b>Figure 1.20</b>	Effect of fucoxanthin on the lipid accumulation in 3T3-L1 cells -----	<b>76</b>
<b>Figure 1.21</b>	Effect of fucoxanthin on the differentiation of adipocytes in 3T3-L1 preadipocytes -----	<b>77</b>
<b>Figure 1.22</b>	Effect of fucoxanthin on the gene expression of adiponectin in 3T3-L1 preadipocytes -----	<b>78</b>
<b>Figure 1.23</b>	Effect of fucoxanthin on adipocyte differentiation in 3T3-L1 cells at various time points (data of Western blot) -----	<b>80</b>
<b>Figure 1.24</b>	Effect of fucoxanthin on adipocyte differentiation in 3T3-L1 cells at various time points (normalization of Figure 1.23) -----	<b>81</b>
<b>Figure 1.25</b>	Effect of fucoxanthin on viability and cytotoxicity of mature 3T3-L1 adipocytes -----	<b>83</b>
<b>Figure 1.26</b>	Effect of fucoxanthin on lipolysis of mature 3T3-L1	



	adipocytes -----	84
<b>Figure 1.27</b>	Effect of fucoxanthin on glucose uptake of mature 3T3-L1 adipocytes -----	85
<b>Figure 1.28</b>	Effect of fucoxanthin on IRS signaling pathway of mature 3T3-L1 adipocytes -----	86
<b>Figure 1.29</b>	Effect of fucoxanthin on phosphorylation of LKB1, AMPK, and ACC in mature 3T3-L1 adipocytes -----	88
<b>Figure 1.30</b>	Effect of fucoxanthin on gene expression of CPT-1a in mature 3T3-L1 adipocytes -----	89

### 1.3. INTRODUCTION

As a major risk factor for many chronic diseases, including type 2 diabetes, hypertension, and atherosclerosis [Kopelman, 2000], obesity is a major obstacle to efforts aimed at improving human health and quality of life. Obesity is characterized by excessive fat deposition associated with morphological and functional changes in adipocytes [Fruhbeck et al., 2001]. Studies of adipose tissue biology have led to an improved understanding of the mechanisms that link metabolic disorders with altered adipocyte functions [Fruhbeck, 2008]. Lipid accumulation is caused not only by adipose tissue hypertrophy but also by adipose tissue hyperplasia [Spiegelman and Flier, 1996]. Although the molecular basis for these associations remains unclear, the experimental evidence suggests that some metabolic disorders might be treatable or preventable through the inhibition of adipogenesis and the modulation of adipocyte function [Trayhurn and Beattie, 2001]. The study of adipogenesis has been greatly facilitated by the establishment of immortal preadipocyte cell lines, such as 3T3-L1 preadipocytes. The adipocytes generated from these cells exhibit most of the key features of adipocytes *in vivo* [Green and Meuth, 1974].

Adipogenesis includes morphological changes, growth arrest, and clonal expansion of adipose cells, followed by a complex sequence of changes in gene expression and lipid storage [Gregoire, 2001]. Adipogenesis is characterized by morphological changes, growth arrest (day 0, D0), and clonal expansion (day 0-2, D0-D2) in adipose cells, followed by a complex sequence of changes in gene expression and lipid storage [Gregoire, 2001]. The master adipogenic transcriptional regulators are members of the CCAAT/enhancer binding protein (C/EBP) family and peroxidase proliferator activated receptor (PPAR)  $\gamma$ . These factors regulate adipocyte differentiation by modulating the

expression of their target genes in a coordinated fashion [MacDougald and Lane, 1995; Rangwala and Lazar; Rosen and Spiegelman, 2000; Rosen et al., 2000]. Recent investigations suggest that sterol regulatory element binding protein 1c (SREBP1c) is the earliest transcription factor involved in adipocyte differentiation [Payne et al., 2009]. It acts to induce the expression of C/EBP  $\alpha$ , PPAR $\gamma$ , and SREBP1c [Darlington et al., 1998; Farmer, 2006; Kim and Spiegelman, 1996]. They act synergistically to induce the expression of C/EBP, PPAR  $\gamma$ , and SREBP1c [Darlington et al., 1998; Farmer, 2006; Kim and Spiegelman, 1996]. C/EBP $\alpha$  and PPAR $\gamma$ , in turn, promote terminal differentiation by activating the transcription of the genes for fatty-acid-binding protein aP2 and fatty acid transporter CD36, which are involved in creating and maintaining the adipocyte phenotype. SREBP1c increases the expression of many lipogenic genes, including fatty acid synthase. Loss-of-function studies have shown that PPAR $\gamma$  is necessary and sufficient to promote adipogenesis [Barak et al., 1999; Koutnikova et al., 2003] and that C/EBP $\alpha$  is influential in maintaining the expression of PPAR $\gamma$  [Wu et al., 1999].

AMP-activated protein kinase (AMPK) is known to be a metabolic master switch that is activated by LKB1 under intracellular stress conditions, including glucose deficiency, hypoxia, and reactive oxygen species (ROS) activity [Fryer et al., 2002; Hardie, 2007]. During energy depletion, AMPK inhibits de novo fatty acid synthesis by inactivating acetyl-CoA carboxylase (ACC) and stimulates fatty acid oxidation by up-regulating the expression of carnitine palmitoyltransferase-1 (CPT-1), PPAR $\alpha$ , and uncoupling protein (UCP) [Saha et al., 2004]. As a cellular energy regulator, AMPK is known to play a major role in glucose and lipid metabolism and to control metabolic disorders such as diabetes, obesity, and cancer [Carling., 2004; Kim et al., 2007]. Thus, AMPK has emerged as a therapeutic target for metabolic disorders [Zhang et al., 2009].

Because the currently available drugs for the treatment of obesity cause undesirable side effects, there is high demand for a safe but therapeutically potent anti-obesity drug. A number of plants, plant extracts, and phytochemicals have anti-obesity properties or have direct effects on adipose tissue and have therefore been used as dietary supplements [Rayalam et al., 2008]. As a result, interest in exploring the applications of medicinally beneficial plants has increased [Kessler et al., 2001].

The edible brown alga *Petalonia binghamiae* (J. Agaradh) Vinogradova is consumed as a traditional food in fishery areas of northeast Asia. The shape of *Petalonia binghamiae* is an aggregate of several leaves that are 15–50 mm in width and 100–250 mm in length (Figure 1.1). Extracts of *Petalonia binghamiae* have anti-oxidant properties [Kuda et al., 2006; Sachindra et al., 2007]. Galactosyldiacylglycerol [Mizushina et al., 2001] and fucoxanthin-related compounds [Mori et al., 2004] isolated from *Petalonia binghamiae* inhibit mammalian DNA polymerase  $\alpha$  and exert suppressive properties on adipocyte differentiation in 3T3-L1 cells, respectively. Moreover, we previously demonstrated that an ethanolic extract of *Petalonia binghamiae* exerts an adipogenic effect in 3T3-L1 cells by acting as a mimetic for insulin, and that it exerts an anti-diabetic effect in a streptozotocin-induced diabetic mice model [Kang et al., 2008]. However, the other potentially beneficial properties of *Petalonia binghamiae* have not been studied. In the present study, we evaluated the anti-obesity potential of enzymetic (PBEE) and ethanolic (PBE) extracts of *Petalonia binghamiae* thalli in murine 3T3-L1 cells and in animal models fed a high-fat-diet (HFD).

Moreover, it is believed that the ingestion of edible brown seaweeds is beneficial to human health. Fucoxanthin, a major marine carotenoid, has been isolated from brown seaweeds, such as *Undaria pinnatifida*, *Hijikia fusiformis*, and *Sargassum fulvellum*. It has several physiological activities, including anti-cancer [Satomi and Nishino, 2007], anti-carcinogenic [Kim et al., 1998],

anti-inflammatory [Shiratori et al., 2005], anti-oxidant [Sachindra et al., 2007], and anti-obesity [Maeda et al., 2005; Maeda et al., 2007] effects. Maeda et al. [Maeda et al., 2006] further reported that fucoxanthin, when applied to cells continuously for 5 days (D2-D7), inhibited the differentiation of 3T3-L1 preadipocytes into adipocytes by down-regulating PPAR $\gamma$ . However, the effects of fucoxanthin on cells at different differentiation stages (early stage, D0-D2; intermediate stage, D2-D4; late stage, D4-D7) and mature adipocytes have not been reported. In this study, we isolated fucoxanthin from the edible seaweed *Petalonia binghamiae* extracts, and investigated its effects on adipogenesis and lipid metabolism in differentiating preadipocytes and fully differentiated adipocytes.





Figure 1.1. Picture of wild *Petalonia binghamiae*. The seaweed was collected in the Jeju island, Republic of Korea.

## 1.4. MATERIALS AND METHODS

### 1.4.1. Reagents

Dulbecco's modified Eagle's medium (DMEM), fetal bovine serum (FBS), bovine calf serum (BCS), and penicillin-streptomycin (PS) were obtained from Gibco BRL (Grand Island, NY, USA). Antibodies to PPAR $\gamma$ , fatty acid-binding protein aP2, C/EBP $\alpha$ , C/EBP $\beta$ , phospho-Ser431-LKB1, phospho-Ser473 protein kinase B (PKB, Akt), insulin receptor substrate (IRS), and phospho-Thr204-ERK 1/2 were purchased from Santa Cruz Biotechnology (Santa Cruz, CA, USA). Antibodies to Akt, phospho-Ser636/639-IRS, phospho-Thr172-AMP-activated protein kinase (p-AMPK)  $\alpha$  and phospho-Ser79-acetyl-CoA carboxylase (p-ACC) were purchased from Cell Signaling Technology (Beverly, MA, USA). Antibody to sterol regulatory element binding protein c (SREBP1c) was obtained from BD Biosciences (San Jose, CA, USA). Phosphate buffered saline (pH 7.4; PBS), 3-isobutyl-1-methylxanthine (IBMX), dexamethasone, insulin, and 3-(4,5-dimethylthiazol-2-yl)-2,5-diphenyl tetrazolium bromide (MTT) were obtained from Sigma Chemical Co. (St. Louis, MO, USA). The lactate dehydrogenase (LDH) Cytotoxicity Detection Kit was purchased from Takara Shuzo Co. (Otsu, Shiga, Japan). 2-Deoxy-D-[ $^3$ H]glucose was obtained from Amersham Biosciences (Piscataway, NJ, USA). All other reagents were purchased from Sigma Chemical Co. unless otherwise noted.

### 1.4.2. Preparation of a water-soluble extract of *Petalonia binghamiae* (PBEE)

Thalli of the brown seaweed *Petalonia binghamiae* were collected from

the coast of Jeju Island, Korea. To enhance water-solubility of seaweed, each 250 g sample of dried seaweed was mixed with 10 L of citric acid buffer solution (pH 4.5) and incubated for 30 min. Then, enzymatic hydrolysis reactions were initiated by the addition of 6.25 mL each of Viscozyme and Celluclast (Novozyme Nordisk, Bagsvaerd, Denmark), and the mixture was incubated at 50°C for 5 h on a platform shaker. After heating at 100°C for 10 min, the enzymatic extract was centrifuged at  $3,000 \times g$  at 4°C for 20 min to recover the supernatant fraction containing the water-soluble extract, designated PBEE. The contents of the total polyphenols (3.96 mg/g) and polysaccharides (424.3 mg/g) in PBEE were comparable to those (25.39 and 8.2 mg/g) of the ethanolic extract in *Petalonia binghamiae* (PBE). The PBEE solution was lyophilized and then stored at -20°C until use.

#### 1.4.3. Preparation of *Petalonia binghamiae* ethanol extract (PBE)

Thalli of brown seaweed *Petalonia binghamiae* were collected from the coast of Jeju Island, South Korea. One kilogram of *Petalonia binghamiae* dried powder was extracted with 80% ethanol (10 L) at room temperature for 48 h. The procedure described above was repeated twice. The combined PBE was concentrated on a rotary evaporator under reduced pressure and freeze-dried to a powder. PBE was stored at -20°C until use.

#### 1.4.4. Preparation of fucoxanthin from *Petalonia binghamiae*

Lyophilized powder (1 kg) of *Petalonia binghamiae* was extracted twice in 10 L of 80% EtOH. Fucoxanthin isolation was performed using a Waters 2695 Alliance HPLC system (Waters Corp., Milford, MA), consisting of two pumps, an autosampler, a column oven, a fraction collector, and a PDA detector (Waters 2998 photodiode array detector; Waters Corp.). Fucoxanthin

separation was performed using a SymmetryPrep C18 column (300 × 7.8 mm ID; 7 μm); the column oven maintained the column temperature at 40°C. *Petalonia binghamiae* extract (40 μL, 100 mg/mL) was injected into the column and was then monitored by recording UV spectra for the irradiated samples at wavelengths between 210 and 600 nm (Figure 1.2, 450 nm). The mobile phase for the prep-HPLC solvent system consisted of methanol (A) and water (B). The gradient mobile phase program was as follows: a 47-min gradient was started with 60% A, linearly increased to 100% A over 36 min, linearly reduced to 60% A over 2 min, and held for 7 min at a flow rate of 1.6 mL/min. The fucoxanthin peak was fractionated using a fraction collector and concentrated in a rotary evaporator at 40°C. <sup>13</sup>C NMR spectra were collected using a JEOL FT/NMR 400 spectrometer (JEOL Ltd., Tokyo, Japan). <sup>13</sup>C NMR data were recorded at 400 and 100 MHz, respectively, with reference to the solvent signals. FAB-MS were obtained with m-nitrobenzyl alcohol matrix on JEOL, JMS-700 spectrometer. The spectral data for fucoxanthin were consistent with those reported previously [Englert et al., 1990; Haugan et al., 1992].

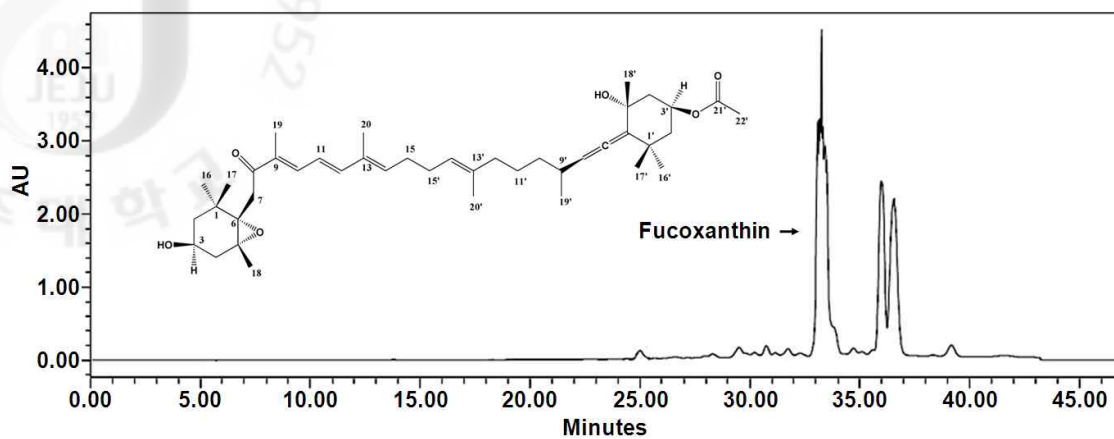


Figure 1.2. HPLC chromatograms of *Petalonia binghamiae* extracts obtained by PDA detector system. Fucoxanthin separation were conducted on a SymmetryPrep C18 column, 40  $\mu$ L injection at 40°C, detection at 450 nm by HPLC.

#### 1.4.5. Cell culture and differentiation

3T3-L1 preadipocyte cells obtained from American Type Culture Collection (Rockville, MD, USA) were cultured in DMEM containing 1% PS and 10% BCS at 37°C under a 5% CO<sub>2</sub> atmosphere.

##### *1.4.5.1 Differentiation I*

To induce differentiation, 2-day post-confluent preadipocytes (designated day 0) were cultured in MDI differentiation medium I (DMEM containing 1% PS, 10% FBS, 0.5 mM IBMX, 1 µM dexamethasone, and 0.5 µg/mL insulin) for 2 days. The cells were then cultured for a further 2 days in DMEM containing 1% PS, 10% FBS, and 0.5 µg/mL insulin. Thereafter, the cells were maintained in post-differentiation medium (DMEM containing 1% PS and 10% FBS), which was replaced every 2 days.

##### *1.4.5.2 Differentiation II*

To induce differentiation, 2-day post-confluent preadipocytes (designated day 0) were cultured in MDI differentiation medium II (DMEM containing 1% PS, 10% FBS, 0.5 mM IBMX, 1 µM dexamethasone, and 5 µg/mL insulin) for 2 days. The cells were then cultured for another 2 days in DMEM containing 1% PS, 10% FBS, and 5 µg/mL insulin. Thereafter, the cells were maintained in post-differentiation medium (DMEM containing 1% PS and 10% FBS), which was replaced every 2 days.

#### 1.4.6. Cell viability and cytotoxicity

The effect of samples on cell viability and cytotoxicity were determined

by the MTT and LDH assay, respectively. ① Preadipocytes were seeded at a density of  $1 \times 10^4$  cell/well into 96-well plate, then treated samples after 24 h, and then incubated for 72 h. ② Mature 3T3-L1 adipocytes were cultured in DMEM containing 1% PS, 10% FBS, and samples for 24 h. MTT (400  $\mu$ g/mL) was added to each well, and the plate incubated at 37°C for 4 h. The MTT (400  $\mu$ g/mL) was added to each well, and the plates incubated for 4 h at 37°C. The liquid in the plate was removed, and dimethyl sulfoxide (DMSO) was added to dissolve the MTT-formazan complex. Optical density was measured at 540 nm. The effect of samples on cell viability was evaluated as the relative absorbance compared with that of control cultures. The cytotoxic effect of samples was measured by LDH Cytotoxicity Detection Kit. The LDH activities in medium and cell lysate were measured for evaluation of cytotoxicity according to the manufacturer's protocol (LDH released into the medium/maximal LDH release  $\times$  100).

#### **1.4.7. Oil Red O staining and cell quantification**

After the induction of differentiation, cells were stained with Oil Red O [6 parts saturated Oil Red O dye (0.6%) in isopropanol plus 4 parts water]. Briefly, the cells were washed twice with PBS, fixed through incubation with 3.7% formaldehyde (Sigma Chemical Co.) in PBS for 1 h, washed an additional three times with water and stained with Oil Red O for 1 h. Excess stain was removed by washing with water, and the stained cells were dried. The stained lipid droplets were dissolved in isopropanol containing 4% Nonidet P-40 and then quantified by measuring the absorbance at 520 nm. Lipid content for each experimental group is expressed relative to that of MDI differentiated cells (designated as 100%).

#### **1.4.8. Western blot analysis**

Adipose tissue was homogenized in ice-cold buffer containing lysis buffer [1× RIPA (Upstate Biotechnology, Temecula, CA, USA), 1 mM PMSF, 1 mM Na<sub>3</sub>VO<sub>4</sub>, 1 mM NaF, and 1 µg/mL each of aprotinin, pepstatin, and leupeptin]. 3T3-L1 cells were washed with ice-cold PBS, collected, and centrifuged. The cell pellets were resuspended in lysis buffer and incubated on ice for 1 h. The adipose tissue and 3T3-L1 cells debris were then removed by centrifugation and protein concentrations in the lysates were determined using Bio-Rad Protein Assay Reagent (Bio-Rad Laboratories, Hercules, CA, USA). The adipose tissue and 3T3-L1 cells lysates were then subjected to electrophoresis on 10–15% polyacrylamide gels containing sodium dodecyl sulfate (SDS) and transferred to polyvinylidene difluoride membranes. The membranes were blocked with a solution of 0.1% Tween-20 in Tris-buffered saline containing 5% bovine serum albumin (BSA) at room temperature for 1 h. After incubation overnight at 4°C with primary antibody, the membranes were incubated with horseradish peroxidase-conjugated secondary antibody at room temperature for 1 h. Immunodetection was carried out using ECL Western blotting detection reagent (Amersham Biosciences, Piscataway, NJ, USA).

#### **1.4.9. RNA preparation and quantitative real-time RT-PCR analysis**

Total RNA was extracted from the adipose tissue and 3T3-L1 adipocytes using the TRIzol reagent according to the manufacturer's instructions and then treated with DNase (Wako Pure Chemical Industries, Ltd., Osaka, Japan). cDNA was synthesized from 1 µg of total RNA in a 20 µL reaction using a Maxime RT PreMix Kit (iNtRON Biotechnology, Seongnam, Kyunggi, Korea). The following primers were used in real-time RT-PCR analysis: adiponectin, 5'-GAC CTG GCC ACT TTC TCC TC-3' and 5'-GTC ATC TTC GGC



ATG ACT GG-3'; carnitine palmitoyltransferase-1a (CPT-1a), 5'-ACC CTG AGG CAT CTA TTG ACA-3' and 5'-TGA CAT ACT CCC ACA GAT GGC-3';  $\beta$ -actin, 5'-AGG CTG TGC TGT CCC TGT AT-3' and 5'-ACC CAA GAA GGA AGG CTG GA-3'. Samples were prepared using iQ SYBR Green Supermix (Bio-Rad Laboratories) according to the manufacturer's instructions. Adiponectin, CPT-1a, and  $\beta$ -actin mRNA expressions were measured by quantitative real-time RT-PCR using the Chromo4 Real-Time PCR System (Bio-Rad Laboratories). The formation of a single product was verified by melting curve analysis. The expression levels of adiponectin and CPT-1a were normalized to that of  $\beta$ -actin. Data were analyzed using Opticon Monitor software (ver. 3.1; Bio-Rad Laboratories).

#### 1.4.10. Flow cytometric analysis of the cell cycle

Post-confluent 3T3-L1 preadipocytes were treated with MDI in the presence or absence of PBEE for 24 h, washed twice with PBS, harvested, and fixed in 70% ethanol at 4°C for 1 h. After the ethanol was removed, the cells were washed twice with PBS and treated with RNase (2  $\mu$ g/mL) for 30 min. The cells were stained with propidium iodide (5  $\mu$ g/mL Sigma Chemical Co.) for 30 min, and the cell cycle distribution was determined by fluorescence activated cell sorting (FACS) on a flow cytometer (FACSCalibur BD Biosciences, Heidelberg, Germany).

#### 1.4.11. Lipolysis assay

To obtain fully differentiated 3T3-L1 cells, confluent cells were induced in MDI differentiation medium II (DMEM containing 1% PS, 10% FBS, 0.5 mM IBMX, 1  $\mu$ M dexamethasone, 5  $\mu$ g/mL insulin) for 2 days. The cells were then cultured for a further 2 days in DMEM containing 1% PS, 10%

FBS, and 5 µg/mL insulin. Then, they were maintained in post-differentiation medium, which was replaced every 2 days. Fully differentiated 3T3-L1 cells were next incubated with serum-free DMEM for 4 h. The cells were then treated with post-differentiation medium containing various concentrations of the fucoxanthin. Culture supernatants were assayed for glycerol levels at 24 or 48 h post-treatment using a free glycerol reagent kit (Sigma-Aldrich).

#### 1.4.12. Glucose uptake activity assay

Glucose uptake activity was analyzed by measuring the uptake of radiolabeled glucose. Briefly, differentiated 3T3-L1 adipocytes grown in 12-well plates were washed twice with serum-free DMEM and incubated for 2 h at 37°C with 1 mL of DMEM containing 0.1% bovine serum albumin (BSA). The cells were then washed three times with Krebs-Ringer-Heps (KRH) buffer [20 mM HEPES (pH 7.4), 136 mM NaCl, 4.7 mM KCl, 1.25 mM MgSO<sub>4</sub>, 1.25 mM CaCl<sub>2</sub>, and 2 mg/mL BSA] and incubated at 37°C for 30 min with 0.9 mL of KRH buffer. They were next incubated with or without samples for 30 min or 4 h at 37°C. Insulin was added, and the cells were incubated at 37°C for a further 15 or 20 min. Glucose uptake was initiated by the addition of 0.1 mL of KRH buffer containing 2-deoxy-D-[<sup>3</sup>H]glucose (37 MBq/L Amersham Bioscience) and glucose (1 mM). After 15 min, glucose uptake was terminated by washing the cells three times with cold PBS. The cells were lysed through incubation for 20 min at 37°C with 0.7 mL of 1% Triton X-100. Levels of radioactivity in the cell lysates were determined using a Tri-Carb 2700TR scintillation counter (Packard, Meriden, CT, USA).

#### 1.4.13. Animals

##### ► Rat

The animal study protocol was approved by the Institutional Animal Care

and Use Committee of Jeju National University. After purchase, 40 male 4-week-old Sprague-Dawley (SD) rats (Orient Bio Inc-QC, Seoul, Korea) were adapted for 1 week to specific conditions of temperature ( $22\pm 2^{\circ}\text{C}$ ), humidity ( $50\pm 5\%$ ), and lighting (light from 08:00 to 20:00). The animals were housed in plastic cages and given free access to drinking water and food as described below. After adaptation, the SD rats (now 5 weeks old  $196.5\pm 1.9$  g) were randomly divided into 4 groups of 10 rats each. One group (ND) was fed a normal basal diet (Harlan, Bemis, Vancouver, Canada protein: 18.9%, carbohydrate: 57.33%, fat: 5% and others 3.3 kcal/g), and three groups (HFD, HFD+PBEE<sub>100</sub>, and HFD+PBEE<sub>500</sub>) were fed a HFD consisting of 40% beef tallow-modified AIN-76A (Jung-Ang Laboratory Animal Inc., Ansong, Korea protein: 17.7%, carbohydrate: 31.4%, fat: 40% and others 5.542 kcal/g). The ND group and the HFD group were provided with tap water. The other two HFD groups were provided with tap water containing PBEE at 100 mg/L (HFD+PBEE<sub>100</sub>) or 500 mg/L (HFD+PBEE<sub>500</sub>).

#### ► Mouse

The animal study protocol was approved by the Institutional Animal Care and Use Committee of Jeju National University. After purchase, 30 male 4 weeks old C57BL/6 mice (Nara Biotech Co., Ltd, Seoul, Korea) were adapted for 1 week to specific temperature ( $22\pm 2^{\circ}\text{C}$ ), humidity ( $50\pm 5\%$ ), and lighting (light from 08:00 to 20:00). The animals were housed in plastic cages (2 mice/cage) and given free access to drinking water and food. After adaptation, the C57BL/6 mice (now 5 weeks old;  $22.5\pm 1.1$  g) were randomly divided into three groups of 10 mice each. One group (normal diet, ND) was fed a 10% kcal fat diet (D12450B, Research Diets, New Brunswick, NJ, USA; protein: 19.2%, carbohydrate: 67.3%, fat: 4.3%, and others; 3.85 kcal/g), and two groups (high-fat-diet, HFD; HFD+PBE) were fed a 60% kcal fat diet

(D12492, Research Diets, New Brunswick, NJ, USA; protein: 26.2%, carbohydrate: 26.3%, fat: 34.9% and, others; 5.24 kcal/g). PBE was dissolved in 0.1% carboxymethyl cellulose (CMC) and administrated orally to the animals at a dosage of 150 mg/kg/day for 70 days. The oral administration volume was approximately 100  $\mu$ L per 10 g weight. Mice in the ND and the HFD groups were given 0.1% CMC.

#### **1.4.14. Measurement of body weight, epididymal adipose tissue weight, and food and water intake**

##### **► Rat**

Body weight was measured at the beginning of the experiment and at 5-day intervals for 30 days. The amount of food and water intake by each group was recorded every week. The epididymal white adipose tissue was weighed after quick removal from sacrificed rats.

##### **► Mouse**

Body weight and food intake were measured once every 5 day throughout the experiment for 70 days. At the end of the feeding period, the mice were anesthetized with diethyl ether after an overnight fast. The epididymal adipose tissue, perirenal adipose tissue, and liver weight were weighed after rapid removal from sacrificed mice.

#### **1.4.15. Biochemical analysis**

##### **► Rat**

After 30 days, the rats were sacrificed by ether anesthesia overdose. Blood samples were collected from the heart and were allowed to stand for 30 min at room temperature for clotting. Serum samples were then collected by centrifugation at 1,000  $\times$  g for 15 min. High density lipoprotein

(HDL)-cholesterol, glutamic oxaloacetic transaminase (GOT), and glutamic pyruvic transaminase (GPT) concentrations in serum were assayed using an automatic blood analyzer (Kuadro, BPC Biosed, Rome, Italy).

▶ Mouse

After 70 days, the mice were sacrificed by ether anesthesia overdose. Blood samples were drawn from the abdominal aorta into a vacuum tube and allowed to stand at room temperature for 30 min for clotting. Serum samples were then collected by centrifugation at  $1,000 \times g$  for 15 min. Triglyceride (TG), glutamic pyruvic transaminase (GPT), and glutamic oxaloacetic transaminase (GOT) concentrations in serum were assayed using commercial Kit (ASANPHARM, Seoul, Korea) and an automatic blood analyzer (Kuadro, BPC Biosed, Rome, Italy).

#### 1.4.16. Histology

▶ Rat

After blood was drained from the livers, the livers were fixed in 10% neutral formalin solution for 48 h. The hepatic tissue was subsequently dehydrated in a graded ethanol series (75-100%) and embedded in paraffin wax. The embedded tissue was sectioned (8- $\mu$ m-thick sections), stained with hematoxylin and eosin (H&E), and examined by light microscopy (Olympus BX51 Olympus Optical, Tokyo, Japan), and then photographed at a final magnification of 100 $\times$ .

▶ Mouse

After blood was drained from the livers, the livers and epididymal adipose tissue were fixed in 10% neutral formalin solution for 48 h. The

tissue was subsequently dehydrated in a graded ethanol series (75–100%) and embedded in paraffin wax. The embedded tissue was sectioned (8- $\mu$ m-thick sections), stained with hematoxylin and eosin (H&E), and examined by light microscopy (Olympus BX51; Olympus Optical, Tokyo, Japan), and then photographed at a final magnification of 50 $\times$ , 100 $\times$  or 200 $\times$ .

#### 1.4.17. Statistical analysis

Values are expressed as means  $\pm$  S.D. or S.E. One-way analysis of variance (ANOVA) was used for multiple comparisons. Treatment effects were analyzed by the paired *t*-test or Duncan's multiple range test using SPSS software (ver. 12.0; SPSS Inc., Chicago, IL, USA). Differences were considered statistically significant at  $p < 0.05$ .

## 1.5. RESULTS

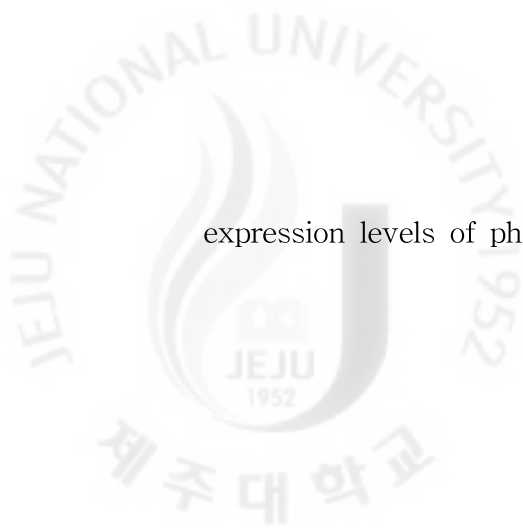
### 1.5.1. Anti-obesity effect of *Petalonia binghamiae* enzymatic extract (PBEE)

#### 1.5.1.1. PBEE inhibits 3T3-L1 adipocyte differentiation by modulating the expression of key transcriptional regulators

First of all, the effect of PBEE on cell viability and cytotoxicity of 3T3-L1 cells were evaluated by the MTT and LDH assay. PBEE at concentration of 500 mg/mL did not affect the viability ( $2.43 \pm 3.30\%$  compared to control) as well as cytotoxicity ( $-1.59 \pm 0.95\%$  compared to control) of the 3T3-L1 cells, as determined by MTT and LDH assays. Then, we tested whether PBEE inhibits MDI-induced differentiation of 3T3-L1 preadipocytes. On day 0, PBEE was added to the MDI differentiation medium (which contains IBMX, dexamethasone, and insulin) on day 8, the adipocytes were stained using Oil Red O. The Oil Red O staining results demonstrated that PBEE treatment at 8, 40, and 200  $\mu\text{g}/\text{mL}$  inhibited 3T3-L1 adipocyte differentiation in a dose-dependent manner. The positive-control cells, which had been treated with 100  $\mu\text{M}$  genistein, exhibited dramatic inhibition of lipid accumulation (Figure 1.3A and B).

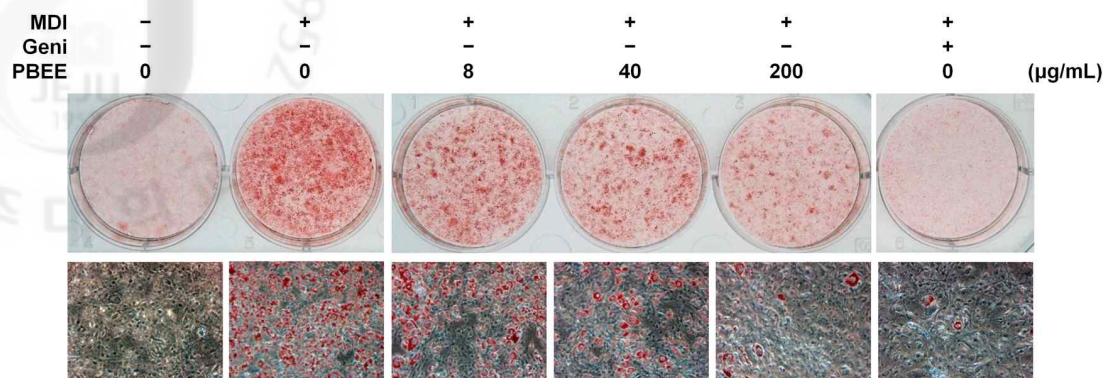
To determine whether PBEE inhibits adipocyte differentiation by negatively regulating the expression of key transcriptional regulators, we examined the expression levels of C/EBP $\alpha$ , C/EBP $\beta$ , and PPAR $\gamma$  during adipocyte differentiation in the presence and absence of PBEE. Expression levels of all three factors were reduced in PBEE-treated cells, as was the expression level of aP2 (Figure 1.4AC and B). However, PBEE did not affect

expression levels of phospho-ERK or SREBP1c (Figure 1.5A and B).





**A**



**B**

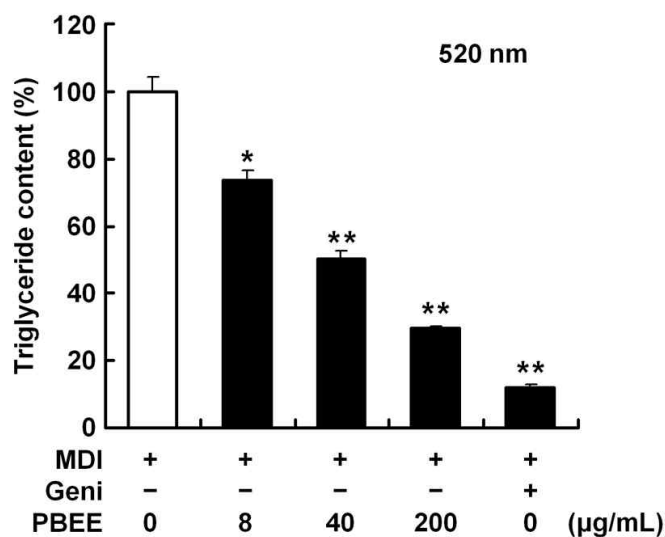
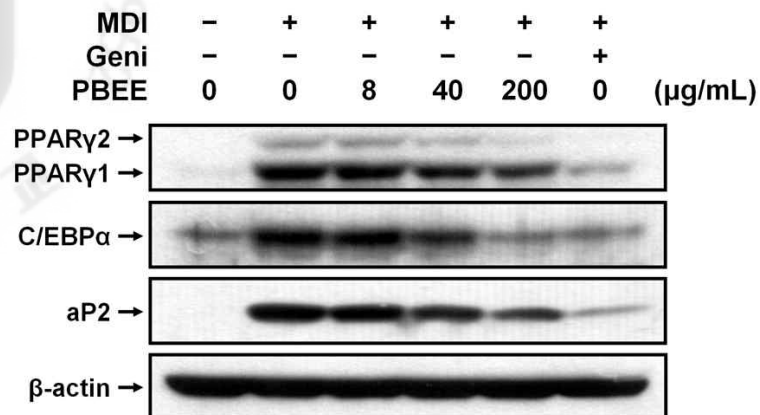


**Figure 1.3. Effect of PBEE on the lipid accumulation in 3T3-L1 cells.** Cells were cultured in MDI differentiation medium in the presence or absence of PBEE (Geni: genistein 100  $\mu\text{M}$ ). (A) Differentiated adipocytes were stained with Oil Red O on day 8. (B) Lipid accumulation was assessed by the quantification of  $\text{OD}_{520}$  as described in the Materials and methods. Results are shown as means  $\pm$  S.D. ( $n=3$ ; \* $p<0.01$  and \*\* $p<0.001$  compared with no PBEE). The data shown are representative of three independent experiments.

**A**



**B**

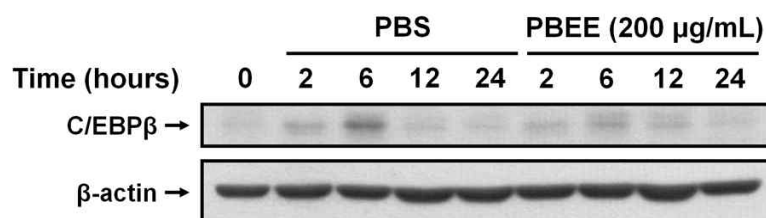
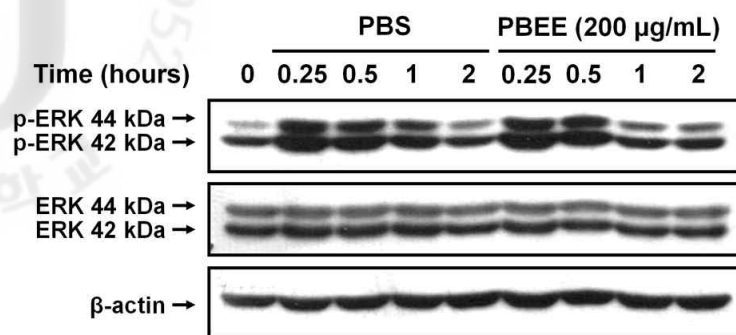


**Figure 1.4. Effect of PBEE on the differentiation of adipocytes in 3T3-L1 preadipocytes.** Cells were cultured in MDI differentiation medium in the presence or absence of PBEE (Geni: genistein 100  $\mu\text{M}$ ) at the indicated times. (A) Western blot analysis of PPAR $\gamma$ , C/EBP $\alpha$ , and aP2 expression. Proteins were prepared from 3T3-L1 cells on day 6. (B) Western blot analysis of C/EBP $\beta$  expression in differentiating 3T3-L1 cells. Proteins were harvested at the indicated times. The data shown are representative of three independent experiments.

**A**



**B**

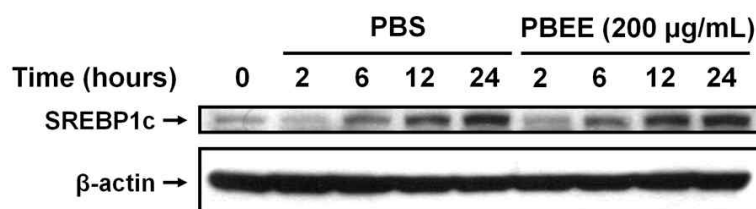
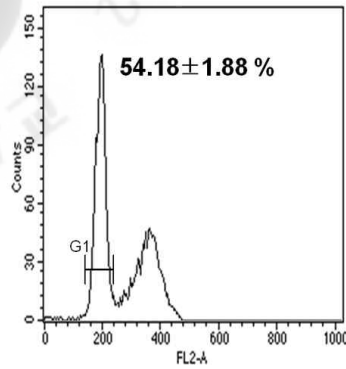


**Figure 1.5.** Effect of PBEE on expression of phospho-ERK and SREBP1c in differentiating 3T3-L1 cells. Cells were cultured in MDI differentiation medium in the presence or absence of PBEE at the indicated times. (A, B) Western blot analysis of phospho-ERK (A), and SREBP1c (B) expression in differentiating 3T3-L1 cells. Proteins were harvested at the indicated times. The data shown are representative of three independent experiments.

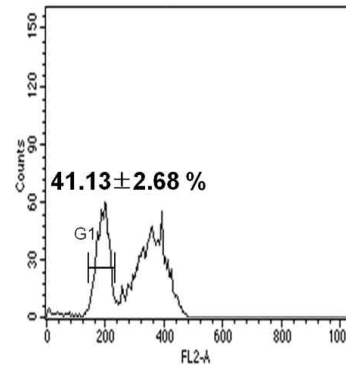
### *1.5.1.2. PBEE blocks cell cycle progression in 3T3-L1 cells*

To confirm the effect of PBEE on cell mitosis after adipogenic induction, the effect of PBEE on the cell cycle was analyzed by FACS. In cells with MDI and PBEE, the G<sub>1</sub>/S transition of the cell cycle was blocked 24 h after induction in a PBEE concentration-dependent manner, as shown in Figure 1.6.

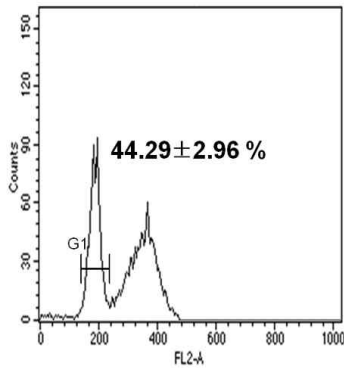
**Negative control**



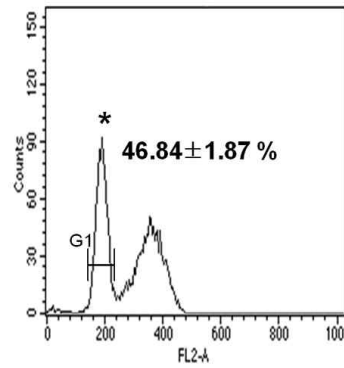
**MDI**



**MDI+PBEE (40 µg/mL)**



**MDI+PBEE (200 µg/mL)**



**MDI+Geni**

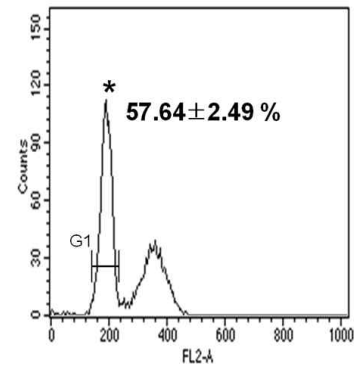


**Figure 1.6. Effect of PBEE on arrest of differentiation-induced 3T3-L1 preadipocytes at G<sub>1</sub>.** The preadipocytes were induced to differentiate in the presence or absence of PBEE. Twenty-four hours after induction, cells were harvested, stained with propidium iodide, and analyzed by FACS. The mean values of the results are shown with the S.D. ( $n=3$ ;  $*p<0.05$  compared with no PBEE) (Geni: genistein 100 µM). The data shown are representative of three independent experiments.

### *1.5.1.3. PBEE inhibits glucose uptake by 3T3-L1 adipocytes*

To investigate the effect of PBEE on glucose uptake, differentiated 3T3-L1 adipocytes were incubated in the presence of radiolabeled glucose and various concentrations of PBEE. As shown in Figure 1.7, PBEE dramatically inhibited glucose uptake in a concentration-dependent manner at the highest PBEE concentration (200  $\mu\text{g/mL}$ ), glucose uptake decreased by 42%. We then examined whether the observed decrease in glucose uptake caused by PBEE was associated with an insulin-dependent signaling pathway by evaluating the phosphorylation of IRS and Akt in PBEE-treated 3T3-L1 adipocytes. PBEE treatment was found to inhibit phosphorylation of both IRS and Akt, comparable to the effect of genistein used as the positive control (Figure 1.8).

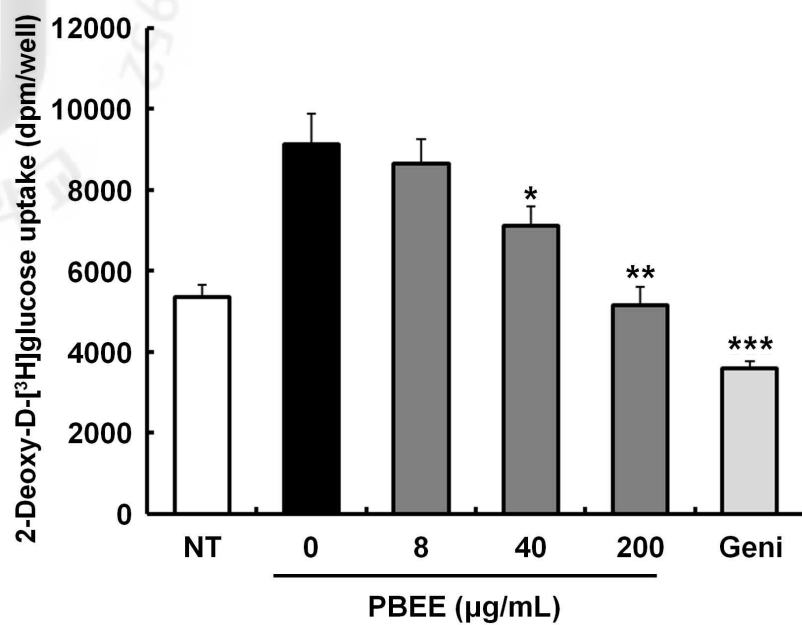
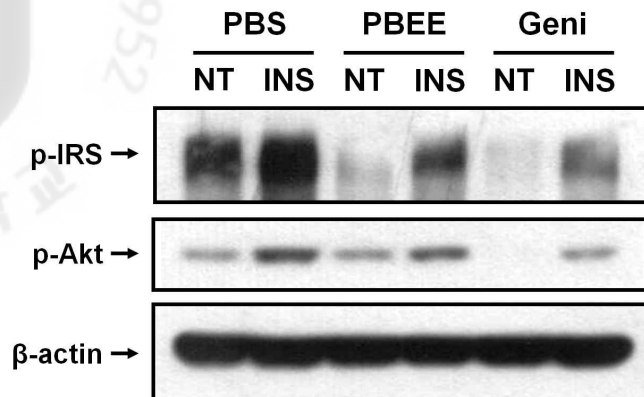


Figure 1.7. Effect of PBEE on glucose uptake in mature 3T3-L1 adipocytes. Mature adipocytes were incubated in 12-well plates in the presence of insulin, PBEE, or genistein (Geni, 100  $\mu$ M) and then assayed for uptake of 2-deoxy-D-[<sup>3</sup>H]glucose. Results are shown as means  $\pm$  S.D. ( $n=3$ ; \* $p<0.05$ , \*\* $p<0.01$ , and \*\*\* $p<0.001$  compared with untreated control). The data shown are representative of three independent experiments.



**Figure 1.8. Effect of PBEE on expression of phospho-IRS in mature 3T3-L1 adipocytes.** Mature adipocytes were incubated in the presence of insulin, PBEE, or genistein (Geni, 100  $\mu$ M) at 15 min. Western blot analysis of phospho-IRS and phospho-Akt levels. Differentiated 3T3-L1 adipocytes were not treated or were treated with insulin (INS; 100  $\mu$ M), PBEE (200  $\mu$ g/mL), or genistein (Geni; 100  $\mu$ M), as indicated. The data shown are representative of three independent experiments.



#### 1.5.1.4. PBEE prevents high-fat-diet (HFD)-induced obesity

As shown in Table 1.1, after 30 days on the HFD, the mean body weight and body weight gain of the HFD rats were more than 10 and 19% higher than those of the ND group ( $p < 0.05$ ), indicating that the HFD did induce obesity. PBEE administration through drinking water (at 100 or 500 mg/L) significantly decreased the body weight and body weight gains of HFD+PBEE rats relative to those of the non-PBEE-treated control HFD group (8 and 12% lower, respectively;  $p < 0.05$ ). The mass of white adipose tissue was also significantly larger in the HFD group (by 38%) than in the ND group ( $p < 0.05$ ). Supplementation of the drinking water of the HFD rats with PBEE at 100 or 500 mg/L significantly decreased their white adipose tissue mass (by 16 or 19%, respectively) relative to that of the non-PBEE-treated HFD group ( $p < 0.05$ , Table 1.1).

Table 1.1. Effects of supplementing PBEE on body weight gain, food and water consumption, energy intake, and white adipose weight in high-fat-diet (HFD)-induced experimental group for 30 days.

Group	ND	HFD	HFD+PBEE <sub>100</sub>	HFD+PBEE <sub>500</sub>
Initial body weight (g)	197.31±2.99	198.59±4.40	195.76±4.08	194.17±4.32
Final body weight (g)	417.86±9.82 <sup>a</sup>	460.90±8.69 <sup>b</sup>	434.99±9.57 <sup>ab</sup>	423.97±13.65 <sup>a</sup>
Body weight gain (g)	220.54±7.02 <sup>a</sup>	262.31±6.33 <sup>b</sup>	239.23±6.37 <sup>a</sup>	229.80±10.33 <sup>a</sup>
Intake of PBEE (mg/kg of body weight/day)	-	-	8.59±0.97	46.71±1.52
Water intake (mL/rat/day)	29.80±0.59	28.80±1.82	28.92±1.07	29.38±1.27
Food intake (g/rat/day)	26.49±0.55 <sup>a</sup>	17.57±0.30 <sup>b</sup>	17.75±0.58 <sup>b</sup>	17.38±0.63 <sup>b</sup>
Energy intake (kcal/rat/day)	87.41±1.18 <sup>a</sup>	97.37±1.69 <sup>b</sup>	98.35±3.22 <sup>b</sup>	96.30±3.51 <sup>b</sup>
White adipose weight (mg/g of body weight)	19.32±0.29 <sup>a</sup>	26.64±1.29 <sup>b</sup>	22.27±1.11 <sup>a</sup>	21.56±1.34 <sup>a</sup>

The values were expressed as mean ± S.E. (*n*=10). Values with different letters in each assay are significantly different from each other between the ND, HFD, HFD+PBEE<sub>100</sub>, and HFD+PBEE<sub>500</sub> groups by Duncan's multiple range test (*p*<0.05).

#### *1.5.1.5. PBEE dramatically decreases signs of liver pathology*

We next examined the effect of PBEE on the levels of serum GPT and GOT in HFD rats. PBEE administration decreased the levels of these markers of cell damage significantly and in a concentration-dependent manner. The levels of serum GPT and GOT were 30 and 17% lower, respectively, in HFD+PBEE<sub>500</sub> rats than in the non-PBEE-treated control HFD group ( $p < 0.05$ , Table 1.2). Moreover, serum HDL-cholesterol levels were also significantly higher (by 26%) in the HFD+PBEE<sub>500</sub> rats ( $p < 0.05$ , Table 1.2).

Photomicrographs of liver samples stained with H&E are shown in Figure 1.9. Livers from the ND group fed tap water for 30 days were normal (Figure 1.9A), and livers from the control group fed a HFD for 30 days exhibited an increased number of fatty droplets (Figure 1.9B). However, livers from the HFD+PBEE groups exhibited a decreased number of fatty droplets relative to the control HFD livers, and the decrease was dose-dependent (Figure 1.9C, D).

Table 1.2. Effects of supplementing PBEE on serum profiles in high-fat-diet (HFD)-induced experimental group for 30 days.

Group	ND	HFD	HFD+PBEE <sub>100</sub>	HFD+PBEE <sub>500</sub>
GPT (IU/L)	38.14±0.83 <sup>a</sup>	47.71±5.45 <sup>b</sup>	35.29±1.85 <sup>a</sup>	33.29±1.95 <sup>a</sup>
GOT (IU/L)	65.29±2.04 <sup>a</sup>	95.86±5.97 <sup>b</sup>	82.57±12.91 <sup>ab</sup>	79.29±4.17 <sup>a</sup>
HDL (mg/dL)	14.00±1.23 <sup>a</sup>	8.71±0.81 <sup>b</sup>	12.86±1.68 <sup>a</sup>	11.00±1.23 <sup>ab</sup>

The values were expressed as mean ± S.E. ( $n=10$ ). Values with different letters in each assay are significantly different from each other between the ND, HFD, HFD+PBEE<sub>100</sub>, and HFD+PBEE<sub>500</sub> groups by Duncan's multiple range test ( $p<0.05$ ).

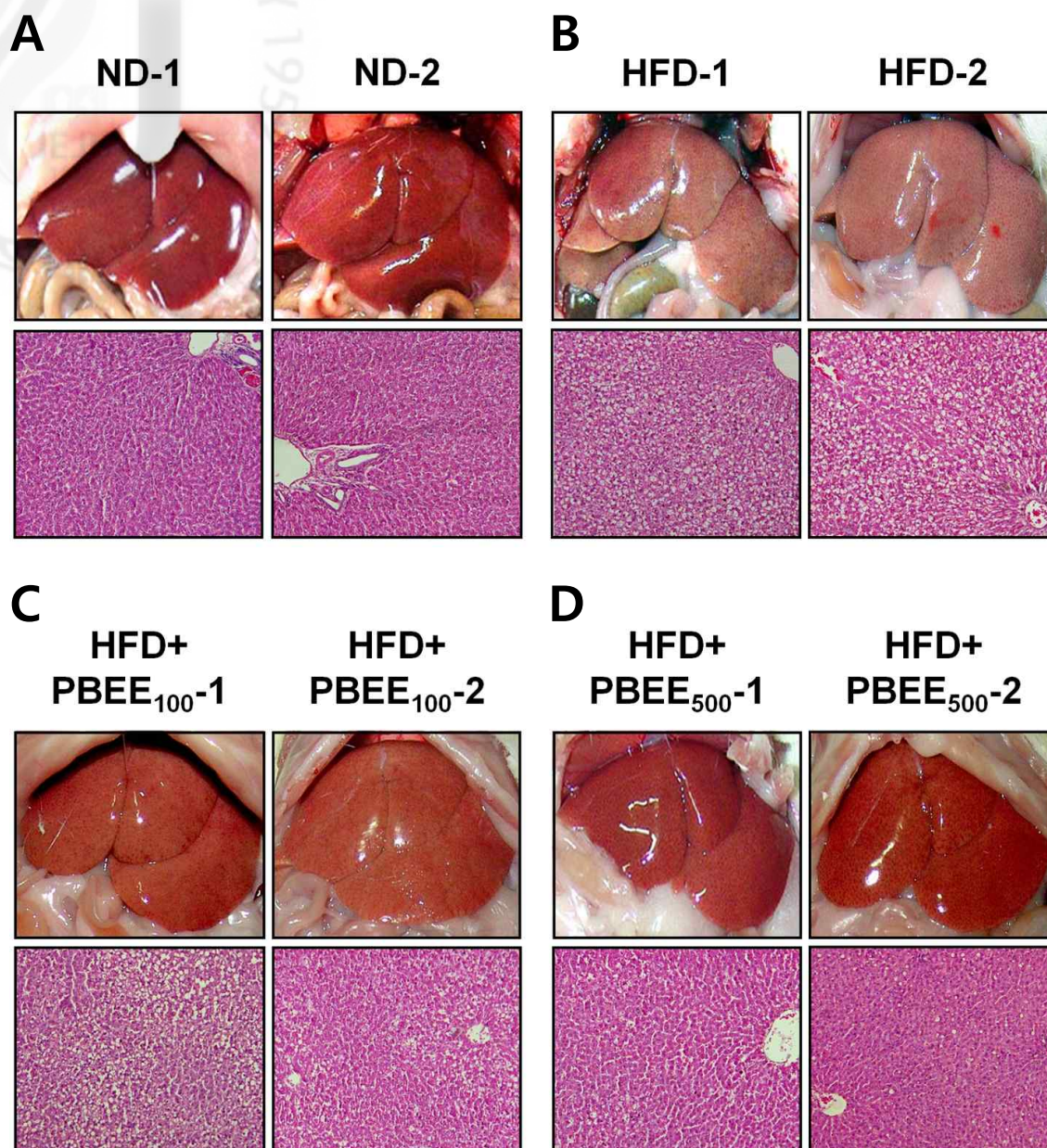


**Figure 1.9.** Effect of PBEE on fatty droplet accumulation in livers of high-fat-diet (HFD)-fed rats. H&E-stained photomicrographs of liver sections are shown at 100 $\times$ . (A) Livers from ND rats appear normal. (B) Livers from HFD-fed control rats exhibit an increased number of fatty droplets after 30 days. (C, D) Drinking water supplementation with PBEE at 100 mg/L (C, PBEE<sub>100</sub>) or 500 mg/L (D, PBEE<sub>500</sub>) decreased fatty droplet accumulation in livers of HFD-fed rats.

## 1.5.2. Anti-obesity effect of *Petalonia binghamiae* ethanolic extract (PBE)

### 1.5.2.1. PBE ameliorated high-fat-diet (HFD)-induced obesity

After 70 days on a HFD, the mean body weight and body weight gain in the HFD group were higher than those in the ND group, indicating that the HFD induced obesity (Figure 1.10, Table 1.3). PBE administration (150 mg/kg/day) significantly decreased body weight and body weight gain in the HFD+PBE group relative to the non-PBE-treated HFD group (11.9% and 28.1% lower, respectively). Moreover, the mRNA expression of adiponectin was lower in the HFD group than in the ND group, but was restored in the HFD+PBE group (Figure 1.11).

Histological analysis of epididymal adipose tissue confirmed that adipocyte size was markedly increased in the HFD group compared with the ND group after 70 days, whereas adipocyte size was markedly decreased in the HFD+PBE group compared with the HFD group (Figure 1.12). Epididymal and perirenal adipose tissue weights were also significantly higher in the HFD group than in the ND group. Epididymal and perirenal adipose tissue weights were significantly lower in the HFD+PBE group (24.8% and 28.5%, respectively) than in the HFD group (Table 1.4). Food intake did not differ significantly among the HFD groups. However, the serum level of TG was significantly lower in the HFD+PBE group (27.8%) than in the HFD group (Table 1.5). Next, we investigated the protein expressions for fatty acid  $\beta$ -oxidation in epididymal adipose tissue. As shown in Figure 1.13, the expressions of phosphorylated forms of AMPK and its immediate substrate (phosphorylated forms of ACC) were higher in the HFD+PBE group than in the HFD group.

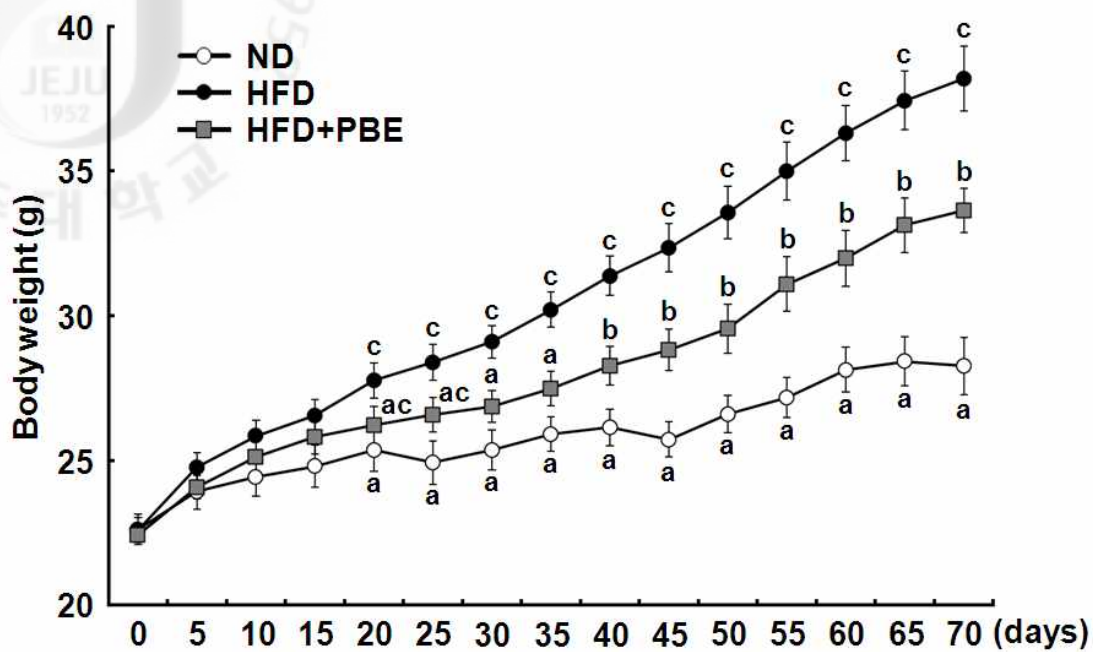


Figure 1.10. Effect of PBE on body weight changes in mice fed a normal diet (ND), high-fat-diet (HFD), or HFD+PBE. Body weights were measured at 5 day intervals for 70 days. Results are shown as means  $\pm$  S.E. ( $n=10$ ). Mean separation was performed using Duncan's multiple range test. <sup>a,b,ac,c</sup> Means not sharing a common superscript are significantly different ( $p<0.05$ ).

Table 1.3. Effects of PBE supplementation on body weight gain in high-fat-diet (HFD)-induced obese experimental group after 70 days.

Group	ND	HFD	HFD+PBE
Initial body weight (g)	22.61±0.53	22.60±0.42	22.43±0.26
Final body weight (g)	28.26±0.99 <sup>a</sup>	38.20±1.12 <sup>c</sup>	33.64±0.77 <sup>b</sup>
Body weight gain (g)	5.65±0.60 <sup>a</sup>	15.60±0.78 <sup>c</sup>	11.21±0.67 <sup>b</sup>
Intake of PBEE (mg/kg of body weight/day)	-	-	150

Values are expressed as means ± S.E. (*n*=10). Values with different letters in each assay are significantly different from each other between the ND, HFD, HFD+PBE groups by Duncan's multiple range test (*p*<0.05).



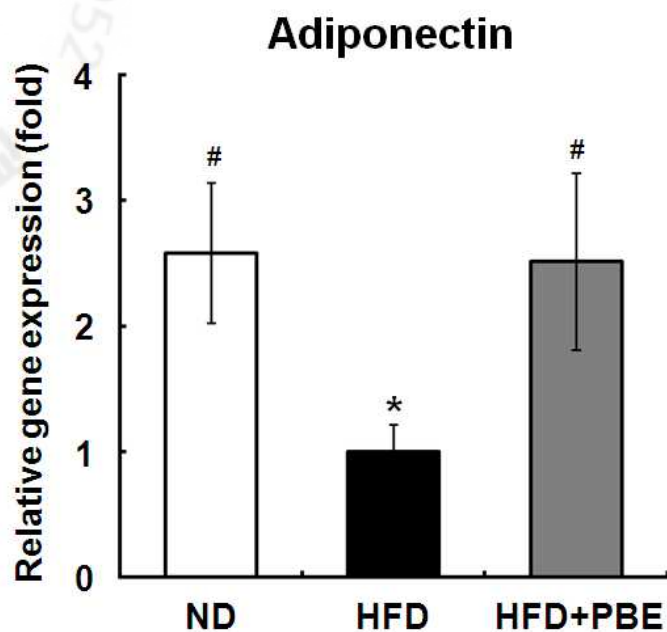


Figure 1.11. Effect of PBE on adiponectin mRNA expression in epididymal adipose tissue of mice fed a normal diet (ND), high-fat-diet (HFD), or HFD+PBE. Real-time RT-PCR analysis of adiponectin mRNA expression in epididymal tissue. All value are presented as means  $\pm$  S.D. ( $n=10$ ;  $*p<0.05$  compared with ND and  $\#p<0.05$  compared with HFD). The data shown are representative of three independent experiments.

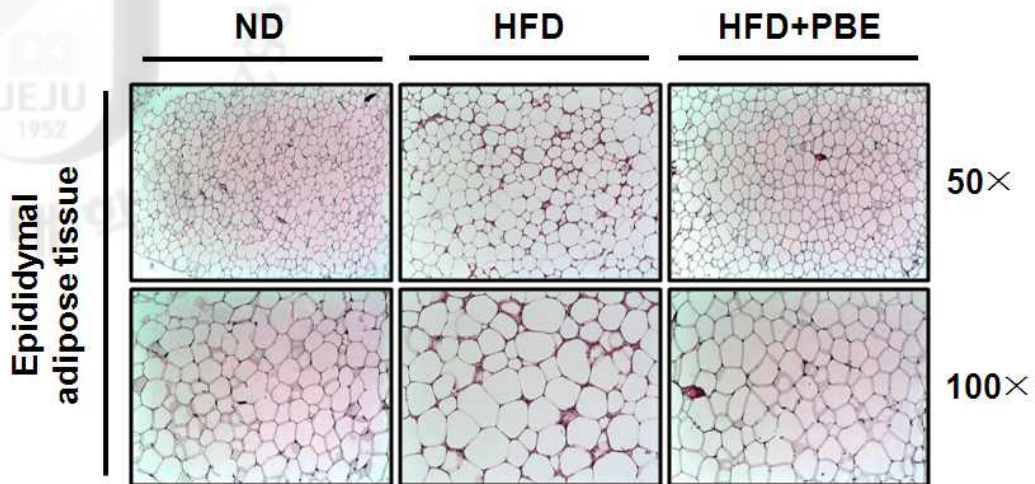


Figure 1.12. Effect of PBE on fatty droplets in epididymal adipose tissue of mice fed a normal diet (ND), high-fat-diet (HFD), or HFD+PBE. Hematoxylin and eosin (H&E)-stained photomicrographs of epididymal adipose sections are shown at 50 $\times$  and 100 $\times$ .

Table 1.4. Effects of PBE supplementation on epididymal adipose tissue weight and perirenal adipose tissue weight in high-fat-diet (HFD)-induced obese experimental group after 70 days.

Group	ND	HFD	HFD+PBE
Epididymal adipose tissue (g)	0.86±0.05 <sup>a</sup>	2.02±0.12 <sup>c</sup>	1.52±0.06 <sup>b</sup>
Perirenal adipose tissue (g)	0.50±0.06 <sup>a</sup>	1.23±0.07 <sup>c</sup>	0.88±0.06 <sup>b</sup>

Values are expressed as means ± S.E. ( $n=10$ ). Values with different letters in each assay are significantly different from each other between the ND, HFD, HFD+PBE groups by Duncan's multiple range test ( $p<0.05$ ).

Table 1.5. Effects of PBE supplementation on food intake and serum levels of TG in high-fat-diet (HFD)-induced obese experimental group after 70 days.

Group	ND	HFD	HFD+PBE
Food intake (g/cage/5 day)	26.57±0.40 <sup>a</sup>	21.19±0.28 <sup>b</sup>	21.07±0.23 <sup>b</sup>
TG (mg/dL)	92.29±4.86 <sup>a</sup>	138.43±9.15 <sup>b</sup>	100.00±7.76 <sup>a</sup>

Values are expressed as means ± S.E. ( $n=10$ ). Values with different letters in each assay are significantly different from each other between the ND, HFD, HFD+PBE groups by Duncan's multiple range test ( $p<0.05$ ).

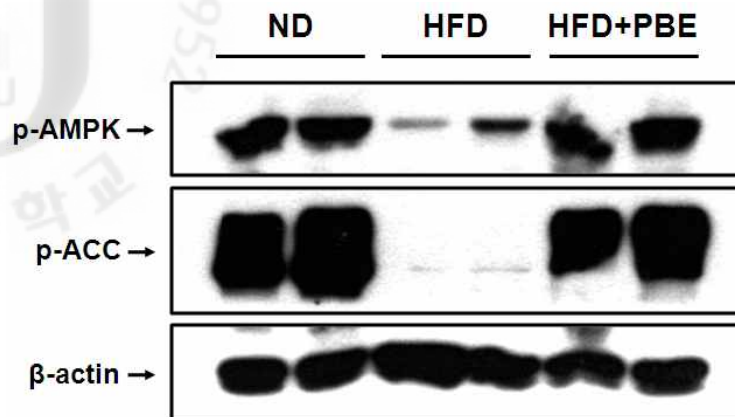


Figure 1.13. Effect of PBE on protein expression in epididymal adipose tissue of mice fed a normal diet (ND), high-fat-diet (HFD), or HFD+PBE. p-AMPK and p-ACC protein expression in epididymal tissue were determined by Western blot analysis. The data shown are representative of three independent experiments.

*1.5.2.2. PBE reduced damage of liver in high-fat-diet (HFD)-induced obese mice*

We next examined the effects of PBE on the levels of serum GPT and GOT in the HFD-induced mice. PBE administration significantly reduced the levels of these markers of cell damage. The levels of serum GPT and GOT were significantly lower in the HFD+PBE group (40.5 and 14.4%, respectively) than in the HFD group (Table 1.6). In addition, liver weight was significantly lower in the HFD+PBE group than in the HFD group.

Figure 1.14 presents representative photomicrographs of liver tissue samples stained with H&E. H&E analysis of the liver revealed greater fatty accumulation in the HFD group compared with the ND group; however, no fatty accumulation was observed in the livers from the HFD+PBE group.

Table 1.6. Effects of PBE supplementation on serum levels of GPT and GOT and liver weight in high-fat-diet (HFD)-induced obese experimental group after 70 days.

Group	ND	HFD	HFD+PBE
GPT (IU/L)	8.57±0.85 <sup>a</sup>	17.29±3.03 <sup>b</sup>	10.29±0.68 <sup>b</sup>
GOT (IU/L)	42.29±1.62 <sup>a</sup>	57.43±3.14 <sup>b</sup>	49.14±1.89 <sup>a</sup>
Liver weight (g)	1.07±0.06 <sup>a</sup>	1.30±0.08 <sup>b</sup>	1.07±0.04 <sup>a</sup>

Values are expressed as means ± S.E. ( $n=10$ ). Values with different letters in each assay are significantly different from each other between the ND, HFD, HFD+PBE groups by Duncan's multiple range test ( $p<0.05$ ).

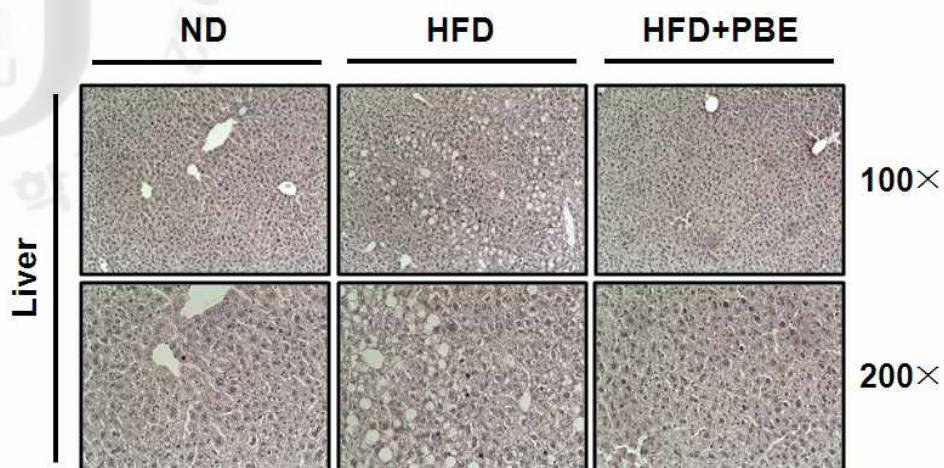


Figure 1.14. Effect of PBE on fatty droplets in the livers of mice fed a normal diet (ND), high-fat-diet (HFD), or HFD+PBE. Hematoxylin and eosin (H&E)-stained photomicrographs of liver tissue sections are shown at 100 $\times$  and 200 $\times$ .



1.5.2.3. PBE reduced the expression of SREBP1c and activated the AMPK pathway in mature 3T3-L1 adipocytes

We first determined the maximal concentration of PBE to be treated to mature 3T3-L1 adipocytes based on MTT and LDH assays (Figure 1.15). Then, we investigated the effects of PBE on the expression of SREBP1c in mature 3T3-L1 adipocytes. PBE reduced dose-dependently the expression of SREBP1c that is a transcription factor regulating the lipogenesis (Figure 1.16).

Also, consistent with the *in vivo* data, PBE markedly induced the phosphorylation of AMPK and ACC in a dose-dependent manner (Figure 1.17). Thus, we investigated the downstream effects of AMPK activation by treating mature 3T3-L1 adipocytes with PBE. PBE increased the expression of CPT-1a mRNA, which is involved in fatty acid  $\beta$ -oxidation (Figure 1.18).

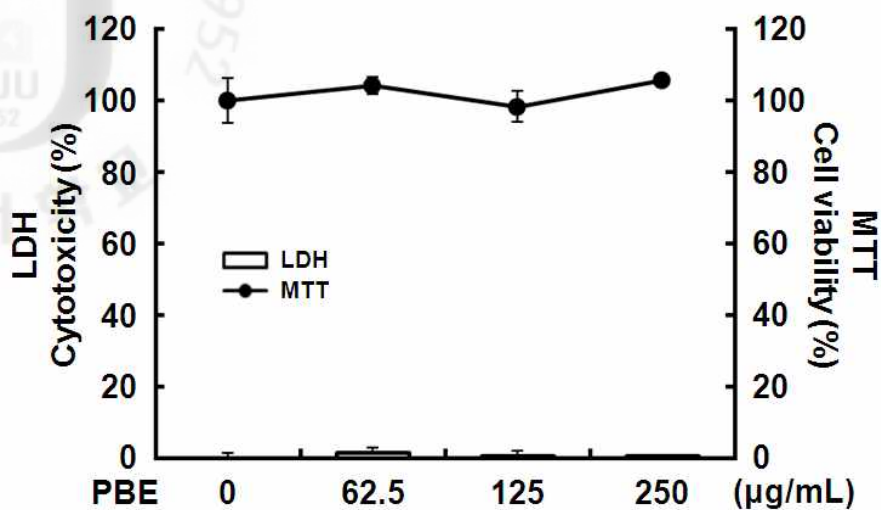
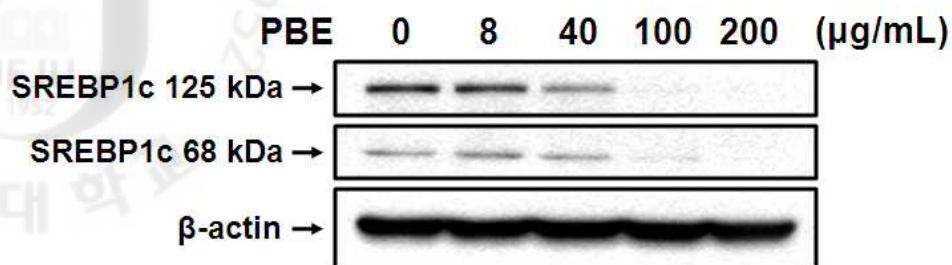
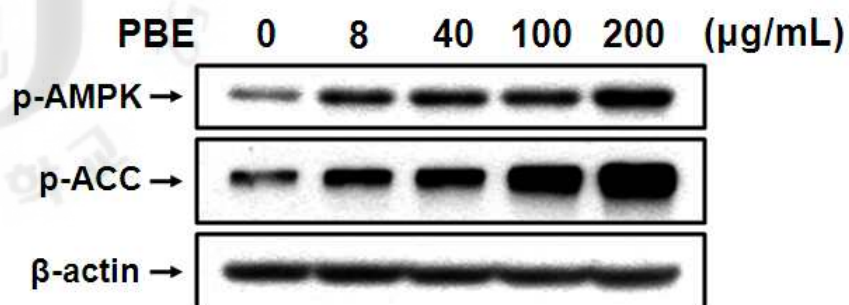


Figure 1.15. Effect of PBE on viability and cytotoxicity of mature 3T3-L1 adipocytes. 3T3-L1 preadipocytes were induced to differentiate as described in the Materials and Methods section. On day 8, viability and cytotoxicity were assessed in MTT and LDH assays for 48 h. All values are presented as means  $\pm$  S.D. ( $n=3$ ;  $*p<0.05$  compared to no PBE). The data shown are representative of three independent experiments.



**Figure 1.16.** Effect of various PBE concentration on expression of SREBP1c in mature 3T3-L1 adipocytes. 3T3-L1 preadipocytes were induced to differentiate as described in the Materials and Methods section. On day 8, mature 3T3-L1 adipocytes were incubated for 16 h with serum-free DMEM containing 0.2% BSA. The cells were then treated with post-differentiation medium containing various PBE concentrations for 24 h. Western blot analysis of the effect of PBE dose on SREBP1c expression. The data shown are representative of three independent experiments.



**Figure 1.17. Effect of various PBE concentration on phosphorylation of AMPK and ACC in mature 3T3-L1 adipocytes.** 3T3-L1 preadipocytes were induced to differentiate as described in the Materials and Methods section. On day 8, mature 3T3-L1 adipocytes were incubated for 16 h with serum-free DMEM containing 0.2% BSA. The cells were then treated with post-differentiation medium containing various PBE concentrations for 24 h. Western blot analysis of the effect of PBE dose on p-AMPK and p-ACC expression. The data shown are representative of three independent experiments.

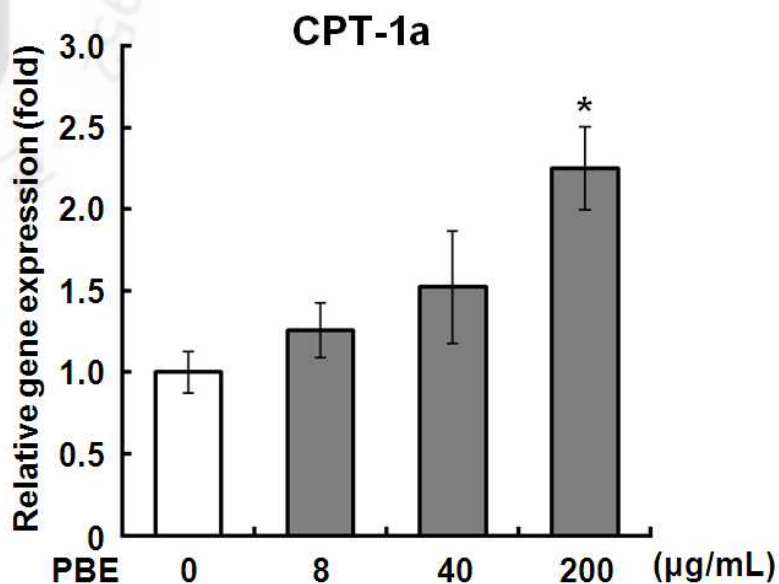


Figure 1.18. Effect of various PBE concentration on gene expression of CPT-1a in mature 3T3-L1 adipocytes. 3T3-L1 preadipocytes were induced to differentiate as described in the Materials and Methods section. On day 8, mature 3T3-L1 adipocytes were incubated for 16 h with serum-free DMEM containing 0.2% BSA. The cells were then treated with post-differentiation medium containing various PBE concentrations for 24 h. Real-time RT-PCR of the effect of PBE on CPT-1a gene expression. All values are presented as means  $\pm$  S.D. ( $n=3$ ;  $*p<0.05$  compared to no PBE). The data shown are representative of three independent experiments.

### 1.5.3. Anti-obesity effect of Fucoxanthin derived from PBE

#### 1.5.3.1. *Fucoxanthin enhances 3T3-L1 adipocyte differentiation at an early stage*

We investigated the effects of treatment with fucoxanthin on cells of different differentiation stages. To identify a concentration of fucoxanthin that did not affect viability or cause cytotoxicity in 3T3-L1 preadipocytes, cell viability and cytotoxicity in 3T3-L1 preadipocytes were evaluated in MTT and LDH assays. At a concentration of 10  $\mu\text{M}$ , fucoxanthin did not affect viability or cause cytotoxicity in 3T3-L1 cells, as determined by MTT and LDH assays (Figure 1.19).

Next, we tested whether fucoxanthin enhanced MDI-induced differentiation in 3T3-L1 preadipocytes. On days 0-2, fucoxanthin was added to the MDI differentiation medium I, containing IBMX, dexamethasone, and insulin; on day 8, the adipocytes were stained using Oil Red O. Oil Red O staining demonstrated that treatment with fucoxanthin at a concentration of 1, 5, or 10  $\mu\text{M}$  dose-dependently enhanced 3T3-L1 adipocyte differentiation and lipid accumulation (Figure 1.20A, B). To determine whether fucoxanthin enhances adipocyte differentiation by increasing the expression of key transcriptional regulators and markers, we measured the expression of PPAR $\gamma$ , C/EBP $\alpha$ , and aP2. Fucoxanthin dose-dependently up-regulated the expression of PPAR $\gamma$  and C/EBP $\alpha$ , master transcription factors involved in the regulation of adipogenic gene expression, and aP2, a marker of adipocyte differentiation (Figure 1.21). Fucoxanthin treatment also significantly increased the expression of the PPAR $\gamma$  target gene adiponectin (Figure 1.22).

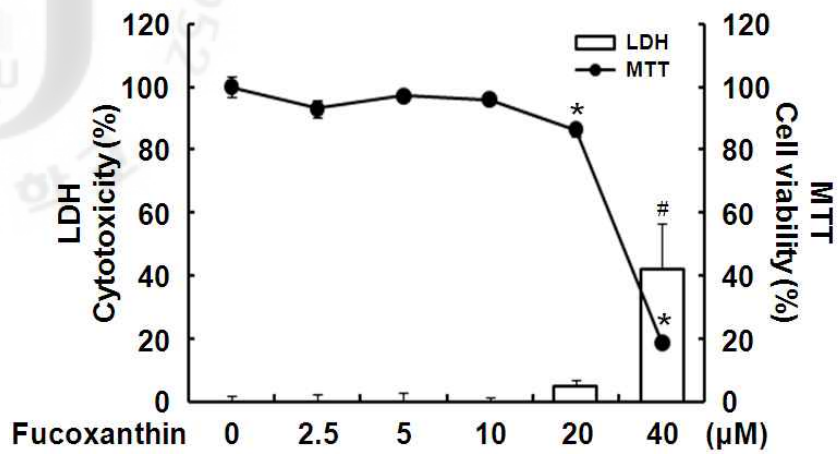
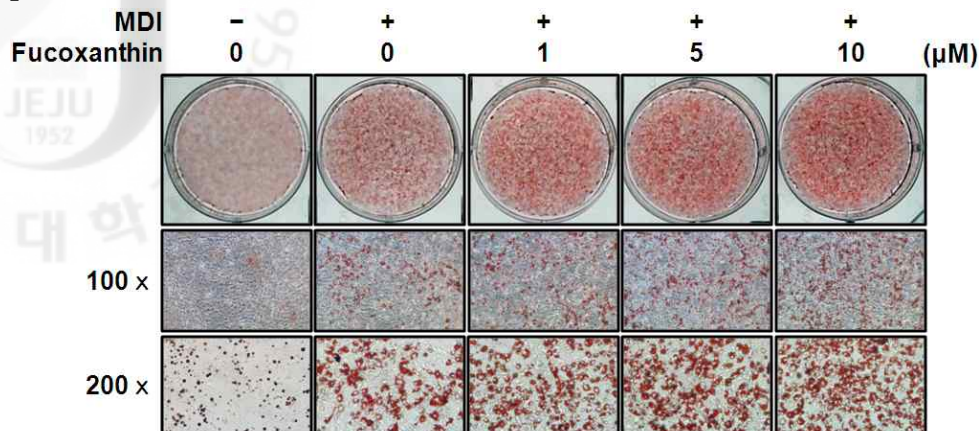
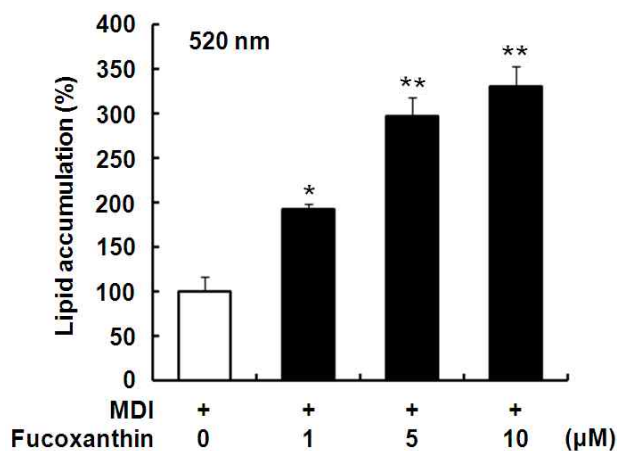


Figure 1.19. Effect of fucoxanthin on viability and cytotoxicity of 3T3-L1 preadipocytes. 3T3-L1 preadipocytes were incubated to evaluate as described in the Materials and Methods section. After 72 h, viability and cytotoxicity were assessed in MTT and LDH assays. All values are presented as means  $\pm$  S.D. ( $n=3$ ;  $*p<0.05$  compared to no fucoxanthin). The data shown are representative of three independent experiments.

**A**



**B**



**Figure 1.20. Effect of fucoxanthin on the lipid accumulation in 3T3-L1 cells.** Cells were cultured in MDI differentiation medium in the presence or absence of fucoxanthin. (A) Differentiated adipocytes were stained with Oil Red O on day 8 (fucoxanthin treatment: day 0-2). The Oil Red O stained adipocytes were photographed at 100× and 200× magnification. (B) Lipid accumulation was assessed by the quantification of OD<sub>520</sub> as described in the Materials and methods. All values are presented as means ± S.D. ( $n=3$ ; \* $p<0.01$  and \*\* $p<0.001$  compared to no fucoxanthin). The data shown are representative of three independent experiments.



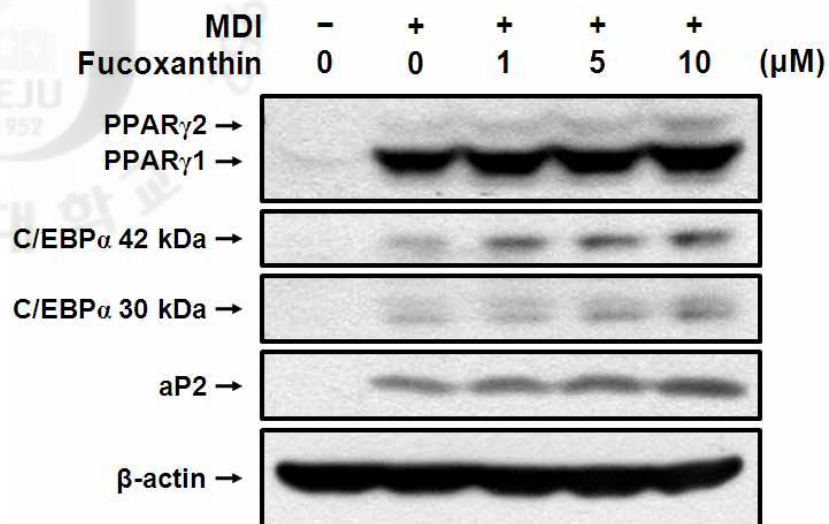


**Figure 1.21. Effect of fucoxanthin on the differentiation of adipocytes in 3T3-L1 preadipocytes.** Cells were cultured in MDI differentiation medium in the presence or absence of fucoxanthin (fucoxanthin treatment: day 0–2). Western blot analysis of PPAR $\gamma$ , C/EBP $\alpha$ , and aP2 expression. Proteins were prepared from 3T3-L1 cells on day 6. The data shown are representative of three independent experiments.

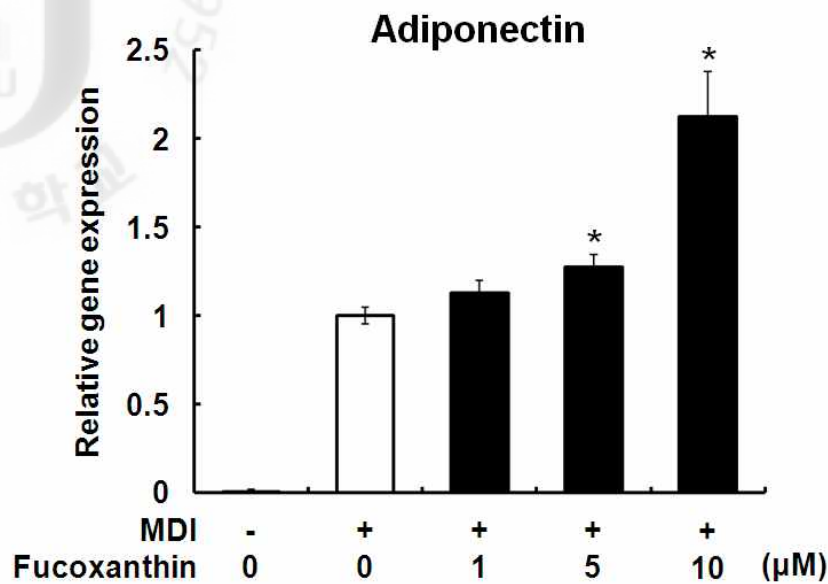
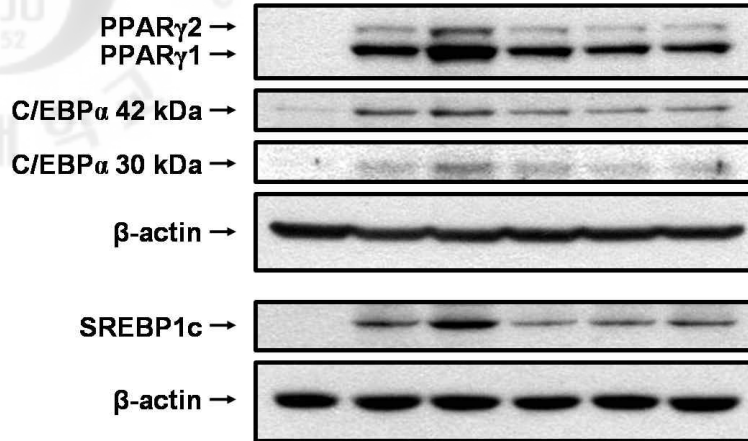


Figure 1.22. Effect of fucoxanthin on the gene expression of adiponectin in 3T3-L1 preadipocytes. Cells were cultured in MDI differentiation medium in the presence or absence of fucoxanthin. Real-time PCR analysis of adiponectin gene expression. Total RNA was prepared from 3T3-L1 cells on day 4. All values are presented as means  $\pm$  S.D. ( $n=3$ ;  $*p<0.01$  compared to no fucoxanthin). The data shown are representative of three independent experiments.

*1.5.3.2. Fucoxanthin inhibits adipocyte differentiation at intermediate and late stages*

We evaluated the effect of fucoxanthin on differentiating 3T3-L1 preadipocytes at various exposure times (D0-D2, D2-D4, D4-D7, and D2-D7) through Western blot analysis of day-7 samples. As shown in Figure 1.23, fucoxanthin significantly up-regulated protein expression of PPAR $\gamma$ , C/EBP $\alpha$ , and SREBP1c at the D0-D2 time point. However, it significantly down-regulated protein expression of PPAR $\gamma$ , C/EBP $\alpha$ , and SREBP1c at the D2-D4, D4-D7, and D2-D7 time points during adipocyte differentiation (Figure 1.24).

MDI	-	+	+	+	+	+
Fuco.	NT	NT	D0-D2	D2-D4	D4-D7	D2-D7



**Figure 1.23. Effect of fucoxanthin on adipocyte differentiation in 3T3-L1 cells at various time points (data of Western blot).** To induce differentiation, 2-day post-confluent preadipocytes were cultured in MDI differentiation medium I for 2 days. The cells were then cultured for a further 2 days in medium containing 0.5  $\mu$ g/mL insulin. Then, the cells were maintained in post-differentiation medium, which was replaced every 2 days. Protein expression after treatment with 10  $\mu$ M fucoxanthin for the indicated periods of time was analyzed by Western blotting. Total protein was extracted at day 7 and the expression of adipocyte-specific protein analyzed by Western blotting. The data shown are representative of three independent experiments.

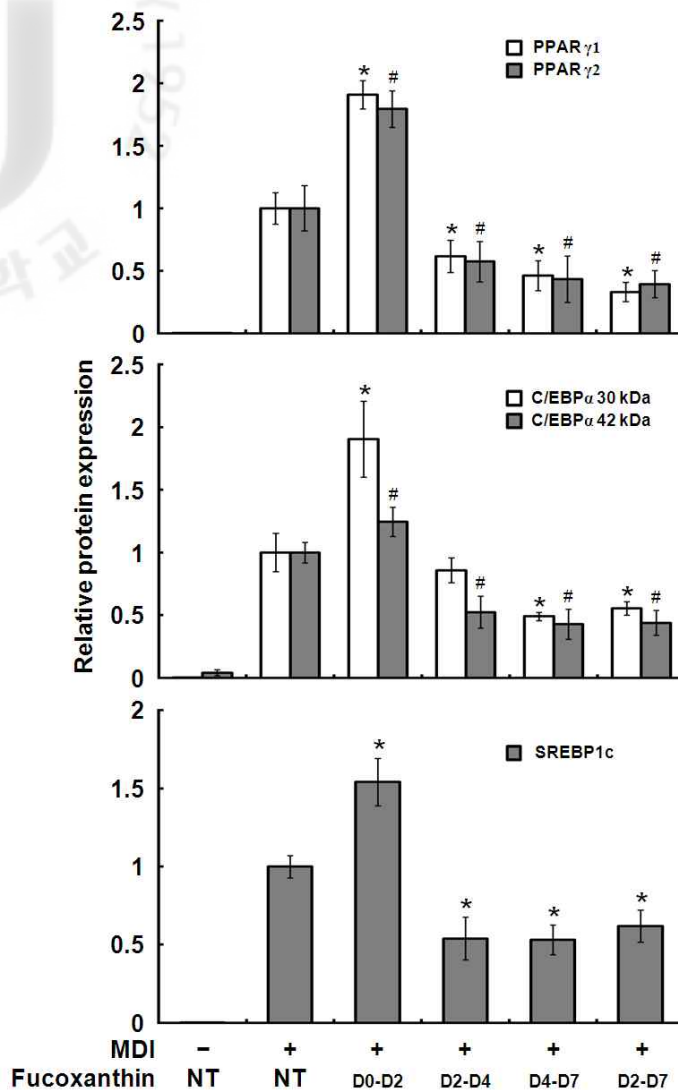


Figure 1.24. Effect of fucoxanthin on adipocyte differentiation in 3T3-L1 cells at various time points (normalization of Figure 1.23). Relative band density was determined by densitometry using the Image J 1.42q software (National Institutes of Health, Bethesda, MD, USA). Target protein expression was normalized to the  $\beta$ -actin expression level and expressed relative to NT protein levels. All values are presented as means  $\pm$  S.D. ( $n=3$ ;  $*p < 0.05$  and  $\#p < 0.05$  with NT (no-treatment control). D0-D2, D2-D4, D4-D7, and D2-D7; times of exposure to 10  $\mu$ M fucoxanthin. The data shown are representative of three independent experiments.

### *1.5.3.3. Fucoxanthin inhibits glucose uptake in mature 3T3-L1 adipocytes*

The cytotoxic effects of fucoxanthin, and its effects on cell viability, were evaluated in mature 3T3-L1 adipocytes in MTT and LDH assays. At a concentration of 10  $\mu$ M, fucoxanthin did not affect viability or cause cytotoxicity in mature 3T3-L1 adipocytes, as determined by MTT and LDH assays (Figure 1.25). We next examined whether fucoxanthin stimulated lipolysis in mature 3T3-L1 adipocytes by measuring levels of glycerol in culture supernatants. Fucoxanthin did not affect lipolysis at 24 or 48 h in mature 3T3-L1 adipocytes (Figure 1.26). Also, to investigate the effect of fucoxanthin on glucose uptake, mature 3T3-L1 adipocytes (D8-) were incubated with radiolabeled glucose and various concentrations of fucoxanthin. As shown in Figure 1.27, fucoxanthin inhibited glucose uptake in a dose-dependent manner. We next examined whether the observed decrease in glucose uptake caused by fucoxanthin was associated with a signaling pathway by evaluating the phosphorylation of IRS and Akt in fucoxanthin-treated 3T3-L1 adipocytes. Fucoxanthin treatment was found to inhibit the phosphorylation of both IRS and Akt (Figure 1.28).

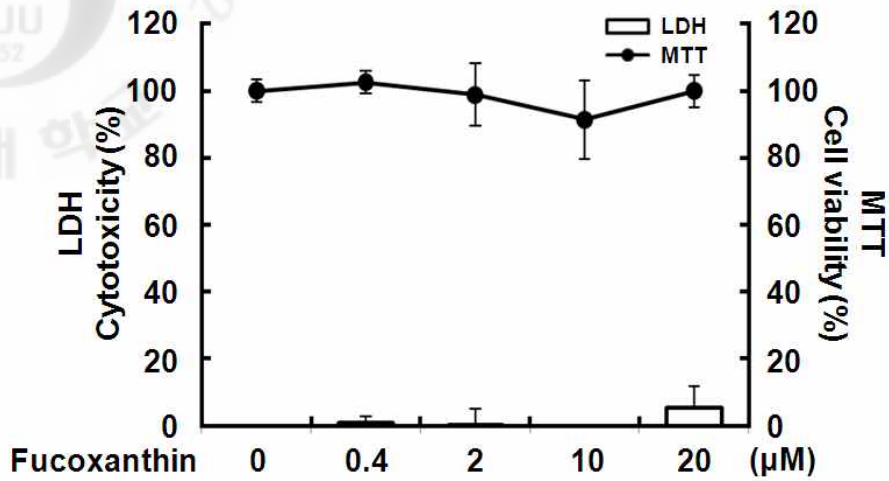
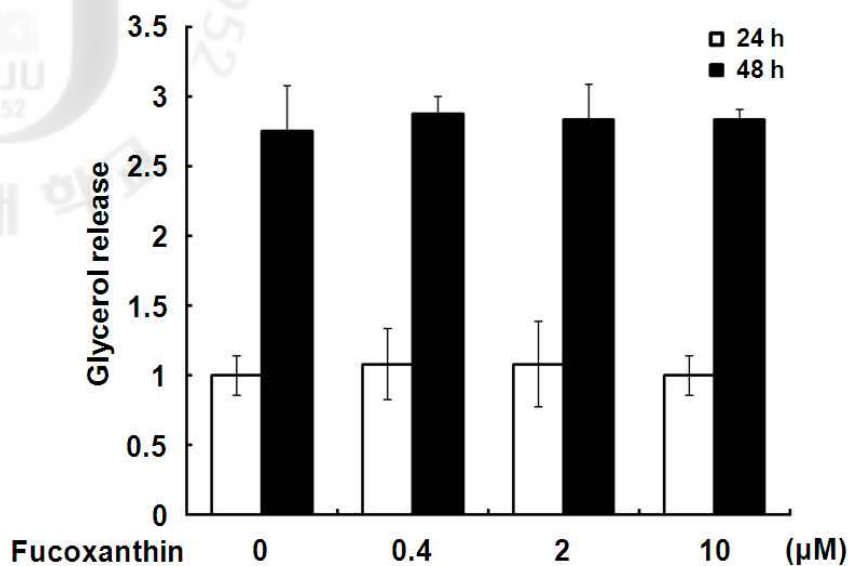
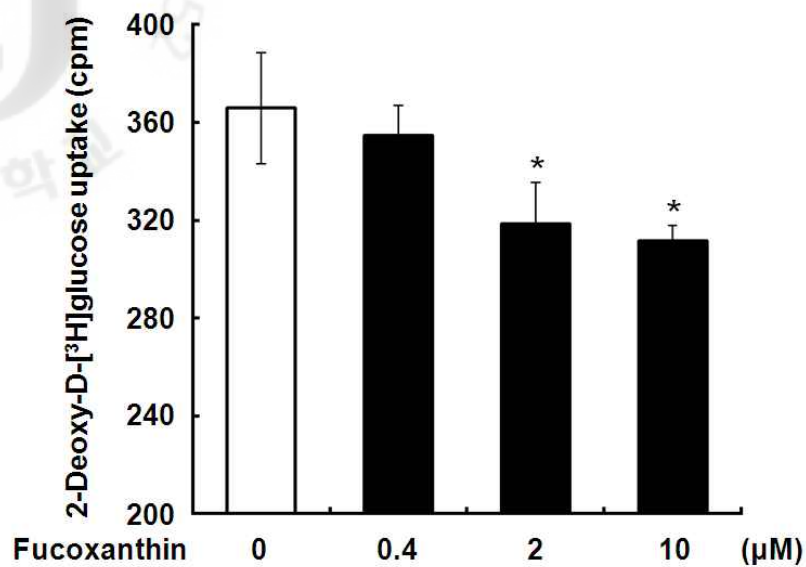


Figure 1.25. Effect of fucoxanthin on viability and cytotoxicity of mature 3T3-L1 adipocytes. To induce differentiation, 2-day post-confluent preadipocytes were cultured in MDI differentiation medium II for 2 days. The cells were then cultured for a further 2 days in medium containing 5 μg/mL insulin. Then, the cells were maintained in post-differentiation medium, which was replaced every 2 days. At day 8, viability and cytotoxicity were assessed in MTT and LDH assay for 48 h. All values are presented as means ± S.D. ( $n=3$ ;  $*p<0.05$  compared to no fucoxanthin). The data shown are representative of three independent experiments.



**Figure 1.26. Effect of fucoxanthin on lipolysis of mature 3T3-L1 adipocytes.** To induce differentiation, 2-day post-confluent preadipocytes were cultured in MDI differentiation medium II for 2 days. The cells were then cultured for a further 2 days in medium containing 5 μg/mL insulin. Then, the cells were maintained in post-differentiation medium, which was replaced every 2 days. At day 8, mature 3T3-L1 adipocytes were incubated with serum-free DMEM for 4 h. The cells were next treated with post-differentiation medium containing various concentration of fucoxanthin for 24 h or 48 h. Glycerol contents relative to control cells (0 μM fucoxanthin) at 24 h (assigned a value of 1). All values are presented as means ± S.D. ( $n=3$ ;  $*p<0.05$  compared to no fucoxanthin). The data shown are representative of three independent experiments.





**Figure 1.27. Effect of fucoxanthin on glucose uptake of mature 3T3-L1 adipocytes.** To induce differentiation, 2-day post-confluent preadipocytes were cultured in MDI differentiation medium II for 2 days. The cells were then cultured for a further 2 days in medium containing 5 μg/mL insulin. Then, the cells were maintained in post-differentiation medium, which was replaced every 2 days. At day 8, mature adipocytes were incubated in 12-well plates in the presence of fucoxanthin and then assayed for uptake of 2-deoxy-D-[<sup>3</sup>H]glucose. All values are presented as means ± S.D. ( $n=3$ ;  $*p<0.05$  compared to no fucoxanthin). The data shown are representative of three independent experiments.

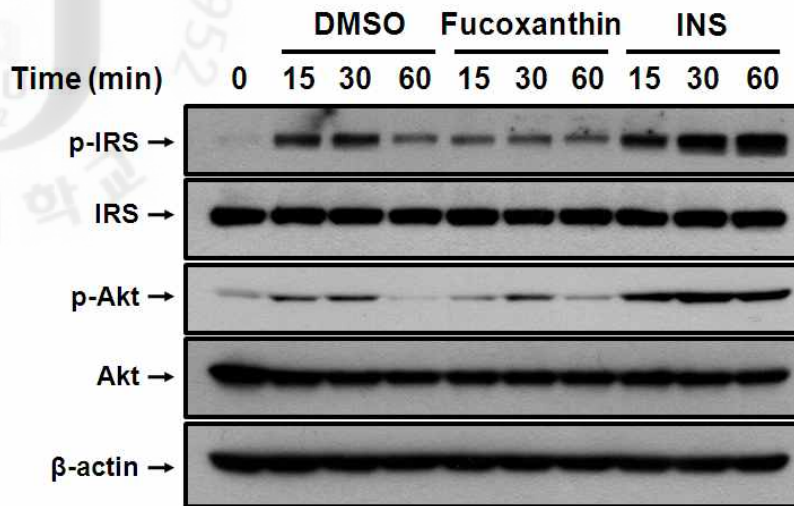


**Figure 1.28. Effect of fucoxanthin on IRS signaling pathway of mature 3T3-L1 adipocytes.** To induce differentiation, 2-day post-confluent preadipocytes were cultured in MDI differentiation medium II for 2 days. The cells were then cultured for a further 2 days in medium containing 5  $\mu\text{g}/\text{mL}$  insulin. Then, the cells were maintained in post-differentiation medium, which was replaced every 2 days. At day 8, mature adipocytes were incubated with serum-free DMEM for 6 h. The expression of signaling pathway proteins in cells treated with post-differentiation medium containing DMSO, 10  $\mu\text{M}$  fucoxanthin, or 100 nM insulin (INS) for the indicated periods of time was analyzed by Western blotting. The data shown are representative of three independent experiments.

*1.5.3.4. Fucoxanthin activated the AMPK pathway in mature 3T3-L1 adipocytes*

We investigated the effect of fucoxanthin which was derived from PBE, on AMPK signaling in mature 3T3-L1 adipocytes. Mature 3T3-L1 adipocytes were cultured in post-differentiation medium, and then exposed to 10  $\mu$ M of fucoxanthin for various periods. Consistent with our PBE data, fucoxanthin markedly induced AMPK and ACC phosphorylation (Figure 1.29). Moreover, fucoxanthin increased the phosphorylation of LKB1, which is responsible for the phosphorylation of AMPK (Figure 1.29). Also, fucoxanthin increased the levels of CPT-1a mRNA (Figure 1.30).

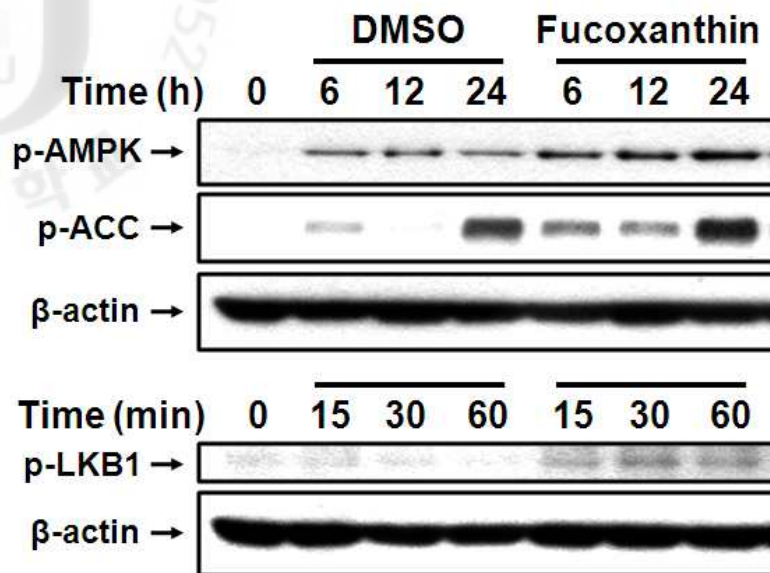


**Figure 1.29.** Effect of fucoxanthin on phosphorylation of LKB1, AMPK, and ACC in mature 3T3-L1 adipocytes. To induce differentiation, 2-day post-confluent preadipocytes were cultured in MDI differentiation medium II for 2 days. The cells were then cultured for a further 2 days in medium containing 5  $\mu\text{g/mL}$  insulin. Then, the cells were maintained in post-differentiation medium, which was replaced every 2 days. At day 8, mature adipocytes were incubated with serum-free DMEM for 16 h. The cells were then treated with post-differentiation medium containing 10  $\mu\text{M}$  of fucoxanthin for various times. The data shown are representative of three independent experiments.

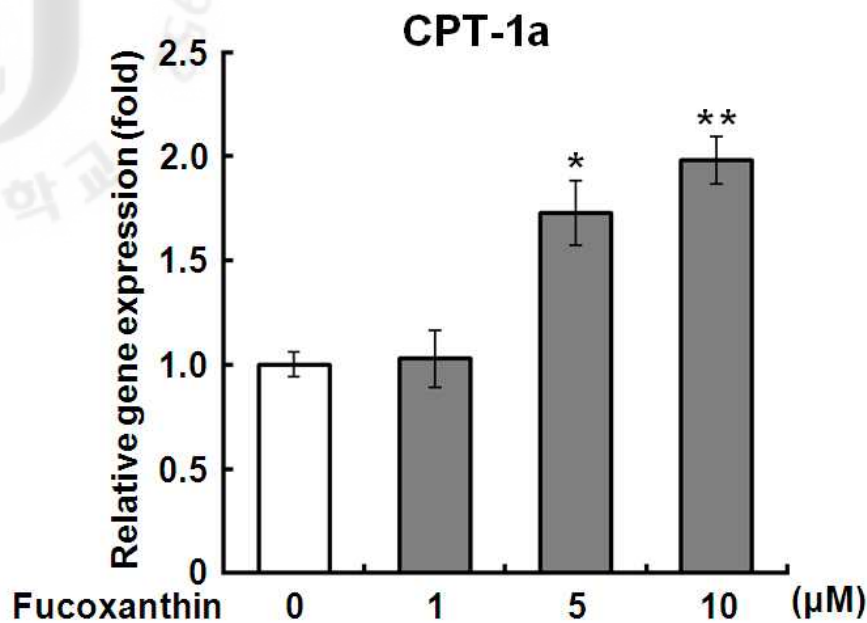


**Figure 1.30.** Effect of fucoxanthin on gene expression of CPT-1a in mature 3T3-L1 adipocytes. To induce differentiation, 2-day post-confluent preadipocytes were cultured in MDI differentiation medium II for 2 days. The cells were then cultured for a further 2 days in medium containing 5 µg/mL insulin. Then, the cells were maintained in post-differentiation medium, which was replaced every 2 days. At day 8, mature adipocytes were incubated with serum-free DMEM for 16 h. The cells were then treated with post-differentiation medium containing various concentration of fucoxanthin for 24 h. All values are presented as means ± S.D. ( $n=3$ ;  $*p<0.01$  and  $**p<0.01$  compared to no fucoxanthin). The data shown are representative of three independent experiments.

## 1.6. DISCUSSION

### 1.6.1. Anti-obesity effect of *Petalonia binghamiae* enzymatic extract (PBEE)

The regulation of adipogenesis involves a number of complex, interconnected cell signaling pathways, thus multiple natural products like edible seaweed extract might have the potential for use in therapy designed to protect metabolic disorder. In this regard, we have been evaluated the potential of several extract of the edible seaweed *Petalonia binghamiae* *in vitro* using murine 3T3-L1 preadipocytes and *in vivo* using animal models [Kang et al., 2008]. In this study, we found that a water-soluble *Petalonia binghamiae* extract, designated PBEE, dose-dependently decreased the levels of triglycerides, PPAR $\gamma$ 1 and 2, C/EBP $\alpha$ , and aP2 in differentiating 3T3-L1 preadipocytes. The PBEE-induced decrease in PPAR $\gamma$  and C/EBP $\alpha$  expression suggested that another PBEE target molecule lay upstream of PPAR $\gamma$  and C/EBP $\alpha$ . To elucidate the signaling pathway through which PBEE affected preadipocyte proliferation, we first examined the possible involvement of ERKs, which have been linked to adipocyte differentiation [Hung et al., 2005; Kim et al., 2007]. However, PBEE treatment did not affect ERK phosphorylation. It also did not affect the expression of SREBP1c, which has been reported to induce the production of an endogenous ligand that enhances PPAR $\gamma$  transcriptional activity [Kim et al., 1998] and can increase the expression of several genes involved in fatty acid metabolism.

C/EBP $\beta$  plays a critical role in adipocyte differentiation [Tang et al., 2003]. It is expressed early in the differentiation program and drives the subsequent expression of C/EBP $\alpha$  [Christy et al., 1991]. Our data showed that PBEE inhibits C/EBP $\beta$  expression in 3T3-L1 cells. Given the importance of

C/EBP during adipocyte differentiation, the inhibition of C/EBP $\beta$  expression by PBEE may be sufficient to block terminal differentiation. Thus, our results suggest that the inhibition of adipocyte differentiation by PBEE correlates with inhibition of C/EBP $\beta$  expression. According to Tang et al. [Tang et al., 2003], mitotic clonal expansion is a prerequisite for differentiation of 3T3-L1 preadipocytes into adipocytes. Also, Harmon and Harp [Harmon and Harp, 2001] have found that genistein inhibits mitotic clonal expansion and induces lipolysis in adipocytes. Our FACS cell cycle data suggest that PBEE affects preadipocyte proliferation. Like genistein, PBEE blocks the cell cycle at the G<sub>1</sub>/S transition. Thus, PBEE might inhibit the differentiation of preadipocytes by preventing them from traversing the G<sub>1</sub>/S checkpoint.

Binding of insulin to its receptor induces tyrosine phosphorylation of the receptor, thereby initiating the insulin signal transduction. Subsequent tyrosine phosphorylation of IRS-1 and -2 leads to activation of phosphatidylinositol 3-kinase (PI3-K) [Youngren, 2007], which produces phosphatidylinositol phospholipids. These phospholipids in turn activate phosphatidylinositol phosphate-dependent kinase-1. The subsequent activation of Akt stimulates glucose uptake into cells by inducing the translocation of glucose transporter 4 from intracellular storage sites to the plasma membrane [Kanzaki, 2006]. We found that PBEE, like the often-used tyrosine kinase inhibitor genistein [Akiyama et al., 1987; Wu-Wong et al., 1999], inhibited insulin-stimulated glucose uptake in mature 3T3-L1 adipocytes by reducing the level of phospho-IRS.

Recently, we demonstrated that an ethanolic extract of *Petalonia binghamiae* (PBE) exerts an adipogenic effect in 3T3-L1 cells and anti-diabetic effect in streptozotocin-induced diabetic mice [Kang et al., 2008]. However, this study revealed that the water-soluble extract of *Petalonia binghamiae* (PBEE) exerts an anti-adipogenic effect in 3T3-L1 cells. We suppose that these different biological activities between PBEE and PBE

occur due to different chemical compound contents by two different extraction methods. The contents of total polyphenol compounds were richer in PBE than in PBEE. On the other hand, total polysaccharides were much lower (about 50-fold) in PBE than in PBEE. Accordingly, the present results indicate that the water-soluble component(s), such as polysaccharide(s), which were contained as major constituents in PBEE, inhibit the adipogenesis and glucose uptake in 3T3-L1 cells. While the lipid-soluble constituents, such as polyphenol compounds, which were contained as major constituents in PBE, may exert adipogenic effect in 3T3-L1 cells. However, identifications of their active compound (s) from PBEE and PBE are to be remained for further research.

Adipose tissue is a dynamic organ that plays an important role in energy balance and changes in mass according to the metabolic requirements of the organism [Harp, 2004]. Consistent with our *in vitro* results, the administration of PBEE (100 or 500 mg per liter drinking water) over 30 days to rats fed a HFD decreased the body weight and adipose tissue weight of the rats without changing their energy intake.

We also analyzed the effects of PBEE on the development of fatty liver, which is strongly associated with obesity [James and Day, 1999]. In HFD rats, livers were enlarged and yellowish, indicating liver steatosis, whereas the livers of the HFD+PBEE rats remained red and healthy-looking. Upon histological analysis, the HFD livers exhibited an accumulation of numerous fat droplets, a typical sign of fatty liver. However, the HFD+PBEE livers exhibited a much smaller degree of lipid accumulation and fewer signs of pathology.

Plasma GOT and GPT levels are clinically and toxicologically important indicators, rising as a result of tissue damage caused by toxicants or disease conditions. In HFD rats, the activities of liver function markers, including serum GOT and GPT, were significantly elevated relative to those in the ND



rats and were improved by PBEE supplementation. Taken together, these results indicate that administration of PBEE can partially suppress the development of HFD-induced fatty liver. PBEE supplementation of drinking water at 500 mg/L also significantly increased serum HDL-cholesterol levels in HFD rats.

In conclusion, we have shown that PBEE inhibits adipogenesis by down-regulating the adipocyte-specific transcriptional regulator C/EBP $\beta$ , C/EBP $\alpha$ , and PPAR $\gamma$ . Furthermore, PBEE attenuates the mitotic clonal expansion process of adipocyte differentiation and significantly inhibits glucose uptake in mature 3T3-L1 adipocytes. Finally, the administration of PBEE to rats with HFD-induced obesity reduces body weight gain, adiposity, and the accumulation of fatty droplets in the liver. Taken together, PBEE (or a biologically active component thereof) may protect against HFD-induced obesity through inhibiting adipocyte differentiation and glucose uptake in mature adipocytes.

### 1.6.2. Anti-obesity effect of *Petalonia binghamiae* ethanolic extract (PBE)

Obesity is a major public health problem in industrialized and developing countries. Currently available drugs for the treatment of obesity have undesirable side effects; therefore, there is great demand for a safe but therapeutically potent anti-obesity drug. Thus, there has been increased interest and in the search for anti-obesity phytonutrients that are effectively reduce visceral fat mass.

*Petalonia binghamiae* ethanolic extract (PBE) is known to exert several pharmacological effects, including lowered blood glucose levels, improved glucose tolerance, increases transcriptional activity of PPAR $\gamma$ , and increased glucose uptake [Kang et al., 2008]. However, no fatty acid  $\beta$ -oxidation effect has as yet been reported. In the present study, we investigated the anti-obesity potential of PBE by targeting fatty acid  $\beta$ -oxidation through AMPK signaling using high-fat-diet-induced obese mice. In this animal model, the body weight gain, adipose tissue weight, and serum TG level were significantly lowered by PBE administration with no change in food intake.

Obesity is caused by an increase in the number and size of adipocytes derived from fibroblastic preadipocytes in adipose tissue [Spiegelman and Flier., 1996]. A greater number of large cells were present in the epididymal adipose tissue of the HFD group, while those the HFD+PBE group exhibited a small number of large cells and fewer pathological signs. Adiponectin mRNA expression in the HFD group was about 2.5 times lower than in the ND group. Interestingly, PBE raised the mRNA expression of adiponectin to about the level seen in the ND group, suggesting that it may be beneficial in metabolic diseases. Adiponectin is a protein hormone that modulates a number of metabolic processes, including glucose regulation and fatty acid catabolism [Diez and Iglesias, 2003]. Obesity, diabetes, and atherosclerosis have been

associated with reduced adiponectin levels [Ahima, 2006].

In general, the development of fatty liver is strongly associated with obesity [James and Day, 1999]. HFD feeding induced an accumulation of numerous fatty droplets, a typical of fatty liver. PBE administration improved morphologically the accumulation of lipids and pathological signs and protected against increased liver tissue weight. Also, it significantly reduced the levels of biochemical makers of liver function, including serum GPT and GOT. These results suggest that PBE protects against the development of HFD-induced fatty liver; however, the molecular mechanisms underlying these beneficial properties of PBE are unknown.

As a metabolic master switch, AMPK activation is associated with metabolic organs, including the liver, skeletal muscle, pancreas, and adipose tissue. At the molecular level, our data showed that HFD feeding significantly depressed the activation of AMPK in C57BL/6 mouse epididymal adipose tissue. However, the level of phosphorylated forms of AMPK was recovered to normal by PBE administration for 70 days, suggesting the beneficial role of PBE in activating AMPK signaling pathway. Therefore, we tested whether PBE affected the AMPK signaling pathway *in vitro* using mature 3T3-L1 adipocytes. Consistent with anti-obesity effect of PBE *in vivo*, our results showed that PBE increased the phosphorylation of AMPK and ACC and the mRNA expression of CPT-1a, while it decreased the expression of SREBP1c, in mature 3T3-L1 adipocytes.

AMPK activation increases fatty acid  $\beta$ -oxidation by reducing malonyl-CoA through the inhibition of ACC, and this process up-regulates CPT-1a expression [Merrill et al., 1997]. CPT-1a regulates long-chain fatty acid transport across the mitochondrial membrane [Hao et al., 2010]. SREBP transcription factors regulate the expression of lipogenic enzymes, including ACC, fatty acid synthase (FAS), and 3-hydroxy-3-methylglutaryl CoA reductase (HMGCR) [Goldstein et al., 2002]. The present study strongly

suggests that the beneficial properties of PBE in HFD-induced obese mice were exerted by both increasing fatty acid  $\beta$ -oxidation through the AMPK signaling pathway and decreasing *de novo* lipogenesis in adipose tissue

In conclusion, PBE administration in mice with HFD-induced obesity reduced body weight gain, adipose tissue weight, adipose tissue cell size, and fatty droplet accumulation in the liver. Also, PBE administration increased AMPK and ACC phosphorylation in animal adipose tissues. Moreover, PBE activated the AMPK signaling pathway, and inhibited the expression of SREBP1c in mature 3T3-L1 adipocytes. Taken together, our findings demonstrate that PBE may improve HFD-induced obesity by increasing fatty acid  $\beta$ -oxidation and inhibiting lipogenesis in the adipose tissue.

### 1.6.3. Anti-obesity effect of Fucoxanthin derived from PBE

Because progression of 3T3-L1 preadipocyte differentiation is divided into early (D0-D2), intermediate (D2-D4), and late stages (D4-) [Ntambi and Kim, 2000]. Fucoxanthin dose-dependently enhanced 3T3-L1 adipocyte differentiation and lipid accumulation. Moreover, fucoxanthin dose-dependently up-regulated the expression of PPAR $\gamma$  and C/EBP $\alpha$ , master transcription factors involved in the regulation of adipogenic gene expression, and aP2, a marker of adipocyte differentiation. Also, fucoxanthin treatment also significantly increased the expression of the PPAR $\gamma$  target gene adiponectin. These results suggest that fucoxanthin enhances 3T3-L1 adipocyte differentiation at an early stage (D0-D2) by modulating the expression of key transcriptional regulators.

It has been reported that fucoxanthin, when applied to cells continuously for 5 days, inhibited the differentiation of 3T3-L1 preadipocytes to adipocytes by down-regulating PPAR $\gamma$ , (D2-D7) [Maeda et al., 2006]. Thus, we evaluated the effect of fucoxanthin on differentiating 3T3-L1 preadipocytes at various exposure times (D0-D2, D2-D4, D4-D7, and D2-D7). Fucoxanthin significantly up-regulated protein expression of PPAR $\gamma$ , C/EBP $\alpha$ , and SREBP1c at the D0-D2 time point. However, it significantly down-regulated protein expression of PPAR $\gamma$ , C/EBP $\alpha$ , and SREBP1c at the D2-D4, D4-D7, and D2-D7 time points during adipocyte differentiation. These results suggest that fucoxanthin enhanced 3T3-L1 adipocyte differentiation at an early stage, while inhibiting it at intermediate and late stages by modulating the expression of key transcriptional regulators. However, how fucoxanthin regulates the expression of PPAR $\gamma$ , C/EBP $\alpha$ , and SREBP1c at the various stages of differentiation requires further study.

We next examined whether fucoxanthin stimulated lipolysis in mature 3T3-L1 adipocytes by measuring levels of glycerol in culture supernatants.

Fucoxanthin did not affect lipolysis at 24 or 48 h in mature 3T3-L1 adipocytes.

Binding of insulin to its receptor induces tyrosine phosphorylation of the receptor, initiating insulin signal transduction. Subsequent tyrosine phosphorylation of IRS-1 and IRS-2 leads to activation of PI3-K [Youngren, 2007], which produces phosphatidylinositol phospholipids. These phospholipids, in turn, activate phosphatidylinositol phosphate-dependent kinase-1. The subsequent activation of Akt stimulates the uptake of glucose into cells by inducing the translocation of glucose transporter 4 from intracellular storage sites to the plasma membrane [Kanzaki, 2006]. Fucoxanthin inhibited glucose uptake in a dose-dependent manner by inhibiting the phosphorylation of IRS and Akt. However, fucoxanthin did not affect lipolysis in mature 3T3-L1 adipocytes. This result suggests that fucoxanthin inhibits glucose uptake by inhibiting the phosphorylation of IRS in mature 3T3-L1 adipocytes.

AMPK is known to be a metabolic master switch that is activated by LKB1 under intracellular stress conditions, including glucose deficiency, hypoxia, and ROS activity [Fryer and Parbu-Patel, 2002; Hardie, 2007]. During energy depletion, AMPK inhibits de novo fatty acid synthesis by inactivating aACC and stimulates fatty acid oxidation by up-regulating the expression of CPT-1, PPAR $\alpha$ , and UCP [Saha et al., 2004]. As a cellular energy regulator, AMPK is known to play a major role in glucose and lipid metabolism and to control metabolic disorders such as diabetes, obesity, and cancer [Carling, 2004; Kim et al., 2007]. Thus, AMPK has emerged as a therapeutic target for metabolic disorders [Zhang et al., 2009]. Also, AMPK activation increases fatty acid  $\beta$ -oxidation by reducing malonyl-CoA through the inhibition of ACC, and this process up-regulates CPT-1a expression [Merrill et al., 1997]. CPT-1a regulates long-chain fatty acid transport across the mitochondrial membrane [Hao et al., 2010]. SREBP transcription factors regulate expression of lipogenic enzymes, such as ACC, FAS, and HMGCR

[Goldstein et al., 2002]. Fucoxanthin increased the phosphorylation of LKB1, AMPK, ACC, and the expression of CPT-1a mRNA on AMPK signaling pathway. Thus, these results suggest that fucoxanthin have properties in promoting the fatty acid  $\beta$ -oxidation.

In conclusion, we showed that fucoxanthin, at various stages of differentiation, has varying effects on the differentiation of 3T3-L1 cells. Collectively, our results suggest that fucoxanthin, when present during the early stage of the differentiation period, enhances adipogenesis by up regulating the adipocyte-specific transcriptional regulators PPAR $\gamma$  and C/EBP $\alpha$ . However, fucoxanthin reduced PPAR $\gamma$  and C/EBP $\alpha$  levels when present during the intermediate and late stages of the differentiation period. Additionally, it inhibited glucose uptake in mature 3T3-L1 adipocytes by inhibiting the phosphorylation of IRS. Finally, fucoxanthin induced fatty acid  $\beta$ -oxidation via an activated AMPK pathway. Our results suggest that fucoxanthin exerts its anti-obesity effect by inhibiting the differentiation of adipocytes at both intermediate and late stages, as well as regulation of lipid metabolism in mature adipocytes.

The logo of Jeju National University is a watermark in the background. It features a stylized flame or 'U' shape with the text 'JEJU NATIONAL UNIVERSITY 1952' around it and 'JEJU 1952' in the center.

## PART 2

Anti-obesity effect of the immature *Citrus sunki* peel  
and sinensetin derived from it

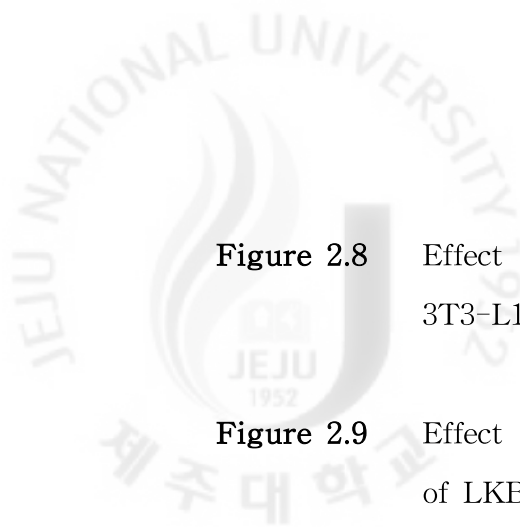


## 2.1. LIST OF TABLES

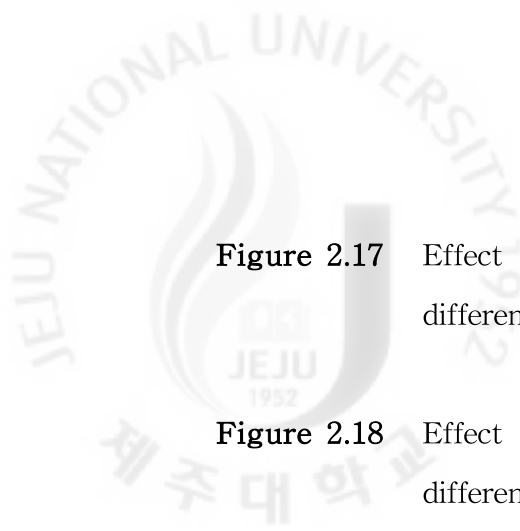
<b>Table 2.1</b>	Flavonoids content (mg/g) in CSE -----	<b>114</b>
<b>Table 2.2</b>	Effects of CSE supplementation on body weight gain, food intake, and liver weight in high-fat-diet (HFD)-induced obese experimental group after 70 days -----	<b>123</b>
<b>Table 2.3</b>	Effects of CSE supplementation on serum levels of T-CHO and TG in high-fat-diet (HFD)-induced obese experimental group after 70 days -----	<b>126</b>
<b>Table 2.4</b>	Effects of CSE supplementation on liver weight in high-fat-diet (HFD)-induced obese experimental group after 70 days -----	<b>129</b>

## 2.2. LIST OF FIGURES

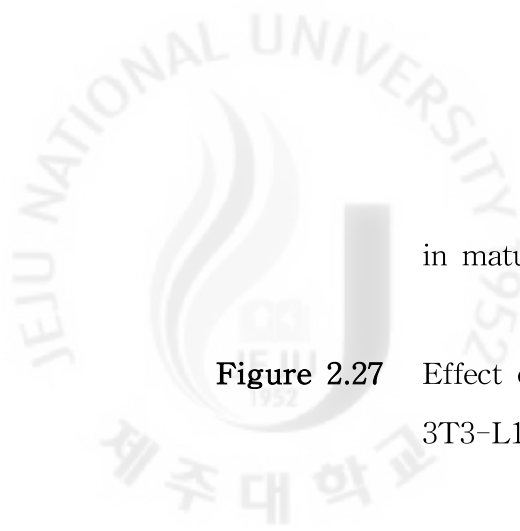
<b>Figure 2.1</b>	Picture of immature <i>Citrus sunki</i> -----	113
<b>Figure 2.2</b>	Effect of CSE on fatty droplets in the epididymal adipose tissue of mice fed a normal diet (ND), high-fat-diet (HFD), or HFD+CSE -----	124
<b>Figure 2.3</b>	Effect of CSE on adipose tissue weight of mice fed a normal diet (ND), high-fat-diet (HFD), or HFD+CSE --	125
<b>Figure 2.4</b>	Effect of CSE on serum levels of GPT, GOT, and LDH in mice fed a normal diet (ND), high-fat-diet (HFD), or HFD+CSE -----	128
<b>Figure 2.5</b>	Effect of CSE on fatty droplets in the livers of mice fed a normal diet (ND), high-fat-diet (HFD), or HFD+CSE -----	130
<b>Figure 2.6</b>	Effect of CSE on protein expression in epididymal adipose tissue of mice fed a normal diet (ND), high-fat-diet (HFD), or HFD+CSE -----	132
<b>Figure 2.7</b>	Effect of CSE on adiponectin mRNA expression in epididymal adipose tissue of mice fed a normal diet (ND), high-fat-diet (HFD), or HFD+CSE -----	133



<b>Figure 2.8</b>	Effect of CSE on viability and cytotoxicity of mature 3T3-L1 adipocytes -----	135
<b>Figure 2.9</b>	Effect of various CSE concentration on phosphorylation of LKB1, AMPK, and ACC in mature 3T3-L1 adipocytes -----	136
<b>Figure 2.10</b>	Effect of CSE on phosphorylation of LKB1, AMPK, and ACC at several times in mature 3T3-L1 adipocytes ----	137
<b>Figure 2.11</b>	Effect of various CSE concentration on gene expression of CPT-1a in mature 3T3-L1 adipocytes -----	138
<b>Figure 2.12</b>	Effect of CSE on lipolysis in mature 3T3-L1 adipocytes -----	140
<b>Figure 2.13</b>	Effect of CSE on phosphorylation of PKA and HSL in mature 3T3-L1 adipocytes -----	141
<b>Figure 2.14</b>	Effect of sinensetin on the lipid accumulation in 3T3-L1 cells -----	143
<b>Figure 2.15</b>	Effect of sinensetin on the differentiation of adipocytes in 3T3-L1 preadipocytes -----	144
<b>Figure 2.16</b>	Effect of sinensetin on the gene expression of adiponectin in 3T3-L1 preadipocytes -----	145



<b>Figure 2.17</b>	Effect of sinensetin on expression of SREBP1c in differentiating 3T3-L1 cells -----	147
<b>Figure 2.18</b>	Effect of sinensetin on expression of C/EBP $\beta$ in differentiating 3T3-L1 cells -----	148
<b>Figure 2.19</b>	Effect of sinensetin on upstream signaling of C/EBP $\beta$ in differentiating 3T3-L1 cells -----	149
<b>Figure 2.20</b>	Effect of sinensetin on phosphorylation of PKA in differentiating 3T3-L1 cells -----	150
<b>Figure 2.21</b>	Effect of sinensetin on production of intracellular cAMP in differentiating 3T3-L1 cells -----	151
<b>Figure 2.22</b>	Effect of sinensetin on lipolysis of mature 3T3-L1 adipocytes -----	153
<b>Figure 2.23</b>	Effect of sinensetin on production of intracellular cAMP in mature 3T3-L1 adipocytes -----	154
<b>Figure 2.24</b>	Effect of sinensetin on phosphorylation of PKA and HSL in mature 3T3-L1 adipocytes -----	155
<b>Figure 2.25</b>	Effect of sinensetin on glucose uptake in mature 3T3-L1 adipocytes -----	157
<b>Figure 2.26</b>	Effect of sinensetin on phosphorylation of IRS and Akt	



	in mature 3T3-L1 adipocytes -----	158
<b>Figure 2.27</b>	Effect of sinensetin on expression of SREBP1c in mature 3T3-L1 adipocytes -----	159
<b>Figure 2.28</b>	Effect of sinensetin on phosphorylation of AMPK and ACC at several times in mature 3T3-L1 adipocytes ----	162
<b>Figure 2.29</b>	Effect of sinensetin on phosphorylation of LKB1 at several times in mature 3T3-L1 adipocytes -----	163
<b>Figure 2.30</b>	Effect of various sinensetin concentration on gene expression levels of CPT-1a in mature 3T3-L1 adipocytes -----	164

## 2.3. INTRODUCTION

Obesity is a leading cause of morbidity and mortality worldwide [World Health Organization, 2002] and is known to arise from an imbalance between energy intake and expenditure. The hypothalamus is the key center for integration of long-term energy balance and is a rich source of satiety regulatory peptides. Many of these peptides are also found in peripheral sites such as the gut and adipose tissue in which they play key physiological roles in body weight homeostasis and contribute to the pathophysiology of insulin resistance and its associated metabolic complications in obesity and diabetes [Hotamisligil et al., 1993; Enriori et al., 2007; Rasouli and Kern, 2008]. Obesity is a major public health problem in both industrialized and developing countries. The condition is characterized by an excess of adipose tissue, which increases one's risk of developing insulin resistance and metabolic syndromes. Metabolic deregulation may lead to such complications as diabetes mellitus, coronary heart disease, and hypertension [Kopelman, 2000]. At the cellular level, obesity is caused by an increase in the number and size of adipocytes derived from fibroblastic preadipocytes in adipose tissue [Spiegelman and Flier, 1996]. Adipose tissue is vital for maintaining metabolic homeostasis, and as an endocrine organ, it secretes various adipokines. Studies on adipose tissue biology have improved our understanding of the mechanisms linking metabolic disorders with altered adipocyte function [Fruhbeck, 2008]. Experimental evidence suggests that some metabolic disorders may be treatable or preventable through the inhibition of adipogenesis and modulation of adipocyte function [Trayhurn and Beattie, 2001].

Adipose tissue is a dynamic organ that plays an important role in energy balance and changes in mass according to the metabolic requirements of the

organism [Harp, 2004]. Adipose tissue has been known as endocrine organ that secretes various kinds of bioactive molecules named adipocytokines. Resistin, plasminogen activator inhibitor-1, and tumor necrosis factor- $\alpha$ , which are increased in obese state and enlarged adipocytes, are implicated in metabolic disorder, whereas adiponectin, which is expressed in small adipocytes, regulates energy metabolism [Yamauchi et al., 2001; Guerre-Millo, 2004]. Thus, increase of small adipocytes is said to be important for maintaining metabolic homeostasis.

Small adipocytes can be provided by differentiation from preadipocytes. The study of adipogenesis has been greatly facilitated by the establishment of immortal preadipocyte cell lines, such as 3T3-L1 preadipocytes. The adipocytes generated from these cells exhibit most of the key features of adipocytes *in vivo* [Green and Meuth., 1974]. Recent investigations suggest that sterol-regulatory element binding protein 1c (SREBP1c) is the earliest transcription factor involved in adipocyte differentiation [Payne et al., 2009]. CCAAT/enhancer binding protein (C/EBP)  $\alpha$  and peroxidase proliferator activated receptor (PPAR)  $\gamma$ , in turn, promote terminal differentiation, by activating transcription of the gene encoding the fatty acid-binding protein aP2, which is involved in establishing and maintaining the adipocyte phenotype. SREBP1c increases the expression of many lipogenic genes, including fatty acid synthase. Loss-of-function studies have shown that PPAR $\gamma$  is necessary and sufficient to promote adipogenesis [Barak et al., 1999; Koutnikova et al., 2003], and that C/EBP $\alpha$  is influential in maintaining the expression of PPAR $\gamma$  [Wu et al., 1999]. 3T3-L1 preadipocytes spontaneously differentiate over a period of several weeks into fat-cell clusters when maintained in culture with fetal calf serum. This can be accelerated by the inducing agents dexamethasone and 3-isobutyl-1-methylxanthine (IBMX). High concentrations of insulin have been used in combination with these inducing agents [Gregoire et al., 1998]. Especially,

IBMX, one of the inducers in the differentiation mixture, is an inhibitor of phosphodiesterase that increases intracellular cAMP, and is a physiological activator of cAMP-dependent protein kinase A (PKA) [Martini et al., 2009].

Adipocytes have an important role in energy homeostasis. Adipose tissue stores energy in the form of lipid and releases fatty acids in response to nutritional signals or energy insufficiency [Spiegelman and Flier, 1996]. Further, adipocytes have endocrine functions by secreting hormones and factors that regulate physiological functions, such as immune response, insulin sensitivity and food intake [Fruhbeck et al., 2001; Gregoire, 2001]. Excessive fat accumulation in the body and white adipose tissue causes obesity and results in an increased risk of many serious diseases, including type II diabetes, hypertension and heart disease. Therefore, prevention and treatment of obesity are relevant to health promotion.

Triglycerids (TG) stored in white adipose tissue is the major energy reserve in mammals. Excess TG accumulation in adipose tissue results in obesity. TG is synthesized and stored in cytosolic lipid droplets during times of energy excess, and is mobilized from lipid droplets, via lipolysis, during times of energy need to generate fatty acids. Whereas, TG synthesis occurs in other organs, such as the liver for VLDL production, lipolysis for the provision of fatty acids as an energy source for other organs is a unique function of adipocytes. Increasing lipolysis in adipocytes may be a potentially useful therapeutic target for treating obesity. However, chronically high levels of fatty acids in the blood, typically observed in obesity, are correlated with many detrimental metabolic consequences such as insulin resistance [Ahmadian et al., 2010]. Therefore, lipolysis and fatty acid oxidation are important mechanisms involved in reducing body fat.

High-fat feeding has commonly been used to induce visceral obesity in rodent animal models [Hansen et al., 1997] because the pathogenesis of obesity is similar to that in humans [Katagiri et al., 2007]. Also, 3T3-L1



preadipocytes are frequently used to study the function of adipocytes *in vitro* due to their ability to differentiate into mature adipocytes [Gregoire et al., 1998]. Currently, however, drugs available for the treatment of obesity have undesirable side effects, and thus a high demand exists for a safe but therapeutically potent anti-obesity drug, which has increased interest in the search for anti-obesity phytonutrients that effectively reduce visceral fat mass.

*Citrus* fruit peel has been used in traditional Asian medicine for centuries to treat indigestion and to improve bronchial and asthmatic conditions [Huang and Wang, 1993]. In modern European herbal medicine, *Citrus* fruit peel is used to treat dyspepsia and related conditions [Wichtl and Bisset, 1994; Blumenthal et al., 1998]. *Citrus* flavonoids are generally categorized into two groups, flavones glycosides (e.g., naringin, hesperidin, nobiletin) and polymethoxylated flavones (PMFs, e.g., sinensetin, tangeretin). These flavonoids have various biological activities, such as anti-atherogenic effects, anti-inflammatory effects, and anticancer activity [Galati et al., 1994; Lee et al., 2001; Ko et al., 2010]. The peel of *Citrus sunki* Hort. ex Tanaka is a rich source of flavanones, as well as many PMFs, which are very rare in other plants [Ko et al., 2010; Choi et al., 2007; Nogata et al., 2006]. In this study, we investigated the anti-obesity potential of immature *Citrus sunki* peel extracts in murine 3T3-L1 adipocytes and mice fed a high-fat diet (HFD).

Moreover, sinensetin, one of polymethoxylated flavones contributes to pharmacological activity such as anti-cancer effect [Dong et al., 2011]. However, the effect of sinensetin on adipocyte functions has not been studied. In the present study, we report that the sinensetin, derived from *Citrus sunki* peel evaluated the adipogenesis potential in 3T3-L1 preadipocytes. Also, we evaluated the lipolysis potential and  $\beta$ -oxidation potential in mature 3T3-L1 adipocytes of sinensetin.

## 2.4. MATERIALS AND METHODS

### 2.4.1. Reagents

Dulbecco's modified Eagle's medium (DMEM), bovine calf serum (BCS), fetal bovine serum (FBS), and penicillin-streptomycin (PS) were purchased from Gibco BRL (Grand Island, NY, USA). Phosphate buffered saline (PBS; pH 7.4), 3-isobutyl-1-methylxanthine (IBMX), dexamethasone, insulin, and 3-(4,5-dimethylthiazol-2-yl)-2,5-diphenyl tetrazolium bromide (MTT), as well as the standards for flavonoid analysis, were obtained from Sigma Chemical Co. (St. Louis, MO, USA). The lactate dehydrogenase (LDH) Cytotoxicity Detection Kit was purchased from Takara Shuzo Co. (Otsu, Shiga, Japan). An antibodies to peroxidase proliferator activated receptor (PPAR)  $\gamma$ , fatty acid-binding protein aP2, CCAAT/enhancer binding protein (C/EBP)  $\alpha$ , C/EBP  $\beta$ , phospho-Ser473 protein kinase B (PKB, Akt), extracellular-signal related kinase 1 and 2 (ERK) 1/2, phospho-Thr204-ERK 1/2, and phosphor-Ser431-LKB1 was acquired from Santa Cruz Biotechnology (Santa Cruz, CA, USA), and antibodies to cAMP-responsive element binding protein (CREB), phospho-Ser133-CREB, adenosine AMP activated protein kinase (AMPK)  $\alpha$ , phospho-Thr172-AMPK $\alpha$ , acetyl-CoA carboxylase (ACC), phospho-Ser79-ACC, phospho-Ser660-hormone sensitive lipase (HSL), phospho-Ser636/639-IRS, Akt, and phospho-Ser/Thr-cAMP-dependent protein kinase A (PKA) substrate were purchased from Cell Signaling Technology (Beverly, MA, USA). Antibody to sterol regulatory element binding protein c (SREBP1c) was obtained from BD Biosciences (San Jose, CA, USA). 2-Deoxy-D-[ $^3$ H]glucose was obtained from Amersham Biosciences (Piscataway, NJ, USA). Sinensetin, nobiletin, and tangeretin were purchased from Wako Pure Chemical Industries, Ltd. (Osaka, Japan). The HPLC-grade

solvents used for extraction and the mobile phase were obtained from Fisher Scientific Korea, Ltd. (Seoul, Republic of Korea). All other reagents were purchased from Sigma Chemical Co., unless otherwise noted.

#### 2.4.2. Preparation of immature *Citrus sunki* peel extract (CSE)

Immature *Citrus sunki* (Figure 2.1) peel was collected from Jeju Island, Republic of Korea. One kilogram of dried peel powder was extracted with 80% ethanol (10 L) twice at room temperature for 48 h. The combined CSE was concentrated on a rotary evaporator under reduced pressure, freeze-dried to a powder, and stored at -20°C until use. To determine the flavonoid content of CSE, high performance liquid chromatography (HPLC) analysis was performed using a Waters 2695 Alliance HPLC system (Waters Corp., Milford, MA, USA) consisting of two pumps, an auto-sampler, a column oven, and a PDA detector (model 2998 photodiode array detector; Waters Corp.). The flavonoid compounds were monitored at 320 nm using a Sunfire™ C18 Column (250 × 4.6 mm, ID; 5 μm; Waters Corp.). The column was operated at 40°C, with a sample injection volume of 10 μl and a flow rate of 1 mL/min. The mobile phase consisted of acetonitrile (MeCN) containing 0.5% acetic acid (A) and water containing 0.5% acetic acid (B). The gradient elution program was as follows: a 25 min gradient was started using 20% A, held for 10 min, linearly increased to 45% A over 12 min, held for 5 min, linearly increased to 75% A over 19 min, and held for 2 min, then finally returned to the initial conditions and held for 3 min. It was confirmed that CSE contained abundant PMFs such as tangeretin and nobiletin (Table 2.1).

Sinensetin were prepared as described previously (Ko et al., 2010). Briefly, dried *Citrus sunki* peel (500 g) was extracted in 5 L of water through incubation at 100°C for 1 h and then filtered through filter paper.

The hot-water extract (1 L) was then fractionated at room temperature with the organic solvents *n*-hexane and chloroform (CHCl<sub>3</sub>). The CHCl<sub>3</sub> fraction was then concentrated and filtered. The sinensetin content of CHCl<sub>3</sub> fraction was analyzed by high-performance liquid chromatography (HPLC) using a Waters 2695 Alliance system (Waters Corp., Milford, MA, USA) equipped with a Waters 2996 photodiode array detector. A fraction collector was used to prepare the sinensetin. The separation of sinensetin was performed using a SymmetryPrep C18 column (300 × 7.8 mm; ID 7 μm). A column oven maintained the column temperature at 40°C. The CHCl<sub>3</sub> fraction (30 μL, 100 mg/mL) was injected into the column and monitored by recording the UV spectra of the irradiated sample at wavelength of 320 nm. The mobile phase in the prep-HPLC solvent system consisted of MeOH (A) and water (B). The gradient mobile phase program consisted of a 45-min gradient started using 20% A, linear increase to 90% A over 36 min, linear decrease to 20% A over 2 min, and finally, 7 min at a flow rate of 1.8 mL/min. The sinensetin peak was fractionated through a fraction collector and concentrated in a rotary evaporator at 40°C. Sinensetin was dissolved in dimethyl sulfoxide (DMSO).



Figure 2.1. Picture of immature *Citrus sunki*. The *Citrus sunki* was collected in the Jeju island, Republic of Korea.

Table 2.1. Flavonoids content (mg/g) in CSE.

Group	CSE	RSD
Rutin	17.02	0.09
Naringin	N.D.	
Hesperidin	17.11	0.08
Quercetin	N.D.	
Naringenin	N.D.	
Hesperetin	N.D.	
Sinensetin	4.23	0.09
Nobiletin	38.83	0.89
Tangeretin	55.13	1.30

Their numerical value are the means calculated from three experiments. RSD, relative standard deviation (%). N.D., not detected.

### **2.4.3. Animals**

The animal study protocol was approved by the Institutional Animal Care and Use Committee of Jeju National University. After purchase, 30 male 4-week-old C57BL/6 mice (Nara Biotech Co., Ltd, Seoul, Republic of Korea) were adapted for 1 week to a specific temperature ( $22\pm 2^{\circ}\text{C}$ ), humidity ( $50\pm 5\%$ ), and lighting (light from 08:00 to 20:00). The animals were housed in plastic cages (2 mice/cage) and given free access to drinking water and food. After adaptation, the C57BL/6 mice (now 5 weeks old;  $22.6\pm 1.2$  g) were randomly divided into three groups of 10 mice each. One group (normal diet, ND) was fed a 10% kcal fat diet (D12450B; Research Diets, New Brunswick, NJ, USA; protein: 19.2%, carbohydrate: 67.3%, fat: 4.3%; and other; 3.85 kcal/g), and two groups (high-fat diet, HFD; HFD+CSE) were fed a 60% kcal fat diet (D12492; Research Diets; protein: 26.2%, carbohydrate: 26.3%, fat: 34.9%; and other; 5.24 kcal/g). CSE was dissolved in 0.1% carboxymethyl cellulose (CMC) and administered orally to the animals at a dosage of 150 mg/kg/day for 70 days. The oral administration volume was approximately 100  $\mu\text{l}$  per 10 g weight. Mice in the ND and the HFD groups were given 0.1% CMC.

### **2.4.4. Measurements of body weight, food intake, liver weight, epididymal adipose tissue weight, and perirenal adipose tissue weight**

Body weight and food intake were measured every 5 days for 70 days. At the end of the feeding period, mice were anesthetized with diethyl ether after an overnight fast. The liver, epididymal adipose tissue, and perirenal adipose tissue were weighed after rapid removal from dead mice.

### **2.4.5. Biochemical analysis**

After 70 days, the mice were killed by ether anesthesia overdose. Blood samples were drawn from the abdominal aorta into a vacuum tube and allowed to clot at room temperature for 30 min. Serum samples were then collected by centrifugation at  $1,000 \times g$  for 15 min. Total cholesterol (T-CHO), triglyceride (TG), glutamic pyruvic transaminase (GPT), glutamic oxaloacetic transaminase (GOT), and lactate dehydrogenase (LDH) concentrations in serum were assayed using a commercial kit (Asanpharm, Seoul, Republic of Korea) and an automatic blood analyzer (Kuadro; BPC Biosed, Rome, Italy).

#### **2.4.6. Histology**

After blood had been drained, the livers and epididymal adipose tissue were fixed in 10% neutral formalin solution for 48 h. The tissue was subsequently dehydrated in a graded ethanol series (75–100%) and embedded in paraffin wax. The embedded tissue was sectioned (8- $\mu\text{m}$ -thick sections), stained with hematoxylin and eosin (H&E), and examined by light microscopy (Olympus BX51; Olympus Optical, Tokyo, Japan), then photographed at final magnifications of 50 $\times$ , 100 $\times$ , or 200 $\times$ .

#### **2.4.7. Cell culture and differentiation**

3T3-L1 preadipocyte cells obtained from American Type Culture Collection (Rockville, MD, USA) were cultured in DMEM containing 1% PS and 10% BCS at 37°C under a 5% CO<sub>2</sub> atmosphere.

##### *2.4.7.1 Differentiation I*



To induce differentiation, 2-day post-confluent preadipocytes (designated day 0) were cultured in MDI differentiation medium I (DMEM containing 1% PS, 10% FBS, 0.5 mM IBMX, 1  $\mu$ M dexamethasone, 1  $\mu$ g/mL insulin) for 2 days. The cells were then cultured for a further 2 days in DMEM containing 1% PS, 10% FBS, and 1  $\mu$ g/mL insulin. Thereafter, the cells were maintained in post-differentiation medium (DMEM containing 1% PS and 10% FBS), which was replaced every 2 days.

#### *2.4.7.2 Differentiation II*

To induce differentiation, 2-day post-confluent preadipocytes (designated day 0) were cultured in MDI differentiation medium II (DMEM containing 1% PS, 10% FBS, 0.5 mM IBMX, 1  $\mu$ M dexamethasone, and 5  $\mu$ g/mL insulin) for 2 days. The cells were then cultured for another 2 days in DMEM containing 1% PS, 10% FBS, and 5  $\mu$ g/mL insulin. Thereafter, the cells were maintained in post-differentiation medium (DMEM containing 1% PS and 10% FBS), which was replaced every 2 days.

#### **2.4.8. Cell viability and cytotoxicity**

The effect of samples on cell viability and cytotoxicity were determined by the MTT and LDH assay, respectively. ① Preadipocytes were seeded at a density of  $1 \times 10^4$  cell/well into 96-well plate, then treated samples after 24 h, and then incubated for 72 h. ② Mature 3T3-L1 adipocytes were cultured in DMEM containing 1% PS, 10% FBS, and samples for 24 h. MTT (400  $\mu$ g/mL) was added to each well, and the plate incubated at 37°C for 4 h. The MTT (400  $\mu$ g/mL) was added to each well, and the plates incubated for 4 h at 37°C. The liquid in the plate was removed, and dimethyl sulfoxide (DMSO) was added to dissolve the MTT-formazan complex. Optical density was

measured at 540 nm. The effect of samples on cell viability was evaluated as the relative absorbance compared with that of control cultures. The cytotoxic effect of samples was measured by LDH Cytotoxicity Detection Kit. The LDH activities in medium and cell lysate were measured for evaluation of cytotoxicity according to the manufacturer's protocol (LDH released into the medium/maximal LDH release  $\times$  100).

#### **2.4.9. Oil Red O staining and cell quantification**

After the induction of differentiation, cells were stained with Oil Red O [6 parts saturated Oil Red O dye (0.6%) in isopropanol plus 4 parts water]. Briefly, the cells were washed twice with PBS, fixed through incubation with 3.7% formaldehyde (Sigma Chemical Co.) in PBS for 1 h, washed an additional three times with water and stained with Oil Red O for 1 h. Excess stain was removed by washing with water, and the stained cells were dried. The stained lipid droplets were dissolved in isopropanol containing 4% Nonidet P-40 and then quantified by measuring the absorbance at 520 nm. Lipid content for each experimental group is expressed relative to that of MDI differentiated cells (designated as 100%).

#### **2.4.10. Western blot analysis**

Adipose tissue was homogenized in ice-cold buffer containing lysis buffer [1 $\times$  RIPA (Upstate Biotechnology, Temecula, CA, USA), 1 mM PMSF, 1 mM Na<sub>3</sub>VO<sub>4</sub>, 1 mM NaF, and 1  $\mu$ g/mL each of aprotinin, pepstatin, and leupeptin]. 3T3-L1 cells were washed with ice-cold PBS, collected, and centrifuged. The cell pellets were resuspended in lysis buffer and incubated on ice for 1 h. The adipose tissue and 3T3-L1 cells debris were then removed by centrifugation and protein concentrations in the lysates were determined using

Bio-Rad Protein Assay Reagent (Bio-Rad Laboratories, Hercules, CA, USA). The adipose tissue and 3T3-L1 cells lysates were then subjected to electrophoresis on 10-15% polyacrylamide gels containing sodium dodecyl sulfate (SDS) and transferred to polyvinylidene difluoride membranes. The membranes were blocked with a solution of 0.1% Tween-20 in Tris-buffered saline containing 5% bovine serum albumin (BSA) at room temperature for 1 h. After incubation overnight at 4°C with primary antibody, the membranes were incubated with horseradish peroxidase-conjugated secondary antibody at room temperature for 1 h. Immunodetection was carried out using ECL Western blotting detection reagent (Amersham Biosciences, Piscataway, NJ, USA).

#### **2.4.11. RNA preparation and quantitative real-time RT-PCR analysis**

Total RNA was extracted from the adipose tissue and 3T3-L1 adipocytes using the TRIzol reagent according to the manufacturer's instructions and then treated with DNase (Wako Pure Chemical Industries, Ltd., Osaka, Japan). cDNA was synthesized from 1 µg of total RNA in a 20 µl reaction using a Maxime RT PreMix Kit (iNtRON Biotechnology, Seongnam, Kyunggi, Korea). The following primers were used in real-time RT-PCR analysis: adiponectin, 5'-GAC CTG GCC ACT TTC TCC TC-3' and 5'-GTC ATC TTC GGC ATG ACT GG-3'; carnitine palmitoyltransferase-1a (CPT-1a), 5'-ACC CTG AGG CAT CTA TTG ACA-3' and 5'-TGA CAT ACT CCC ACA GAT GGC-3'; β-actin, 5'-AGG CTG TGC TGT CCC TGT AT-3' and 5'-ACC CAA GAA GGA AGG CTG GA-3'. Samples were prepared using iQ SYBR Green Supermix (Bio-Rad Laboratories) according to the manufacturer's instructions. Adiponectin, CPT-1a, and β-actin mRNA expressions were measured by quantitative real-time RT-PCR using the Chromo4 Real-Time PCR System (Bio-Rad Laboratories). The formation of a single product was

verified by melting curve analysis. The expression levels of adiponectin and CPT-1a were normalized to that of  $\beta$ -actin. Data were analyzed using Opticon Monitor software (ver. 3.1; Bio-Rad Laboratories).

#### **2.4.12. Lipolysis assay**

To obtain fully differentiated 3T3-L1 cells, confluent cells were induced in MDI differentiation medium II (DMEM containing 1% PS, 10% FBS, 0.5 mM IBMX, 1  $\mu$ M dexamethasone, 5  $\mu$ g/mL insulin) for 2 days. The cells were then cultured for a further 2 days in DMEM containing 1% PS, 10% FBS, and 5  $\mu$ g/mL insulin. Then, they were maintained in post-differentiation medium, which was replaced every 2 days. Fully differentiated 3T3-L1 cells were next incubated with serum-free DMEM for 4 h. The cells were then treated with post-differentiation medium containing various concentrations of the fucoxanthin. Culture supernatants were assayed for glycerol levels at 24 or 48 h post-treatment using a free glycerol reagent kit (Sigma-Aldrich).

#### **2.4.13. Glucose uptake activity assay**

Glucose uptake activity was analyzed by measuring the uptake of radiolabeled glucose. Briefly, differentiated 3T3-L1 adipocytes grown in 12-well plates were washed twice with serum-free DMEM and incubated for 3 h at 37°C with 1 mL of DMEM containing 0.1% bovine serum albumin (BSA). The cells were then washed three times with Krebs-Ringer-Heps (KRH) buffer [20 mM HEPES (pH 7.4), 136 mM NaCl, 4.7 mM KCl, 1.25 mM MgSO<sub>4</sub>, 1.25 mM CaCl<sub>2</sub>, and 2 mg/mL BSA] and incubated at 37°C for 30 min with 0.9 mL of KRH buffer. They were next incubated KRH buffer containing insulin with or without tricin for 6 h at 37°C. Glucose uptake was initiated by the addition of 0.1 mL of KRH buffer containing

2-deoxy-D-[<sup>3</sup>H]glucose (37 MBq/L Amersham Bioscience) and glucose (1 mM). After 20 min, glucose uptake was terminated by washing the cells three times with cold PBS. The cells were lysed through incubation for 20 min at 37°C with 0.7 mL of 1% Triton X-100. Levels of radioactivity in the cell lysates were determined using a Tri-Carb 2700TR scintillation counter (Packard, Meriden, CT, USA).

#### **2.4.14. Measurement of cellular cAMP levels**

Fully differentiated 3T3-L1 cells were incubated with serum-free DMEM containing 0.2% BSA for 16 h. The cell were then treated with serum-free DMEM containing various concentration of the sinensetin for 30 min. The effect of sinensetin was measured using a cAMP Complete ELISA Kit (Enzo Life Sciences, Farmingdale, NY, USA). The cAMP levels were measured, according to the manufacturer's protocol.

#### **2.4.15. Statistical Analysis**

Values are expressed as means ± S.D. or S.E.. A one-way analysis of variance (ANOVA) was used for multiple comparisons. Treatment effects were analyzed using the paired t-test or Duncan's multiple range test using the SPSS software package (ver. 12.0; SPSS Inc., Chicago, IL, USA). Differences were considered statistically significant at  $p < 0.05$ .

## 2.5. RESULTS

### 2.5.1. Anti-obesity effect of *Citrus sunki* ethanolic extract (CSE)

#### 2.5.1.1. CSE improved high-fat-diet (HFD)-induced obesity

After 70 days on the HFD, the mean body weight and body weight gain in the HFD group were 35.2% and 176.1% higher, respectively, than those in the ND group, indicating that the HFD induced obesity (Table 2.2). CSE administration (150 mg/kg/day) significantly decreased both body weight and body weight gain in the HFD+CSE group relative to those in the non-CSE-treated HFD group (16.9% and 40.7% lower, respectively). Histological analysis of epididymal adipose tissue confirmed that adipocyte size was markedly elevated in the HFD group compared to the ND group after 70 days, whereas adipocyte size markedly decreased in the HFD+CSE group compared to the HFD group (Figure 2.2). The weights of epididymal and perirenal adipose tissue were also significantly higher in the HFD group (134.2% and 146.9%, respectively) than in the ND group. Epididymal and perirenal adipose tissue weights were significantly lower in the HFD+CSE group (35.6% and 35.9%, respectively) than in the HFD group (Figure. 2.3A, B).

Food intake did not significantly differ among the HFD groups (Table 2.2). However, serum T-CHO and TG levels were significantly lower in the HFD+CSE group (17.6% and 39.3%, respectively) than the HFD group (Table 2.3).

Table 2.2. Effects of CSE supplementation on body weight gain, food intake, and liver weight in high-fat-diet (HFD)-induced obese experimental group after 70 days.

Group	ND	HFD	HFD+CSE
Initial body weight (g)	22.61±0.53	22.60±0.42	22.50±0.31
Final body weight (g)	28.26±0.99 <sup>a</sup>	38.20±1.12 <sup>c</sup>	31.75±1.38 <sup>b</sup>
Body weight gain (g)	5.65±0.60 <sup>a</sup>	15.60±0.78 <sup>c</sup>	9.25±1.20 <sup>b</sup>
Intake of PBEE (mg/kg of body weight/day)	-	-	150
Food intake (g/cage/5 day)	26.57±0.40 <sup>a</sup>	21.19±0.28 <sup>b</sup>	20.81±0.23 <sup>b</sup>
Liver weight (g)	1.07±0.06 <sup>a</sup>	1.30±0.08 <sup>b</sup>	0.98±0.04 <sup>a</sup>

Values are expressed as means ± S.E. ( $n=10$ ). Values with different letters in each assay are significantly different from each other between the ND, HFD, HFD+CSE groups by Duncan's multiple range test ( $p<0.05$ ).

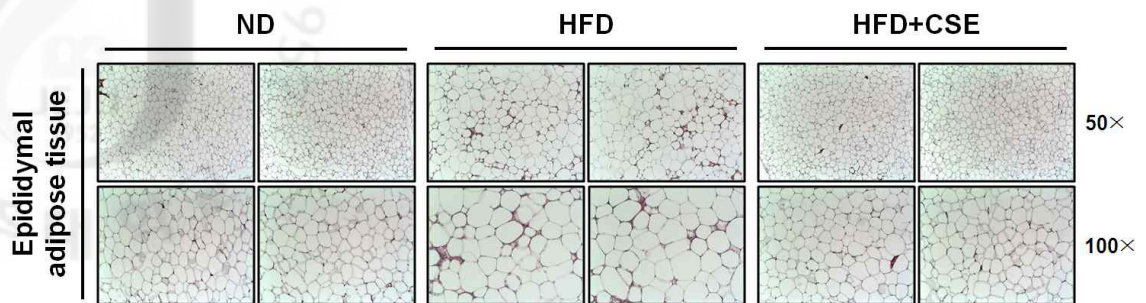


Figure 2.2. Effect of CSE on fatty droplets in the epididymal adipose tissue of mice fed a normal diet (ND), high-fat-diet (HFD), or HFD+CSE. Hematoxylin and eosin (H&E)-stained photomicrographs of epididymal adipose sections are shown at 50 $\times$  and 100 $\times$ .



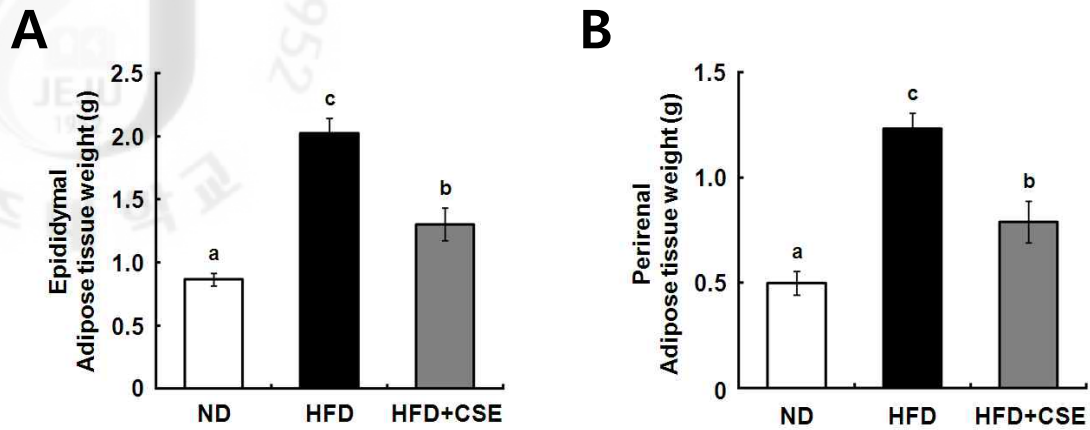


Figure 2.3. Effect of CSE on adipose tissue weight of mice fed a normal diet (ND), high-fat-diet (HFD), or HFD+CSE. (A) Epididymal and (B) perirenal adipose tissue weight were evaluated. Results are shown as means  $\pm$  S.E. ( $n=10$ ). Values with different letters in each assay are significantly different from each other between the ND, HFD, HFD+CSE groups by Duncan's multiple range test ( $p<0.05$ ).

Table 2.3. Effects of CSE supplementation on serum levels of T-CHO and TG in high-fat-diet (HFD)-induced obese experimental group after 70 days.

Group	ND	HFD	HFD+CSE
T-CHO (mg/dL)	119.71±4.09 <sup>a</sup>	179.14±3.90 <sup>c</sup>	147.57±5.53 <sup>b</sup>
TG (mg/dL)	92.29±4.86 <sup>a</sup>	138.43±9.15 <sup>b</sup>	84.00±2.66 <sup>a</sup>

Values are expressed as means ± S.E. ( $n=10$ ). Values with different letters in each assay are significantly different from each other between the ND, HFD, HFD+CSE groups by Duncan's multiple range test ( $p<0.05$ ).

*2.5.1.2. CSE reduced damage of liver in high-fat-diet (HFD)-induced obese mice*

We next examined the effect of CSE on serum GPT, GOT, and LDH levels in HFD mice. CSE administration significantly reduced the levels of these markers of cell damage. The levels of serum GPT and GOT were significantly lower in the HFD+CSE group (56.2% and 19.2%, respectively) than in the HFD group (Figure 2.4A, B). Serum LDH level was also significantly lower in the HFD+CSE group (43.6%) than in the HFD group (Figure 2.4C). In addition, liver weight was significantly lower in the HFD+CSE group than in the HFD group (Table 2.4).

Figure 2.5 shows photomicrographs of H&E-stained liver tissue. H&E analysis of the liver revealed fatty accumulation in the HFD group compared to the ND group; however, no fatty accumulation was observed in the livers of the HFD+CSE group.

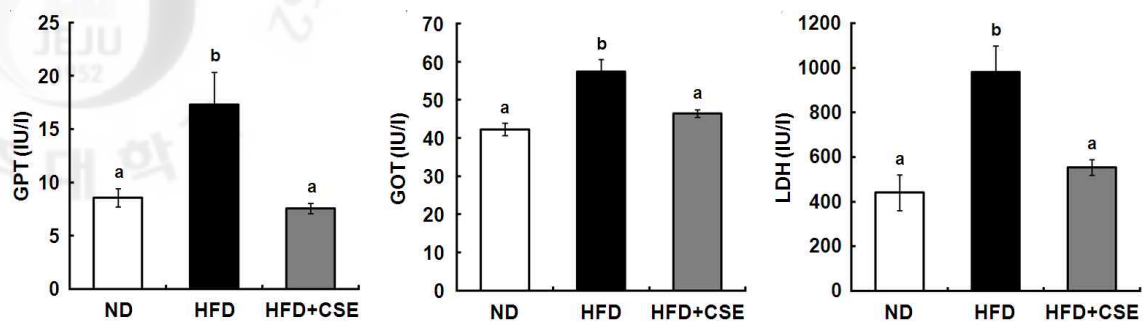


Figure 2.4. Effect of CSE on serum levels of GPT, GOT, and LDH in mice fed a normal diet (ND), high-fat-diet (HFD), or HFD+CSE. The serum levels of (A) glutamic pyruvic transaminase (GPT), (B) glutamic oxaloacetic transaminase (GOT), and (C) lactate dehydrogenase (LDH) were evaluated. Results are shown as means  $\pm$  S.E. ( $n=10$ ). Values with different letters in each assay are significantly different from each other between the ND, HFD, HFD+CSE groups by Duncan's multiple range test ( $p<0.05$ ).

Table 2.4. Effects of CSE supplementation on liver weight in high-fat-diet (HFD)-induced obese experimental group after 70 days.

Group	ND	HFD	HFD+CSE
Liver weight (g)	1.07±0.06 <sup>a</sup>	1.30±0.08 <sup>b</sup>	0.98±0.04 <sup>a</sup>

Values are expressed as means ± S.E. (*n*=10). Values with different letters in each assay are significantly different from each other between the ND, HFD, HFD+CSE groups by Duncan's multiple range test (*p*<0.05).

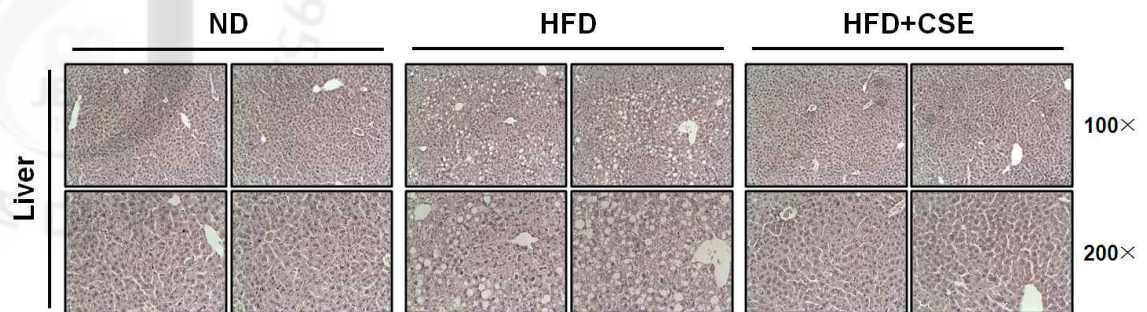


Figure 2.5. Effect of CSE on fatty droplets in the livers of mice fed a normal diet (ND), high-fat-diet (HFD), or HFD+CSE. Hematoxylin and eosin (H&E)-stained photomicrographs of liver tissue sections are shown at 100 $\times$  and 200 $\times$ .

*2.5.1.3. CSE restored AMPK phosphorylation and adiponectin expression in epididymal adipose tissue*

Next, we investigated the expression of proteins responsible for fatty acid  $\beta$ -oxidation in epididymal adipose tissue. As shown in Figure 2.6, expression of the phosphorylated forms of AMPK and its immediate substrate (phosphorylated forms of ACC) were higher in the HFD+CSE group than in the HFD group after 70 days. After 70 days on the HFD, expression of the adiponectin gene was lower in the HFD group than in the ND group (Figure 2.7) but was restored in the HFD+CSE group.

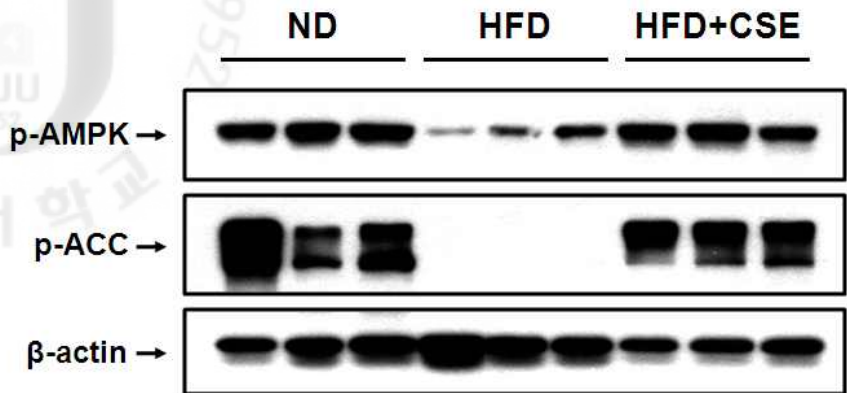


Figure 2.6. Effect of CSE on protein expression in epididymal adipose tissue of mice fed a normal diet (ND), high-fat-diet (HFD), or HFD+CSE. p-AMPK and p-ACC protein expression levels in epididymal tissue were determined by Western blot analysis. The data shown are representative of three independent experiments



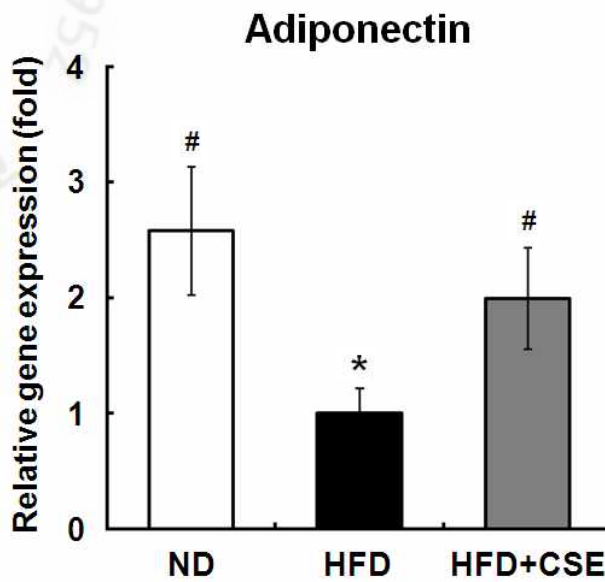


Figure 2.7. Effect of CSE on adiponectin mRNA expression in epididymal adipose tissue of mice fed a normal diet (ND), high-fat-diet (HFD), or HFD+CSE. Real-time RT-PCR analysis of adiponectin mRNA expression in epididymal tissue. All value are presented as means  $\pm$  S.D. ( $n=10$ ;  $*p<0.05$  compared with ND and  $\#p<0.05$  compared with HFD). The data shown are representative of three independent experiments.

#### 2.5.1.4. CSE activated the AMPK pathway in mature 3T3-L1 adipocytes

The effect of CSE on the viability and cytotoxicity of mature 3T3-L1 adipocytes was first evaluated by MTT and LDH assays. A CSE concentration of 250  $\mu\text{g}/\text{mL}$  did not affect viability ( $111.22 \pm 1.51\%$  compared to the control) or cytotoxicity ( $2.97 \pm 2.55\%$  compared to the control) of the mature 3T3-L1 adipocytes (Figure 2.8). To characterize the effects of CSE on the phosphorylation of LKB1, AMPK, and ACC *in vitro*, we treated mature 3T3-L1 adipocytes with various concentrations of CSE. Consistent with the *in vivo* data, CSE markedly induced phosphorylation of LKB1, AMPK, and ACC in a dose-dependent manner (Figure 2.9). After mature 3T3-L1 adipocytes were cultured in post-differentiation medium and then exposed to 200  $\mu\text{g}/\text{mL}$  CSE for 2, 6, 12, and 24 h, CSE markedly induced phosphorylation of LKB1, AMPK, and ACC beginning 2 h after treatment (Figure 2.10). Thus, we investigated the effects downstream of AMPK activation by treating mature 3T3-L1 adipocytes with CSE. CSE increased dose-dependently the levels of CPT-1a mRNA, which is involved in fatty acid oxidation (Figure 2.11).

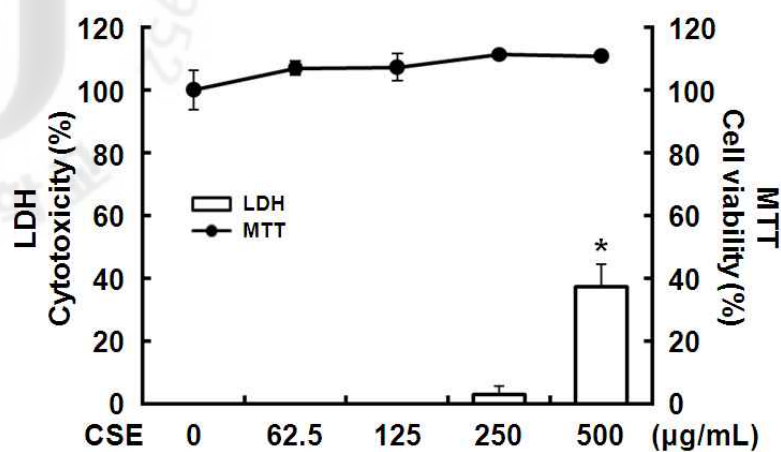


Figure 2.8. Effect of CSE on viability and cytotoxicity of mature 3T3-L1 adipocytes. 3T3-L1 preadipocytes were induced to differentiate as described in the Materials and Methods section. On day 8, viability and cytotoxicity were assessed in MTT and LDH assays for 48 h. All values are presented as means  $\pm$  S.D. ( $n=3$ ;  $*p<0.05$  compared to no CSE). The data shown are representative of three independent experiments.

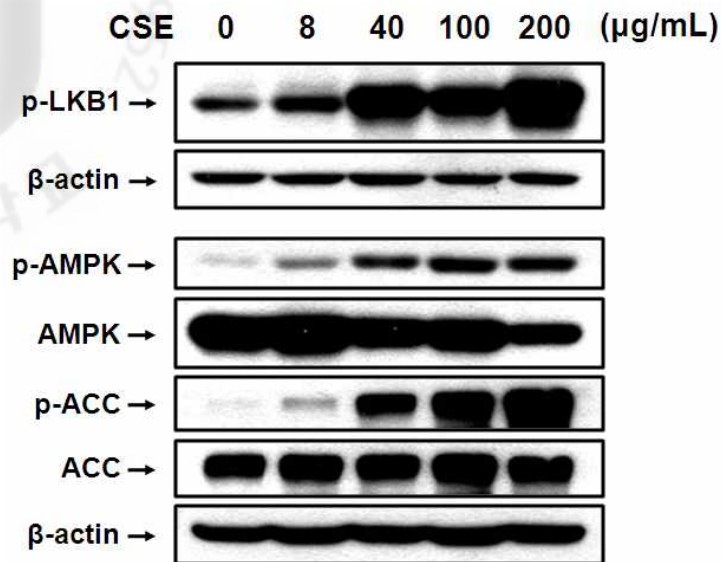
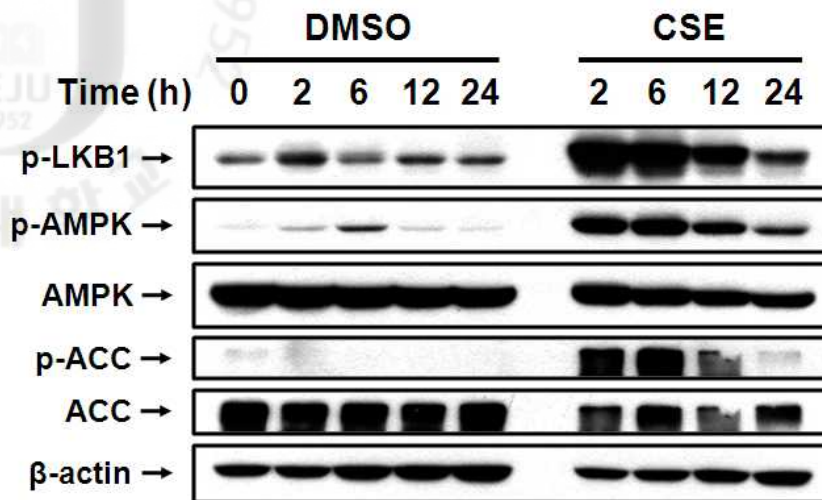


Figure 2.9. Effect of various CSE concentration on phosphorylation of LKB1, AMPK, and ACC in mature 3T3-L1 adipocytes. 3T3-L1 preadipocytes were induced to differentiate as described in the Materials and Methods section. On day 8, mature 3T3-L1 adipocytes were incubated for 16 h with serum-free DMEM containing 0.2% BSA. The cells were then treated with post-differentiation medium containing various CSE concentrations for 24 h. Western blot analysis of the effect of CSE dose on p-LKB1, p-AMPK, AMPK, p-ACC, and ACC expression. The data shown are representative of three independent experiments.



**Figure 2.10.** Effect of CSE on phosphorylation of LKB1, AMPK, and ACC at several times in mature 3T3-L1 adipocytes. 3T3-L1 preadipocytes were induced to differentiate as described in the Materials and Methods section. On day 8, mature 3T3-L1 adipocytes were incubated for 16 h with serum-free DMEM containing 0.2% BSA. The cells were then treated with post-differentiation medium containing CSE (200  $\mu\text{g}/\text{mL}$ ) at the indicated times. Western blot analysis of the time course of p-LKB1, p-AMPK, AMPK, p-ACC, and ACC expression. The data shown are representative of three independent experiments.

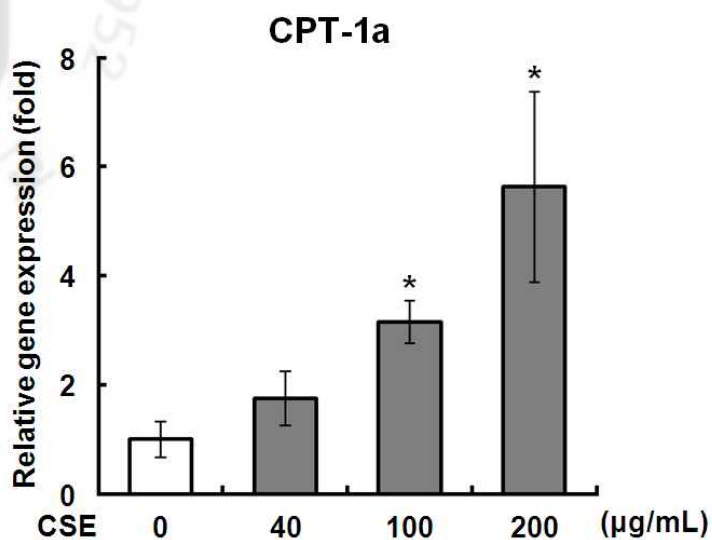
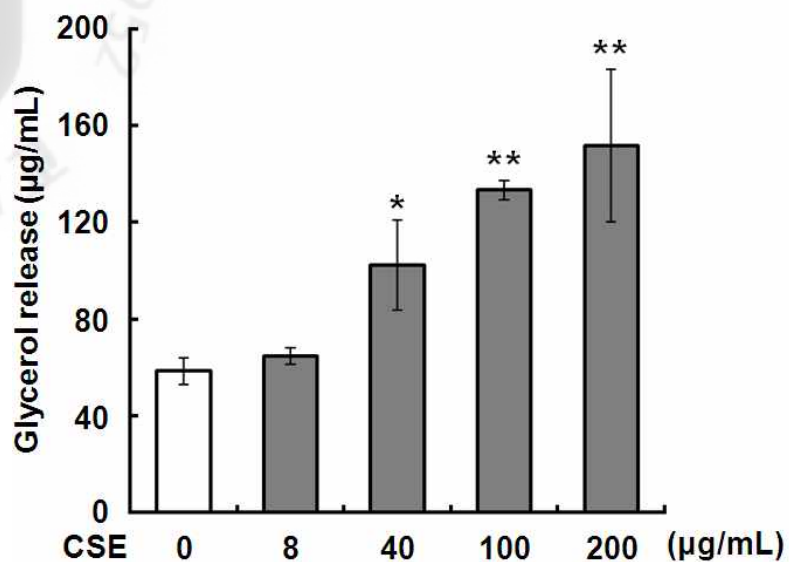


Figure 2.11. Effect of various CSE concentration on gene expression of CPT-1a in mature 3T3-L1 adipocytes. 3T3-L1 preadipocytes were induced to differentiate as described in the Materials and Methods section. On day 8, mature 3T3-L1 adipocytes were incubated for 16 h with serum-free DMEM containing 0.2% BSA. The cells were then treated with post-differentiation medium containing various CSE concentrations for 24 h. Real-time RT-PCR of the effect of CSE on CPT-1a gene expression. All values are presented as means  $\pm$  S.D. ( $n=3$ ;  $*p<0.05$  compared to no CSE). The data shown are representative of three independent experiments.

#### *2.5.1.5. CSE activated the PKA pathway in mature 3T3-L1 adipocytes*

We next examined whether CSE stimulated lipolysis in mature 3T3-L1 adipocytes by measuring glycerol levels in culture supernatants. CSE significantly increased lipolysis at 24 h in a dose-dependent manner (Figure 12). We next examined whether the increase in lipolysis caused by CSE was associated with a signaling pathway by evaluating the phosphorylated forms of PKA and its immediate substrate (HSL) in CSE-treated mature 3T3-L1 adipocytes. CSE treatment was found to stimulate the phosphorylation of both PKA substrate and HSL (Figure 13).



**Figure 2.12.** Effect of CSE on lipolysis in mature 3T3-L1 adipocytes. 3T3-L1 preadipocytes were induced to differentiate as described in the Materials and Methods section. On day 8, mature 3T3-L1 adipocytes were incubated for 16 h with serum-free DMEM containing 0.2% BSA. The cells were then treated with post-differentiation medium containing various concentrations of CSE for 24 h. Glycerol release into the medium was measured. All values are presented as means±SD ( $n=3$ ;  $*p<0.05$  and  $**p<0.01$  compared to no CSE). The data shown are representative of three independent experiments.



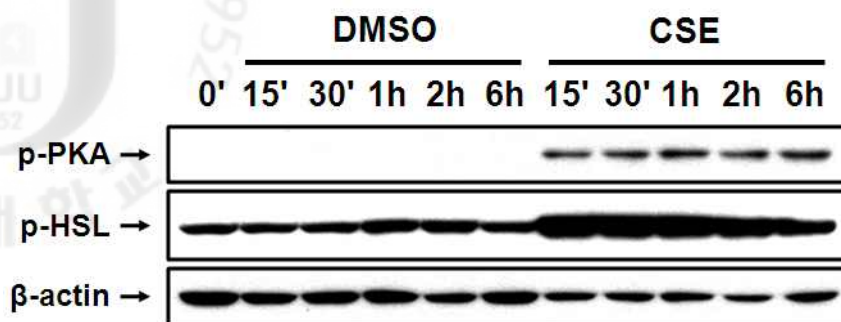
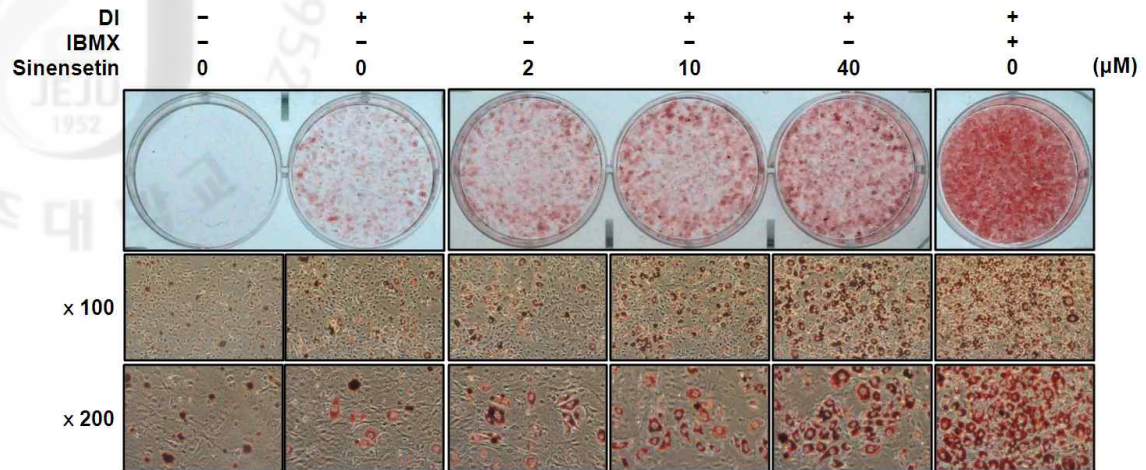
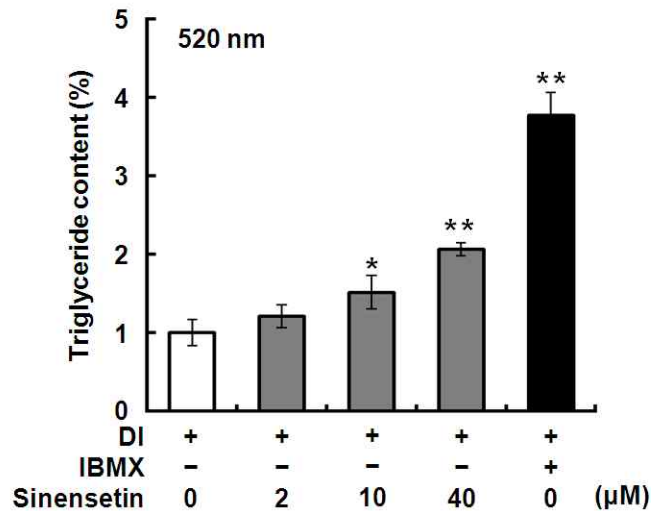


Figure 2.13. Effect of CSE on phosphorylation of PKA and HSL in mature 3T3-L1 adipocytes. 3T3-L1 preadipocytes were induced to differentiate as described in the Materials and Methods section. On day 8, mature 3T3-L1 adipocytes were incubated for 16 h with serum-free DMEM containing 0.2% BSA. The cells were then treated with post-differentiation medium containing CSE (200  $\mu\text{g}/\text{mL}$ ) at the indicated times. Western blot analysis of the time course of p-PKA and p-HSL expression. The data shown are representative of three independent experiments.

## 2.5.2. Anti-obesity effect of Sinensetin derived from CSE

### 2.5.2.1. *Sinensetin enhances adipogenesis in 3T3-L1 preadipocytes in the absence of IBMX*

First of all, the effect of sinensetin on cytotoxicity of 3T3-L1 cells was evaluated by the LDH assay. At a concentration of 50  $\mu\text{M}$ , sinensetin did not cause in 3T3-L1 cells ( $-0.50 \pm 1.31\%$  compared to control). Next, the adipogenic potential of sinensetin was assessed by inducing the differentiation of 3T3-L1 preadipocytes in incomplete differentiation medium containing dexamethasone and insulin, but with sinensetin in place of IBMX. On day 8, the adipocytes were stained using Oil Red O. Oil Red O staining demonstrated that treatment with sinensetin at concentrations of 2, 10, and 40  $\mu\text{M}$  enhanced 3T3-L1 adipocyte differentiation in a dose-dependent manner (Figure 2.14A) and increased triglyceride content (Figure 2.14B), though the effect of 40  $\mu\text{M}$  sinensetin was not strong compared with positive control cells that had been treated with 0.5 mM IBMX. To determine whether sinensetin enhances adipocyte differentiation by positively regulating the expression of key transcriptional regulators, we examined the expression levels of PPAR $\gamma$ 1, 2, and C/EBP $\alpha$  during adipocyte differentiation in the presence and absence of sinensetin. Expression levels of two factors were induced in sinensetin-treated cells, as was the expression level of aP2 (Figure 2.15). Sinensetin treatment also significantly increased the expression of the PPAR $\gamma$  target gene adiponectin (Figure 2.16).

**A****B**

**Figure 2.14. Effect of sinensetin on the lipid accumulation in 3T3-L1 cells.** Cells were cultured in DI differentiation medium (excluding IBMX) with various concentration of sinensetin (IBMX: 0.5 mM). (A) Differentiated adipocytes were stained with Oil Red O on day 8 (after 2 days of sinensetin treatment). (B) Lipid accumulation was assessed by the quantification of OD<sub>520</sub> as described in the Materials and methods. Results are shown as means ± S.D. ( $n=3$ ; \* $p<0.05$  and \*\* $p<0.001$  compared with no sinensetin). The data shown are representative of three independent experiments.

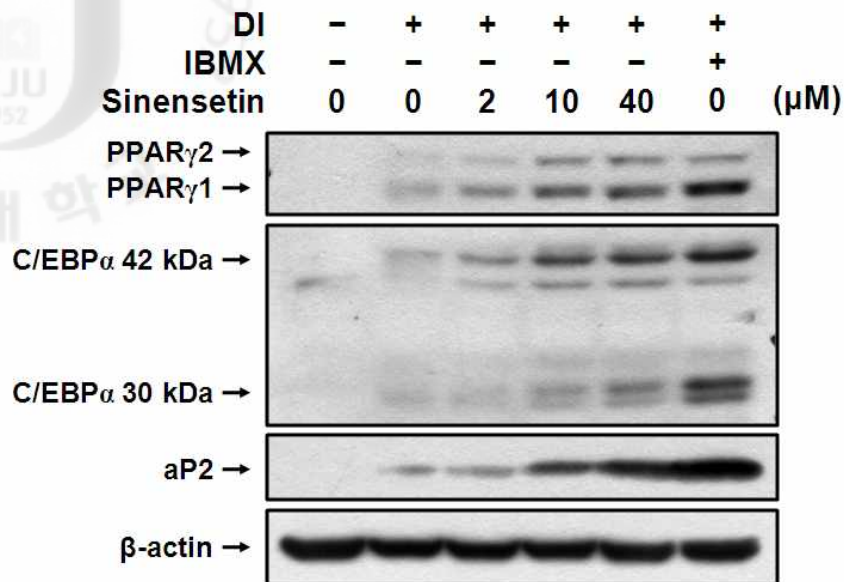


**Figure 2.15. Effect of sinensetin on the differentiation of adipocytes in 3T3-L1 preadipocytes.** Western blot analysis of PPAR $\gamma$ , C/EBP $\alpha$ , and aP2 expression. Proteins were prepared from 3T3-L1 cells on day 6. Cells were cultured in DI differentiation medium (excluding IBMX) with various concentration of sinensetin (IBMX: 0.5 mM). The data shown are representative of three independent experiments.

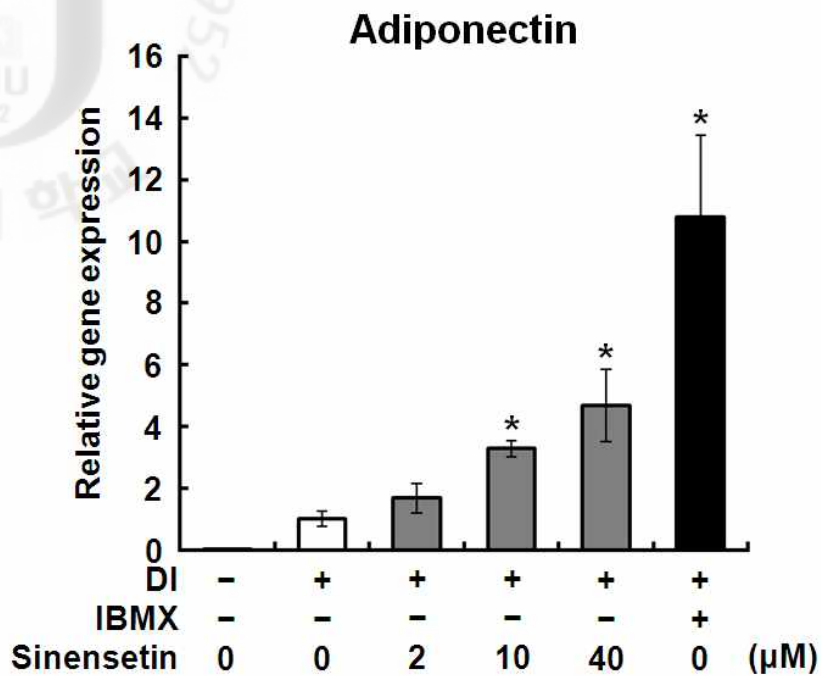
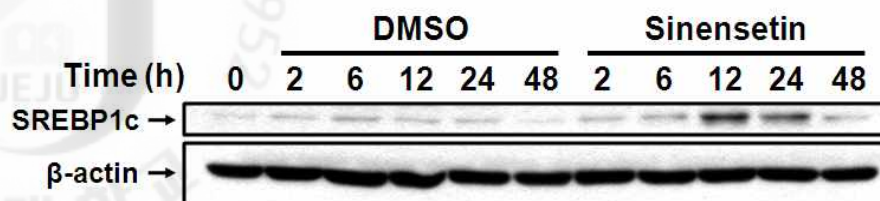


Figure 2.16. Effect of sinensetin on the gene expression of adiponectin in 3T3-L1 preadipocytes. Real-time PCR analysis of adiponectin gene expression. Total RNA was prepared from 3T3-L1 cells on day 4. Cells were cultured in DI differentiation medium (excluding IBMX) with various concentration of sinensetin (IBMX: 0.5 mM). All values are presented as means  $\pm$  S.D. ( $n=3$ ;  $*p<0.05$  compared to no sinensetin). The data shown are representative of three independent experiments.

### *2.5.2.2. Sinensetin activates 3T3-L1 adipocyte differentiation signal at an early stage*

To determine the effect of sinensetin on the early stages after adipogenic induction, its effects on the expression of early adipogenic transcription factors were analyzed by Western blotting. Sinensetin markedly increased protein expression of SREBP1c (Figure 2.17) and also increased the expression of C/EBP $\beta$ , which is responsible for the expression of PPAR $\gamma$  (Figure 2.18). We next examined the effect of sinensetin on the phosphorylation of CREB and ERK in 3T3-L1 preadipocytes. As shown in Figure 2.19, cells treated with sinensetin showed increased phosphorylation of CREB and ERK compared with control cells treated with DMSO. In sinensetin-treated early differentiating 3T3-L1 preadipocytes, these proteins were more strongly activated and remained active until 0.25 h. We next examined whether the increase in phosphorylation of CREB caused by sinensetin was associated with a signaling pathway by evaluating the phosphorylated forms of PKA in sinensetin-treated 3T3-L1 cells. Sinensetin treatment was found to stimulate the phosphorylation of PKA substrate (Figure 2.20). Moreover, we next examined whether the increase in phosphorylation of PKA caused by sinensetin was associated with a signaling pathway by evaluating the cAMP levels in sinensetin-treated 3T3-L1 preadipocytes. Sinensetin treatment at 2, 10, and 40  $\mu$ M was significantly found to increase the cAMP levels at 30 min in a dose-dependent manner (Figure 2.21).



**Figure 2.17. Effect of sinensetin on expression of SREBP1c in differentiating 3T3-L1 cells.** Western blot analysis of SREBP1c expression in differentiating 3T3-L1 cells. Cells were cultured in DMEM containing 10% FBS in the presence or absence of sinensetin (40  $\mu$ M) at the indicated times. Proteins were harvested at the indicated times. The data shown are representative of three independent experiments.

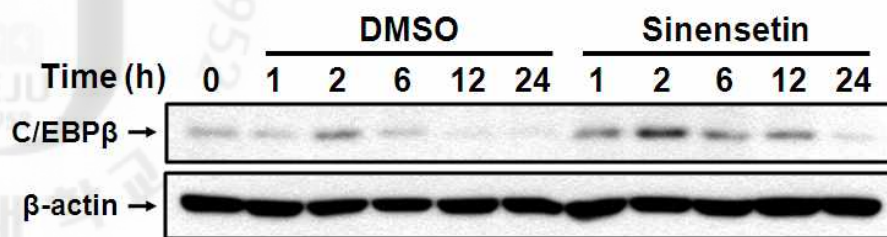


**Figure 2.18. Effect of sinensetin on expression of C/EBPβ in differentiating 3T3-L1 cells.** Western blot analysis of C/EBPβ expression in differentiating 3T3-L1 cells. Cells were cultured in DMEM containing 10% FBS in the presence or absence of sinensetin (40 μM) at the indicated times. Proteins were harvested at the indicated times. The data shown are representative of three independent experiments.



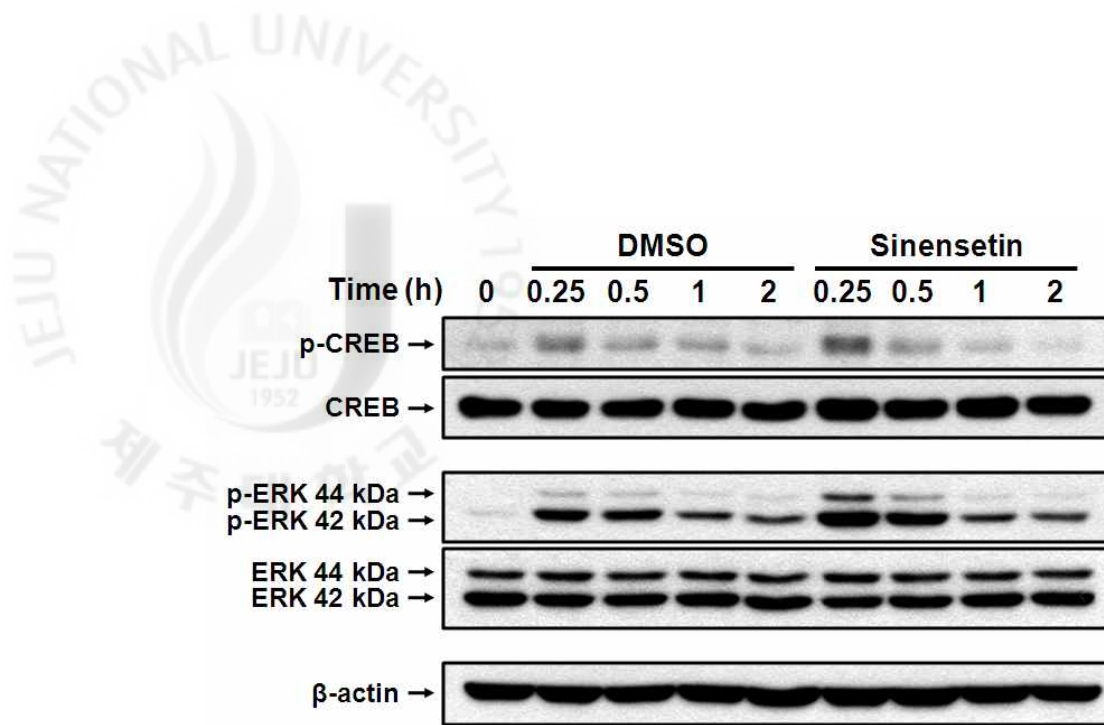


**Figure 2.19. Effect of sinensetin on upstream signaling of C/EBP $\beta$  in differentiating 3T3-L1 cells.** Western blot analysis of CREB and ERK activation in differentiating 3T3-L1 cells. Cells were cultured in DMEM containing 10% FBS in the presence or absence of sinensetin (40  $\mu$ M) at the indicated times. Proteins were harvested at the indicated times. The data shown are representative of three independent experiments.

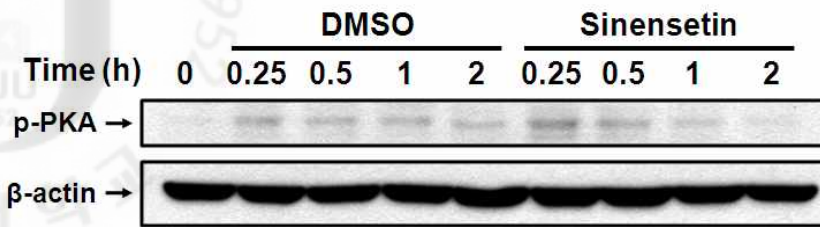
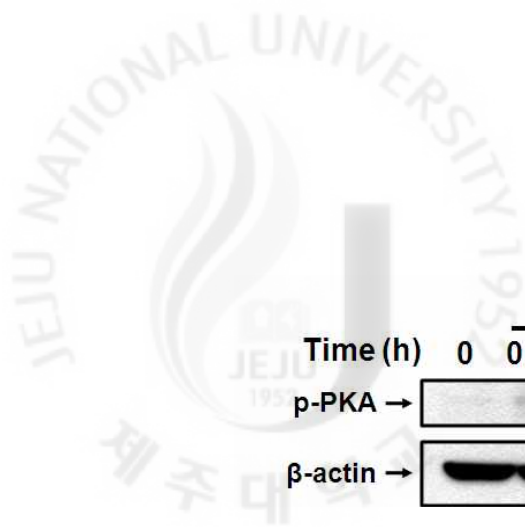
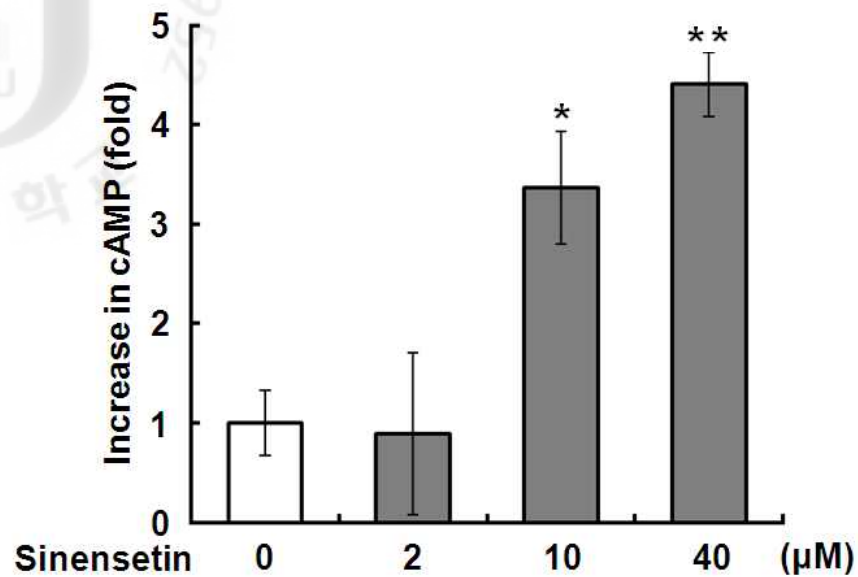


Figure 2.20. Effect of sinensetin on phosphorylation of PKA in differentiating 3T3-L1 cells. Western blot analysis of PKA acitivation in differentiating 3T3-L1 cells. Cells were cultured in DMEM containing 10% FBS in the presence or absence of sinensetin (40  $\mu$ M) at the indicated times. Proteins were harvested at the indicated times. The data shown are representative of three independent experiments.



**Figure 2.21. Effect of sinensetin on production of intracellular cAMP in differentiating 3T3-L1 cells.** Measurement of cellular cAMP levels in differentiating 3T3-L1. Cells were cultured in serum-free DMEM with various concentration of sinensetin. Cell lysates were prepared 30 min after treatment of sinensetin in 3T3-L1 preadipocyte. All values are presented as means  $\pm$  S.D. ( $n=3$ ;  $*p<0.05$  and  $**p<0.01$  compared to no sinensetin). The data shown are representative of three independent experiments.

### *2.5.2.3. Sinensetin stimulates lipolysis in mature 3T3-L1 adipocyte*

To investigate the effects of sinensetin on lipolysis in mature 3T3-L1 adipocytes, glycerol levels in culture supernatants were measured. Sinensetin significantly increased lipolysis at 24 h and 48 h (Figure 2.22). Also, we next examined whether the increase in phosphorylation of PKA caused by sinensetin was associated with a signaling pathway by evaluating the cAMP levels in sinensetin-treated mature 3T3-L1 adipocytes. Sinensetin treatment at 2, 10, and 40  $\mu\text{M}$  was significantly found to increase the cAMP levels at 30 min in a dose-dependent manner (Figure 2.23). We next examined whether the decrease in lipolysis caused by sinensetin was associated with a signaling pathway by evaluating the phosphorylated forms of PKA and its immediate substrate (HSL) in sinensetin-treated mature 3T3-L1 adipocytes. Sinensetin treatment was found to stimulate the phosphorylation of both PKA (Figure 2.24A) and HSL (Figure 2.24B).

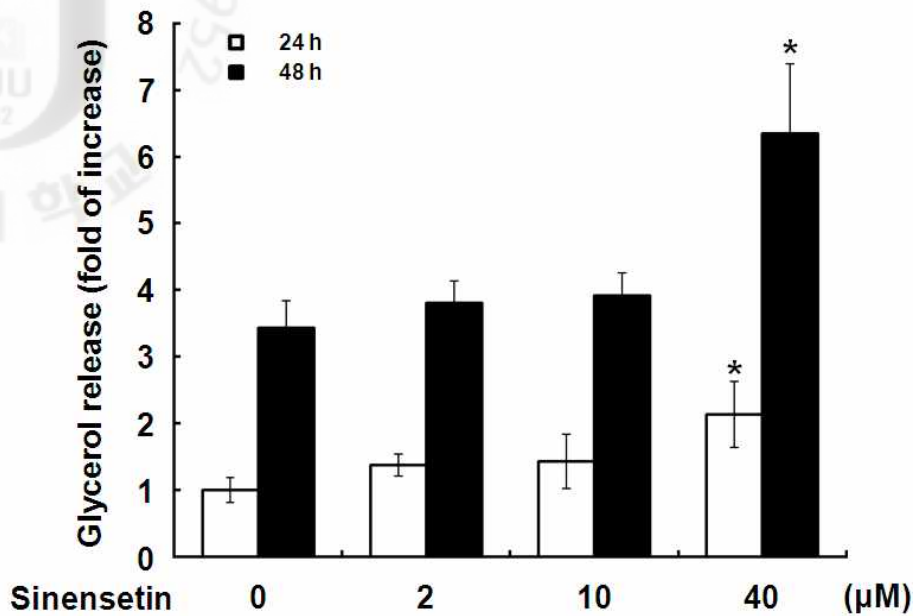


**Figure 2.22. Effect of sinensetin on lipolysis of mature 3T3-L1 adipocytes.** To induce differentiation, 2-day post-confluent preadipocytes were cultured in MDI differentiation medium II for 2 days. The cells were then cultured for a further 2 days in medium containing 5 µg/mL insulin. Then, the cells were maintained in post-differentiation medium, which was replaced every 2 days. At day 8, mature 3T3-L1 adipocytes were incubated with serum-free DMEM for 4 h. The cells were next treated with post-differentiation medium containing various concentration of sinensetin for 24 h or 48 h. Glycerol contents relative to control cells (0 µM sinensetin) at 24 h (assigned a value of 1). All values are presented as means ± S.D. ( $n=3$ ;  $*p<0.05$  compared to no sinensetin). The data shown are representative of three independent experiments.

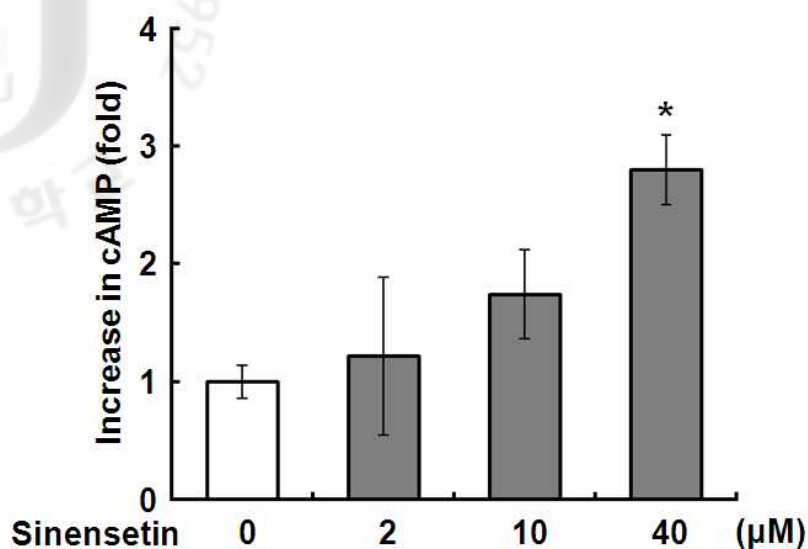


**Figure 2.23. Effect of sinensetin on production of intracellular cAMP in mature 3T3-L1 adipocytes.** Measurement of cellular cAMP levels in mature 3T3-L1 adipocytes. To induce differentiation, 2-day post-confluent preadipocytes were cultured in MDI differentiation medium II for 2 days. The cells were then cultured for a further 2 days in medium containing 5 µg/mL insulin. Then, the cells were maintained in post-differentiation medium, which was replaced every 2 days. At day 8, mature 3T3-L1 adipocytes were incubated with serum-free DMEM for 4 h. Cells were cultured in serum-free DMEM with various concentration of sinensetin. Cell lysates were prepared 30 min after treatment of sinensetin in 3T3-L1 preadipocyte. All values are presented as means ± S.D. ( $n=3$ ;  $*p<0.05$  compared to no sinensetin). The data shown are representative of three independent experiments.

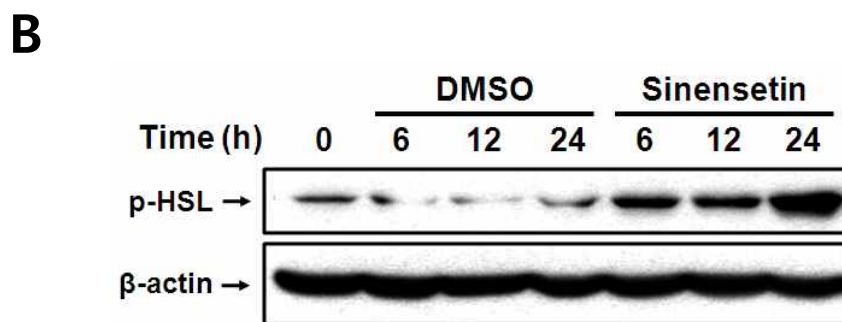
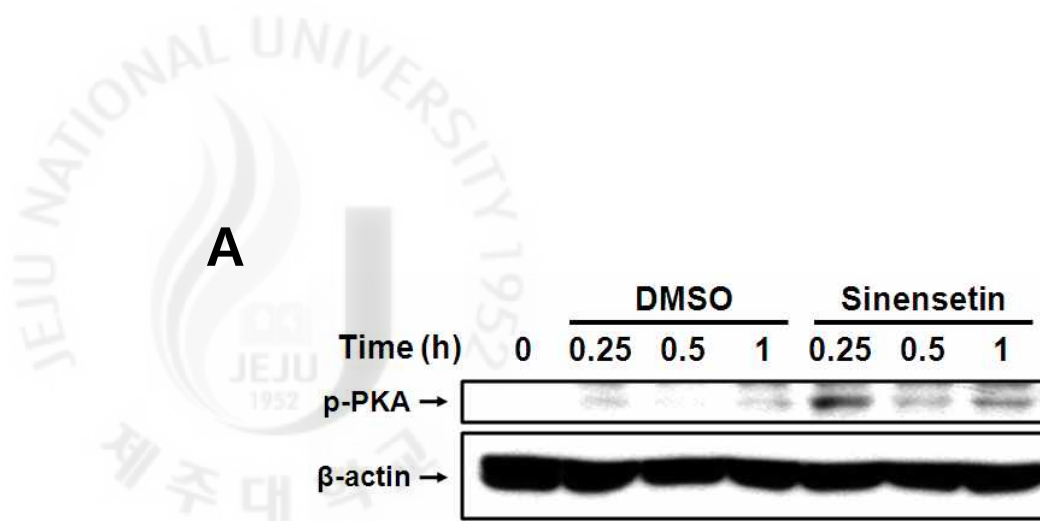


**Figure 2.24.** Effect of sinensetin on phosphorylation of PKA and HSL in mature 3T3-L1 adipocytes. To induce differentiation, 2-day post-confluent preadipocytes were cultured in MDI differentiation medium II for 2 days. The cells were then cultured for a further 2 days in medium containing 5  $\mu\text{g}/\text{mL}$  insulin. Then, the cells were maintained in post-differentiation medium, which was replaced every 2 days. At day 8, mature 3T3-L1 adipocytes were incubated for 16 h with serum-free DMEM containing 0.2% BSA. The cells were then treated with post-differentiation medium containing sinensetin (40  $\mu\text{M}$ ) at the indicated times. Western blot analysis of the time course of p-PKA (A) and p-HSL (B) expression. The data shown are representative of three independent experiments.

#### *2.5.2.4. Sinensetin inhibits glucose uptake and lipogenesis in mature 3T3-L1 adipocyte*

To investigate the effect of sinensetin on glucose uptake, differentiated 3T3-L1 adipocytes were incubated in the presence of radiolabeled glucose and various concentrations of sinensetin. As shown in Figure 2.25, sinensetin dramatically inhibited glucose uptake in a concentration-dependent manner; at the highest sinensetin concentration (40  $\mu$ M), glucose uptake decreased by 39%. We then examined whether the observed decrease in glucose uptake caused by sinensetin was associated with an insulin-dependent signaling pathway by evaluating the phosphorylation of IRS and Akt in sinensetin-treated 3T3-L1 adipocytes. Sinensetin treatment was found to inhibit phosphorylation of both IRS and Akt (Figure 2.26). Also, to characterize the effects of sinensetin on the expression SREBP1c, mature 3T3-L1 adipocytes were exposed to 40  $\mu$ M sinensetin for 6, 12, and 24 h. Sinensetin significantly decreased the expression of SREBP1c that is a transcription factor regulating the lipogenesis (Figure 2.27A and B).



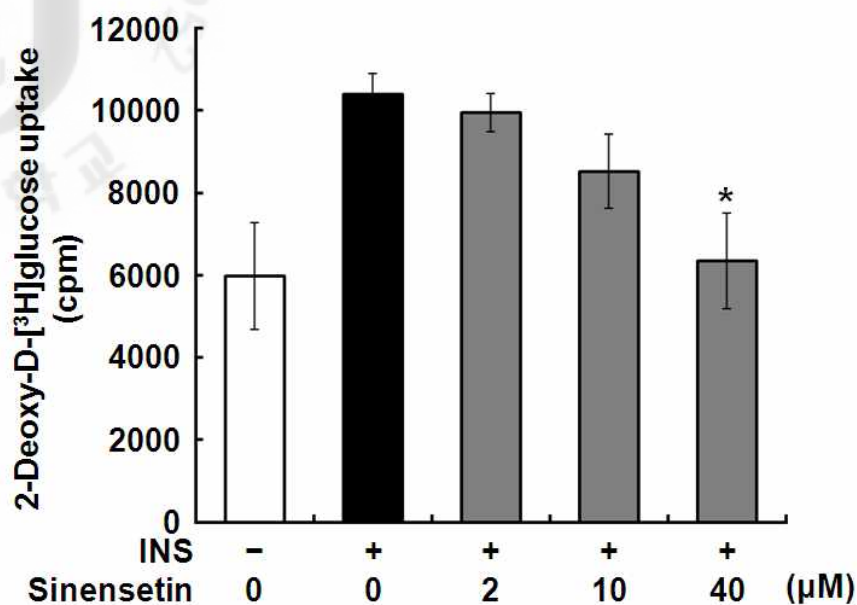


**Figure 2.25. Effect of sinensetin on glucose uptake in mature 3T3-L1 adipocytes.** To induce differentiation, 2-day post-confluent preadipocytes were cultured in MDI differentiation medium II for 2 days. The cells were then cultured for a further 2 days in medium containing 5 μg/mL insulin. Then, the cells were maintained in post-differentiation medium, which was replaced every 2 days. At day 8, mature adipocytes were incubated in 12-well plates in the presence of insulin (100 nM), sinensetin and then assayed for uptake of 2-deoxy-D-[<sup>3</sup>H]glucose. All values are presented as means ± S.D. ( $n=3$ ;  $*p<0.05$  compared to no sinensetin). The data shown are representative of three independent experiments.

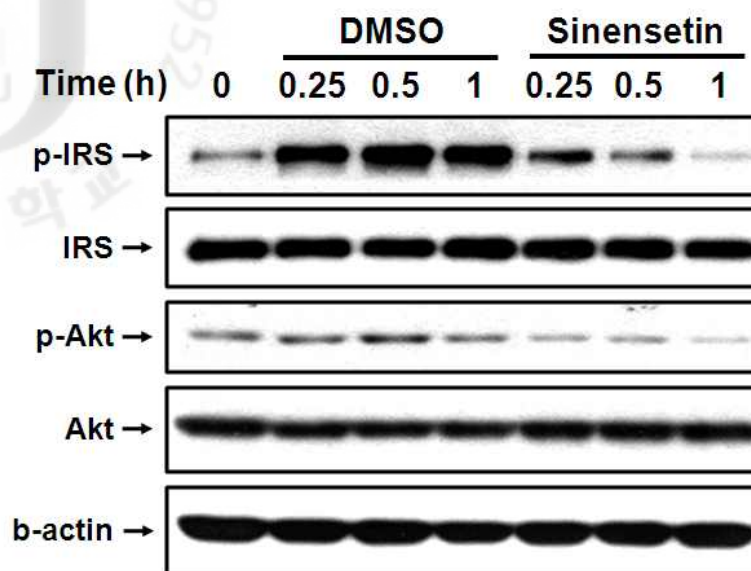


**Figure 2.26. Effect of sinensetin on phosphorylation of IRS and Akt in mature 3T3-L1 adipocytes.** Western blot analysis of the time course of p-IRS and Akt activation. To induce differentiation, 2-day post-confluent preadipocytes were cultured in MDI differentiation medium II for 2 days. The cells were then cultured for a further 2 days in medium containing 5  $\mu\text{g}/\text{mL}$  insulin. Then, the cells were maintained in post-differentiation medium, which was replaced every 2 days. At day 8, mature 3T3-L1 adipocytes were incubated for 16 h with serum-free DMEM containing 0.2% BSA. The cells were then treated with post-differentiation medium containing sinensetin (40  $\mu\text{M}$ ) at the indicated times. The data shown are representative of three independent experiments.

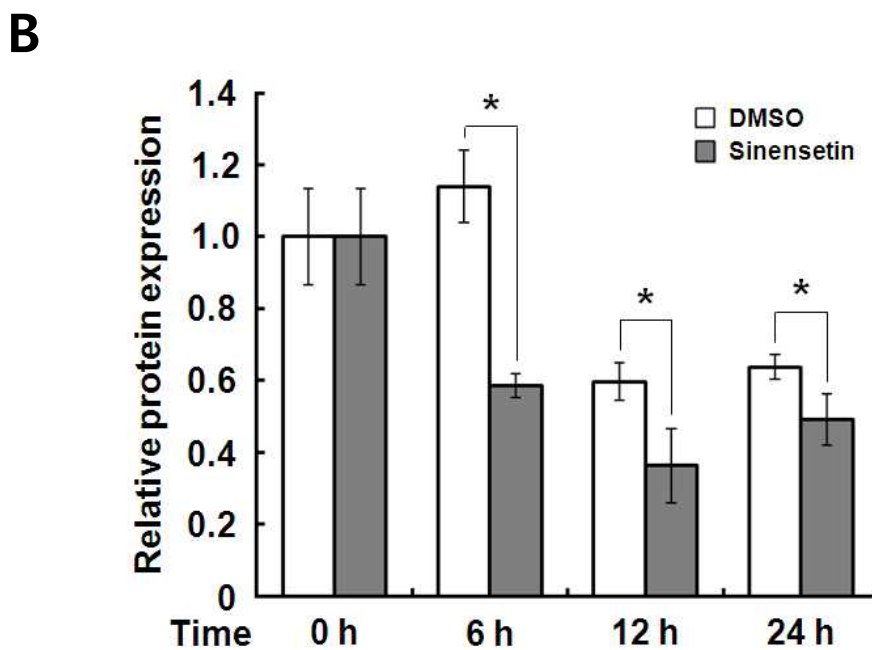
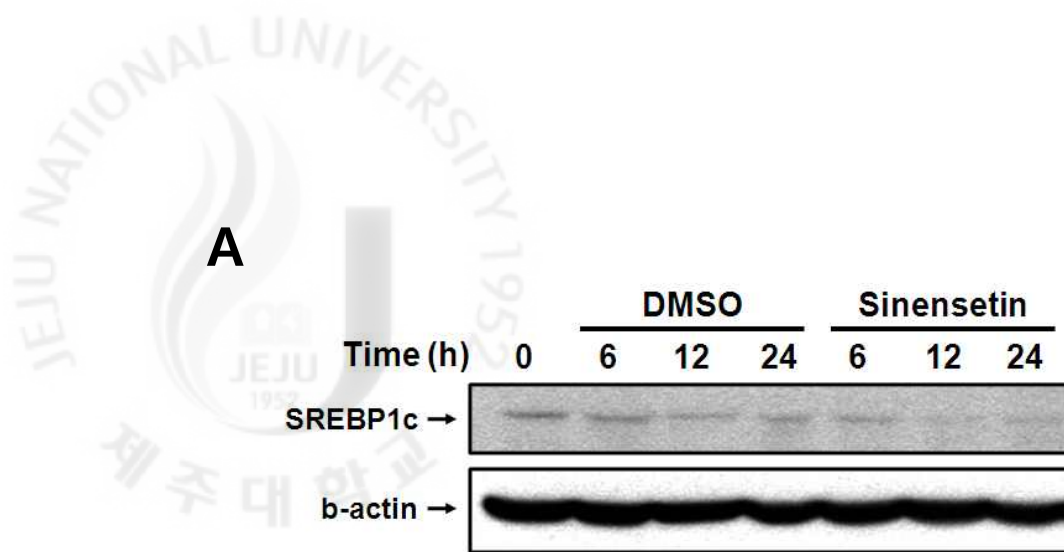


**Figure 2.27. Effect of sinensetin on expression of SREBP1c in mature 3T3-L1 adipocytes.** To induce differentiation, 2-day post-confluent preadipocytes were cultured in MDI differentiation medium II for 2 days. The cells were then cultured for a further 2 days in medium containing 5  $\mu\text{g}/\text{mL}$  insulin. Then, the cells were maintained in post-differentiation medium, which was replaced every 2 days. At day 8, mature 3T3-L1 adipocytes were incubated for 16 h with serum-free DMEM containing 0.2% BSA. The cells

were then treated with post-differentiation medium containing sinensetin (40  $\mu$ M) at the indicated times (A) Western blot analysis of the time course of SREBP1c expression. (B) Relative band density was determined by densitometry using the Image J 1.42q software (National Institutes of Health, Bethesda, MD, USA). SREBP1c protein expression was normalized to the  $\beta$ -actin expression level and expressed relative to 0 h levels. All values are presented as means  $\pm$  S.D. ( $n=3$ ;  $*p<0.05$  compared with no sinensetin. The data shown are representative of three independent experiments.

*2.5.2.5. Sinensetin activated the fatty acid  $\beta$ -oxidation in mature 3T3-L1 adipocyte*

To characterize the effects of sinensetin on the phosphorylation of AMPK and ACC, mature 3T3-L1 adipocytes were exposed to 40  $\mu$ M sinensetin for 6, 12, and 24 h, sinensetin markedly induced phosphorylation of AMPK and ACC (Figure 2.28). Thus, we investigated the effects upstream of AMPK activation by treating mature 3T3-L1 adipocytes with sinensetin. Mature 3T3-L1 adipocytes were exposed to 40  $\mu$ M sinensetin for 0.25, 0.5, and 1 h, sinensetin markedly increased the phosphorylation of LKB1 (Figure 2.29). Finally, we examined the effects downstream of AMPK activation by treating mature 3T3-L1 adipocytes with sinensetin. Sinensetin significantly increased dose-dependently the levels of CPT-1a mRNA, which is involved in fatty acid oxidation (Figure 2.30).

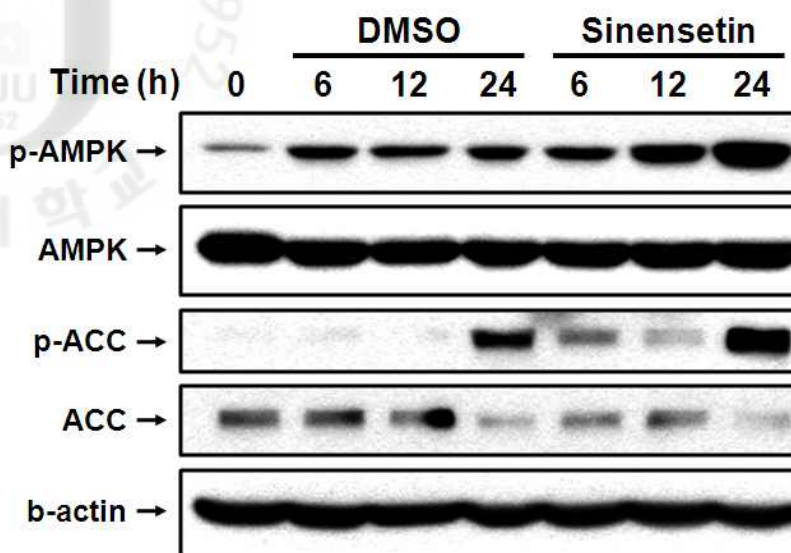


**Figure 2.28. Effect of sinensetin on phosphorylation of AMPK and ACC at several times in mature 3T3-L1 adipocytes.** Western blot analysis of the time course of AMPK and ACC phosphorylation. To induce differentiation, 2-day post-confluent preadipocytes were cultured in MDI differentiation medium II for 2 days. The cells were then cultured for a further 2 days in medium containing 5  $\mu\text{g}/\text{mL}$  insulin. Then, the cells were maintained in post-differentiation medium, which was replaced every 2 days. At day 8, mature 3T3-L1 adipocytes were incubated for 16 h with serum-free DMEM containing 0.2% BSA. The cells were then treated with post-differentiation medium containing sinensetin (40  $\mu\text{M}$ ) at the indicated times. The data shown are representative of three independent experiments.

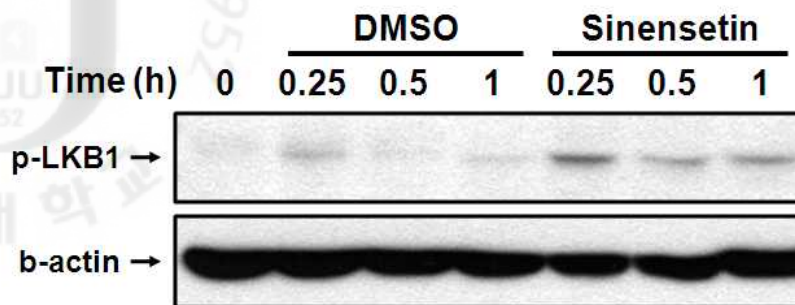


**Figure 2.29. Effect of sinensetin on phosphorylation of LKB1 at several times in mature 3T3-L1 adipocytes.** Western blot analysis of the time course of LKB1 phosphorylation. To induce differentiation, 2-day post-confluent preadipocytes were cultured in MDI differentiation medium II for 2 days. The cells were then cultured for a further 2 days in medium containing 5  $\mu\text{g}/\text{mL}$  insulin. Then, the cells were maintained in post-differentiation medium, which was replaced every 2 days. At day 8, mature 3T3-L1 adipocytes were incubated for 16 h with serum-free DMEM containing 0.2% BSA. The cells were then treated with post-differentiation medium containing sinensetin (40  $\mu\text{M}$ ) at the indicated times. The data shown are representative of three independent experiments.

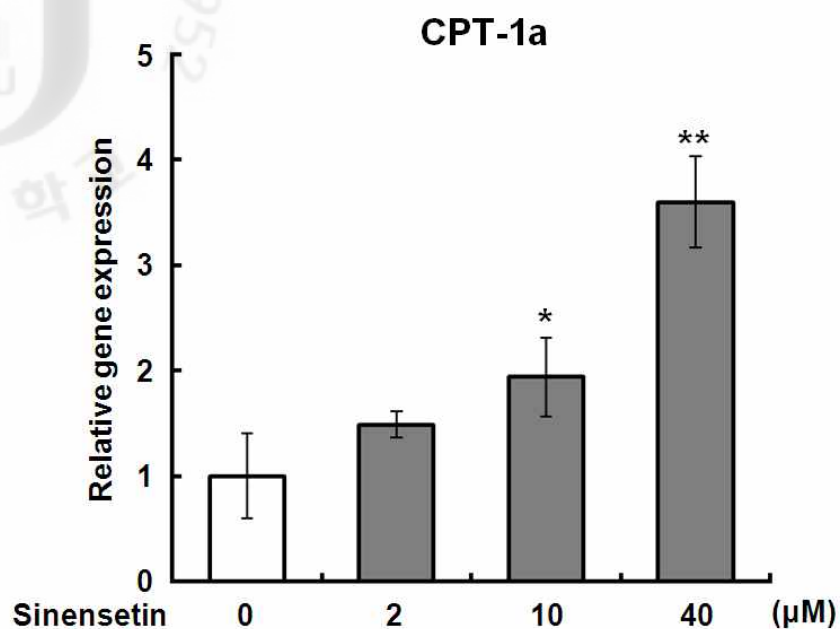


**Figure 2.30.** Effect of various sinensetin concentration on gene expression of CPT-1a in mature 3T3-L1 adipocytes. Real-time RT-PCR of the effect of sinensetin on CPT-1a gene expression. To induce differentiation, 2-day post-confluent preadipocytes were cultured in MDI differentiation medium II for 2 days. The cells were then cultured for a further 2 days in medium containing 5 μg/mL insulin. Then, the cells were maintained in post-differentiation medium, which was replaced every 2 days. At day 8, mature 3T3-L1 adipocytes were incubated for 16 h with serum-free DMEM containing 0.2% BSA. The cells were then treated with post-differentiation medium containing various sinensetin concentrations for 24 h. Real-time RT-PCR of the effect of sinensetin on CPT-1a gene expression. All values are presented as means ± S.D. ( $n=3$ ;  $*p<0.05$  and  $**p<0.01$  compared to no sinensetin). The data shown are representative of three independent experiments.



## 2.6. DISCUSSION

### 2.6.1. Anti-obesity effect of *Citrus sunki* ethanolic extract (CSE)

Adipose tissue is a dynamic organ that plays an important role in energy balance and changes in mass according to the metabolic requirements of the organism [Harp, 2004]. We examined the effects of CSE on HFD-induced fat accumulation in the adipose tissue of C57BL/6 mice. Body weight gain, adipose tissue weight, and T-CHO and TG serum levels were significantly lowered in CSE-treated mice compared to the HFD group, with no change in food intake. Moreover, histological analysis revealed a greater number of large cells in the epididymal adipose tissue of the HFD group, a typical sign of obese adipose tissue. However, the epididymal adipose tissue of the HFD+CSE group exhibited few large cells and fewer pathological signs. Also, we examined the effects of CSE on the levels of adiponectin in adipose tissue of the HFD-induced mice. Adiponectin is a protein hormone that modulates a number of metabolic processes, including glucose regulation and fatty acid catabolism [Díez and Iglesias, 2003]. Obesity, diabetes, and atherosclerosis have been associated with reduced adiponectin levels [Ahima, 2006]. In the present study, CSE recovered the expression of adiponectin mRNA, which had been lowered in C57BL/6 mice fed the HFD. These results indicate that CSE might have anti-obesity activities *in vivo*, without affecting the amount of food intake.

We also analyzed the effects of CSE on the development of fatty liver, which is strongly associated with obesity [James and Day, 1999]. Upon histological analysis, the livers of the HFD group exhibited an accumulation of numerous fatty droplets, a typical sign of fatty liver. However, the livers of the HFD+CSE group exhibited a much smaller degree of lipid accumulation

and fewer pathological signs. Moreover, liver weight was significantly lower in the HFD+CSE group than in the HFD group. Serum GPT, GOT, and LDH levels are clinically and toxicologically important indicators, and rise as a result of tissue damage caused by toxicants or disease conditions. In the HFD group, the activities of liver function markers, including serum GPT, GOT, and LDH, were significantly elevated relative to those in the ND group and were improved by CSE supplementation. These results indicate that administration of CSE can dramatically suppress the development of HFD-induced fatty liver.

AMPK is known to play a major role in glucose and lipid metabolism and to control metabolic disorders such as diabetes, obesity, and cancer [Carling, 2004]. To detect other specific molecular targets through which CSE exerted inhibitory effects on obesity, we examined the effects on AMPK signaling in epididymal adipose tissue and mature 3T3-L1 adipocytes. AMPK is known to be a metabolic master switch that is activated by LKB1 under intracellular stress conditions, including glucose deficiency, hypoxia, and reactive oxygen species (ROS) activity [Hardie, 2007]. AMPK activation is associated with metabolic organs including the liver, skeletal muscle, pancreas, and adipose tissue; thus, AMPK has been targeted in the development of drugs to treat metabolic diseases [Zhang and Zhou, 2009]. In the present study, CSE recovered the expression of phosphorylated forms of AMPK, which had been reduced in C57BL/6 mice fed the HFD. Furthermore, treatment with CSE induced AMPK phosphorylation by stimulating LKB1 phosphorylation in a dose-dependent manner, and the activation of this kinase led to the phosphorylation of its substrate, ACC, in mature 3T3-L1 adipocytes. These results suggest that CSE influenced metabolic processes related to the AMPK signaling pathway. AMPK activation increases fatty acid oxidation by reducing malonyl-CoA through the inhibition of ACC, and this process upregulates CPT-1a expression [Merrill et al., 1997]. CPT-1a

regulates long-chain fatty acid transport across the mitochondrial membrane [Hao et al., 2010]. CSE enhanced the expression of CPT-1a mRNA in a dose-dependent manner in mature 3T3-L1 adipocytes. These results suggest that CSE promotes fatty acid  $\beta$ -oxidation by activating AMPK in HFD-induced obese mice and mature 3T3-L1 adipocytes.

The major physiological role of white adipose tissue fat stores is to supply lipid energy when it is needed by other tissues. This is achieved by a highly regulated pathway whereby the triglycerides stored in adipocytes are hydrolyzed, and fatty acids are delivered to the plasma. Lipolysis plays a pivotal role in controlling the quantity of triglycerides stored in fat depots and in determining plasma free fatty acid levels. Hence, modulators of lipolysis may exert beneficial properties if the same molecule or another compound stimulates the oxidation of fatty acids and energy expenditure [Langin, 2006]. The effects of the CSE on lipolysis were examined in mature 3T3-L1 adipocytes. Compared to control adipocytes, medium glycerol concentration was dose-dependently increased by the CSE. Lipolysis is triggered by an increase in the intracellular cAMP level, which in turn activates PKA and HSL [Mauriege et al., 1988]. The CSE stimulated the activation of PKA and HSL. These results suggest that CSE promotes lipolysis by activating PKA in mature 3T3-L1 adipocytes.

In this study, we did not determine the active components exerting antiobesity effects. However, we confirmed that CSE contained abundant PMFs as compared to other Citrus species [Choi et al., 2007; Nogata et al., 2006]. PMFs decrease plasma cholesterol and TG levels at lower doses than hesperidin and narigenin in hamsters with diet-induced hypercholesterolemia [Kurowska and Manthey, 2004]. Supplementation with PMFs and palm tocotrienols decrease plasma TG and cholesterol levels in humans [Roza et al., 2007]. Recently, Lee et al. [Lee et al., 2011] reported that PMFs-rich Citrus depressa extract has antiobesity effects in HFD-induced obese mice. Thus,

PMFs might be major components that mediate the antiobesity effect of CSE.

In conclusion, we showed that administration of CSE to mice with HFD-induced obesity reduced body weight gain, adipose tissue weight, the cell size of adipose tissue, and the accumulation of fatty droplets in the liver. CSE reduces serum total-cholesterol and triglycerides, thereby regulating lipid metabolism. Also, CSE increased  $\beta$ -oxidation in epididymal adipose tissue and mature 3T3-L1 adipocytes by activating the phosphorylation of AMPK and ACC. CSE markedly enhanced lipolysis in mature 3T3-L1 adipocytes by stimulating the phosphorylation of PKA. Taken together, our findings demonstrate that CSE improves HFD-induced obesity through elevated  $\beta$ -oxidation and lipolysis in adipose tissue.

### 2.6.2. Anti-obesity effect of Sinensetin derived from CSE

In this study, we found that a sinensetin dose-dependently increased the PPAR $\gamma$ 1 and 2, C/EBP $\alpha$ , and aP2 excluding IBMX in differentiating 3T3-L1 preadipocytes. The sinensetin-induced increase in PPAR $\gamma$  and C/EBP $\alpha$  expression suggested that another sinensetin target molecule lay upstream of PPAR $\gamma$  and C/EBP $\alpha$ . Moreover, it also increase expression of SREBP1c, which has been reported to induce the production of an endogenous ligand that enhances PPAR $\gamma$  transcriptional activity [Kim et al., 1996] and can increase the expression of several genes involved in fatty acid metabolism. These results strongly suggest that sinensetin exerts adipogenesis effects via expression of adipogenic transcription factors.

C/EBP $\beta$  plays a critical role in adipocyte differentiation [Tang et al., 2003]. It is expressed early in the differentiation program and drives the subsequent expression of C/EBP $\alpha$  [Christy et al., 1991]. Moreover, C/EBP $\beta$  is rapidly induced by stimulation of hormone signaling and function as transcriptional regulator of PPAR $\gamma$  [Hamm et al., 2001]. Our data showed that sinensetin enhances C/EBP $\beta$  expression in differentiating 3T3-L1 cells. In addition, cAMP-responsive element-binding protein (CREB) is a central transcriptional activator of the adipocyte differentiation program. The expression of C/EBP $\beta$  is regulated by CREB, which is activated in early stage of adipogenesis [Niehof et al., 1997; Zhang et al., 2004]. CREB protein is required for phosphorylation on Ser 133 to exhibit transcriptional activity [Gonzalez and Montminy, 1989]. Also, activation of C/EBP $\beta$  is required for phosphorylation by extracellular signal-regulated kinase (ERK) and glycogen synthase kinase  $\beta$  [Park et al., 2004; Tang et al., 2005]. In this study, we found that sinensetin markedly increased the phosphorylation of CREB and ERK in differentiating 3T3-L1 cells. These results suggested that sinensetin could stimulate the activation of CREB and ERK, both are critical for the

expression and transcriptional activity of C/EBP $\beta$ , led to the enhanced expression of PPAR $\gamma$  and adipocyte differentiation. Moreover, CREB is activated by cAMP/PKA pathway [Niehof et al., 1997; Zhang et al., 2004]. We ascertained that sinensetin dose-dependently elevated intracellular cAMP levels in differentiating 3T3-L1 cells and phosphorylation of PKA. These results strongly indicate that sinensetin enhances adipogenesis effects via cAMP/PKA pathway in differentiating 3T3-L1 cells.

The white adipose tissue was the capacity to store triglycerides (TG) and to mobilize fatty acids and glycerol, according to energetic demands. Approximately 90% of the adipocyte volume is TG located in a only lipid droplet that dislocates the nucleus to the periphery, resulting in limited cytosolic space [Thompson et al., 2010; Meex et al., 2009]. The effects of sinensetin on lipolysis were examined in mature 3T3-L1 adipocytes. Compared to control adipocytes, medium glycerol concentration was dose-dependently increased by the sinensetin. Lipolysis in adipocytes is known to be triggered by increase of intracellular cAMP level, which in turn activates PKA and downstream lipases (HSL) [Mauriège et al., 1988]. The effects of the sinensetin on lipolysis were examined in mature 3T3-L1 adipocytes. Compared to control adipocytes, medium glycerol concentration was increased by the sinensetin. Moreover, we found that a sinensetin significantly increased the intracellular cAMP levels. Also, sinensetin stimulated the activation of PKA and HSL. These results suggest that sinensetin promotes lipolysis effects in mature 3T3-L1 adipocytes.

Obesity is characterized by increased fat deposition in visceral and subcutaneous depots and is an underlying feature of several related metabolic defects including insulin resistance, dyslipidemia, hypertension, and cardiovascular disease [Zimmet et al., 2001]. Central events in obesity development include defective adipose tissue lipolysis, increased lipogenesis, and reduced oxidative capacity [Bogacka et al., 2005; Choo et al., 2006;

Wilson-Fritch et al., 2004; Arner, 2005].

Phosphorylation of IRS leads to activation of phosphatidylinositol 3-kinase (PI3-K) [Youngren, 2007]. Subsequent activation of Akt by PI3-K stimulates glucose uptake into cells by inducing the translocation of glucose transporter 4 from intracellular storage sites to the plasma membrane [Kanzaki, 2006]. We found that sinensetin inhibited insulin-stimulated glucose uptake in mature 3T3-L1 adipocytes by reducing the level of phospho-IRS and phosphor-Akt. Moreover, Activation of Akt leads to activation of phosphodiesterase 3B (PDE3B) [Ahmadian et al., 2010]. Lipid metabolism in adipocytes is controlled by the concerted actions of cAMP-elevating hormones and insulin. Insulin counteracts catecholamine-induced lipolysis (hydrolysis of triglycerides) mainly by inducing phosphorylation and activation of PDE3B [Choi et al., 2006; Elks and Manganiello, 1985; Eriksson et al., 1995]. Activation of PDE3B leads to increased hydrolysis of cAMP, resulting in reduced activity of PKA, which phosphorylates and activates HSL as well as other target enzymes that carry out or regulate lipolysis [Holm et al., 2000; Londos et al., 1995]. Overexpression and site-directed mutagenesis studies have suggested that PKB is the upstream kinase that phosphorylates PDE3B in response to insulin [Ahmad et al., 2000; Kitamura et al., 1999]. Our data showed that sinensetin stimulates lipolysis by reducing phosphorylation of IRS in mature 3T3-L1 adipocytes.

SREBP transcription factors that regulate expression of lipogenic enzymes, such as ACC, fatty acid synthase (FAS), and 3-hydroxy-3-methylglutaryl CoA reductase (HMGCR) [Goldstein et al., 2002]. Sinensetin significantly reduced the expression of SREBP1c in mature 3T3-L1 adipocytes. These results suggest that sinensetin inhibites lipogenesis by reducing SREPB1c in mature 3T3-L1 adipocytes.

The major physiological role of white adipose tissue fat stores is to supply lipid energy when it is needed by other tissues. This is achieved by a

highly regulated pathway whereby the TG stored in adipocytes are hydrolyzed, and fatty acids are delivered to the plasma. Lipolysis plays a pivotal role in controlling the quantity of triglycerides stored in fat depots and in determining plasma free fatty acid levels. Hence, modulators of lipolysis may exert beneficial properties if the same molecule or another compound stimulates the oxidation of fatty acids and energy expenditure [Langine, 2006].

AMPK is known to play a major role in glucose and lipid metabolism and to control metabolic disorders such as diabetes, obesity, and cancer [Carling., 2004]. AMPK has emerged as a therapeutic target for metabolic disorders [Zhang et al., 2009]. To detect other specific molecular targets through which sinensetin exerted inhibitory effects on obesity, we examined the effects on AMPK signaling in epididymal adipose tissue and mature 3T3-L1 adipocytes. AMPK is known to be a metabolic master switch that is activated by LKB1 under intracellular stress conditions, including glucose deficiency, hypoxia, and reactive oxygen species (ROS) activity [Hardie, 2007]. AMPK activation is associated with metabolic organs including the liver, skeletal muscle, pancreas, and adipose tissue; thus, AMPK has been targeted in the development of drugs to treat metabolic diseases [Zhang et al., 2009]. In the present study, sinensetin enhanced the phosphorylation of AMPK. Furthermore, treatment with sinensetin induced AMPK phosphorylation by stimulating LKB1 phosphorylation, and the activation of this kinase led to the phosphorylation of its substrate, ACC in mature 3T3-L1 adipocytes. These results suggest that sinensetin influenced metabolic processes related to the AMPK signaling pathway. AMPK activation increases fatty acid  $\beta$ -oxidation by reducing malonyl-CoA through the inhibition of ACC, and this process up-regulates CPT-1a expression [Merrill et al., 1997]. CPT-1a regulates long-chain fatty acid transport across the mitochondrial membrane [Hao et al., 2010]. Sinensetin increased the expression of CPT-1a mRNA in a dose-dependent manner in mature 3T3-L1 adipocytes. These results suggest



that sinensetin promotes fatty acid  $\beta$ -oxidation by activating AMPK in mature 3T3-L1 adipocytes.

In conclusion, we showed that sinensetin could enhance differentiation of preadipocytes by cAMP/PKA pathway. Also, sinensetin stimulates lipolysis and inhibits glucose uptake by down-regulating the phosphorylation of IRS and Akt in mature 3T3-L1 adipocytes. Furthermore, sinensetin attenuates the lipogenesis by down-regulating the expression of SREBP1c in mature 3T3-L1 adipocytes. Finally, sinensetin increased fatty acid  $\beta$ -oxidation in mature 3T3-L1 adipocytes by phosphorylation of AMPK and ACC. Taken together, our results suggest that sinensetin exerts its anti-obesity effect by inhibiting lipogenesis and stimulating the lipolysis, as well as enhancing the fatty acid  $\beta$ -oxidation in mature 3T3-L1 adipocytes.



## PART 3

Anti-obesity effect of the *Sasa quepaertensis* leaf

### 3.1. LIST OF TABLES

<b>Table 3.1</b>	Effects of SQE supplementation on body weight gain in high-fat-diet (HFD)-induced obese experimental group after 70 days -----	<b>191</b>
<b>Table 3.2</b>	Effects of SQE supplementation on epididymal adipose tissue weight and perirenal adipose tissue weight in high-fat-diet (HFD)-induced obese experimental group after 70 days -----	<b>192</b>
<b>Table 3.3</b>	Effects of SQE supplementation on serum levels of T-CHO, TG, and food intake in high-fat-diet (HFD)-induced obese experimental group after 70 days -----	<b>194</b>
<b>Table 3.4</b>	Effects of SQE supplementation on serum levels of GPT, GOT, and LDH and liver weight in high-fat-diet (HFD)-induced obese experimental group after 70 days -----	<b>196</b>

## 3.2. LIST OF FIGURES

<b>Figure 3.1</b>	Picture of <i>Sasa quepaertensis</i> -----	182
<b>Figure 3.2</b>	HPLC chromatogram of SQE -----	183
<b>Figure 3.3</b>	Effect of SQE on body weight changes in mice fed a normal diet (ND), high-fat-diet (HFD), or HFD+SQE --	190
<b>Figure 3.4</b>	Effect of SQE on fatty droplets in epididymal adipose tissue of mice fed a normal diet (ND), high-fat-diet (HFD), or HFD+SQE -----	193
<b>Figure 3.5</b>	Effect of SQE on fatty droplets in the livers of mice fed a normal diet (ND), high-fat-diet (HFD), or HFD+SQE -----	197
<b>Figure 3.6</b>	Effect of SQE on protein expression in epididymal adipose tissue of mice fed a normal diet (ND), high-fat-diet (HFD), or HFD+SQE -----	199
<b>Figure 3.7</b>	Effect of SQE on adiponectin mRNA expression in epididymal adipose tissue of mice fed a normal diet (ND), high-fat-diet (HFD), or HFD+SQE -----	200
<b>Figure 3.8</b>	Effect of SQE on viability and cytotoxicity of mature 3T3-L1 adipocytes -----	202

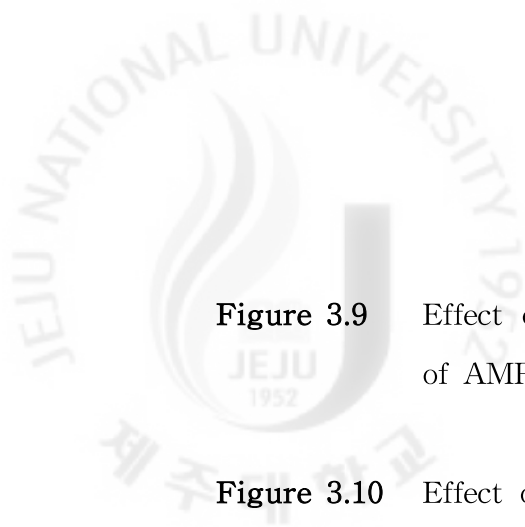


**Figure 3.9** Effect of various SQE concentration on phosphorylation of AMPK and ACC in mature 3T3-L1 adipocytes ----- 203

**Figure 3.10** Effect of various SQE concentration on gene expression of CPT-1a in mature 3T3-L1 adipocytes ----- 204

### 3.3. INTRODUCTION

As a major risk factor for many chronic diseases, including hypertension, hyperlipidemia, cardiovascular disease, atherosclerosis, and type 2 diabetes [Kopelman, 2000; Stephane et al., 2007], obesity is a major obstacle in efforts to improve human health and quality of life. Obesity is characterized by excessive fat deposition associated with morphological and functional changes in adipocytes [Fruhbeck et al., 2001]. Studies of adipose tissue biology have led to an improved understanding of the mechanisms that link metabolic disorders with altered adipocyte functions [Fruhbeck, 2008]. Lipid accumulation is caused not only by adipose tissue hypertrophy but also by adipose tissue hyperplasia [Spiegelman and Flier, 1996]. Although the molecular basis for these associations remains unclear, the experimental evidence suggests that some metabolic disorders might be treatable or preventable through the inhibition of adipogenesis and the modulation of adipocyte function [Trayhurn and Beattie, 2001].

High-fat feeding has commonly been used to induce visceral obesity in rodent models [Hansen et al., 1997] because the pathogenesis of obesity is similar to that found in humans [Katagiri et al., 2007]. Preventive or therapeutic strategies to control most human obesity should target these abnormalities. Anti-obesity foods and food ingredients may avert the condition, possibly leading to the prevention of lifestyle-related diseases, if they can effectively reduce visceral fat mass [Saito et al., 2005].

Because currently available drugs for the treatment of obesity cause undesirable side effects, there is high demand for a safe but therapeutically potent anti-obesity drug. Several plants, plant extracts, and phytochemicals have anti-obesity properties or exert direct effects on adipose tissue, and have thus been used as dietary supplements [Rayalam et al., 2008; Kang et

al., 2010; Kang et al., 2011].

The genus *Sasa* (Poaceae) is composed of perennial plants commonly known as bamboo grasses, and various *Sasa* species are distributed widely in Asian countries, including Korea, Japan, China, and Russia [Okabe et al., 1975]. *Sasa* leaves have been used in traditional medicine due to their anti-inflammatory, antipyretic, and diuretic properties [Bae, 2000]. Bamboo leaves have also been used in clinical settings to treat hypertension, cardiovascular disease, and cancer [Shibata et al., 1975].

*Sasa queipaertensis* Nakai is a bamboo grass native to Korea that grows only on Mt. Halla on Jeju Island, Korea. Young leaves of *Sasa queipaertensis* are used in a popular bamboo tea, but their beneficial health effects and the bioactive compounds contained in the plant have not yet been identified. In this study, we evaluated the anti-obesity potential of *Sasa queipaertensis* leaf extract (SQE) in mice fed a high-fat diet (HFD) and in murine 3T3-L1 adipocytes. In these model systems, SQE demonstrated anti-obesity effects.

## 3.4. MATERIALS AND METHODS

### 3.4.1. Reagents

Dulbecco's modified Eagle's medium (DMEM), bovine calf serum (BCS), fetal bovine serum (FBS), and penicillin-streptomycin (PS) were obtained from Gibco BRL (Grand Island, NY, USA). Phosphate-buffered saline (PBS; pH 7.4), 3-isobutyl-1-methylxanthine (IBMX), dexamethasone, insulin, and 3-(4,5-dimethylthiazol-2-yl)-2,5-diphenyl tetrazolium bromide (MTT) were obtained from Sigma Chemical Co. (St. Louis, MO, USA). The lactate dehydrogenase (LDH) Cytotoxicity Detection Kit was purchased from Takara Shuzo Co. (Otsu, Shiga, Japan). An antibodies to peroxidase proliferator activated receptor (PPAR)  $\gamma$ , fatty acid-binding protein aP2, and CCAAT/enhancer binding protein (C/EBP)  $\alpha$  was acquired from Santa Cruz Biotechnology (Santa Cruz, CA, USA). Antibodies to AMP activated protein kinase (AMPK) $\alpha$ , phospho-Thr172-AMPK $\alpha$ , acetyl-CoA carboxylase (ACC), and phospho-Ser79-ACC were purchased from Cell Signaling Technology (Beverly, MA, USA). Antibody to sterol regulatory element binding protein c (SREBP1c) was obtained from BD Biosciences (San Jose, CA, USA). 2-Deoxy-D-[ $^3\text{H}$ ]glucose was obtained from Amersham Biosciences (Piscataway, NJ, USA). All other reagents were purchased from Sigma Chemical Co. unless otherwise noted.

### 3.4.2. Preparation of *Sasa quepaertensis* extract (SQE) and HPLC analysis

Leaves of *Sasa quepaertensis* (Figure 3.1) were collected from Mt. Halla on Jeju Island, South Korea. One kilogram of dried leaves was mixed with



water (13 L) and incubated for 30 min. Then, the mixture was incubated at 90°C for 4 h on a platform shaker. The extract (SQE) was filtered and concentrated on a rotary evaporator under reduced pressure, then freeze-dried to a powder. SQE was stored at -20°C until use. The main constituents in SQE were analyzed by high performance liquid chromatography (HPLC) using an Waters 2695 Alliance system (Waters Corp., Milford, MA, USA) equipped with a system controller, auto-injector, column oven and Waters 2998 photodiode array (PDA) detector. Qualitative analysis of SQE was performed using a Sunfire RP 18 column (250 × 4.6 mm ID; 5 μm) at 30°C. The mobile phase consisted of acetonitrile (A) and water containing 1.0 % acetic acid (B). The gradient elution program was as follows: a 52 min gradient was started using 15% A, linearly increased to 100% over 40 min, held for 5 min, then finally returned to the initial conditions and for 5 min with a flow rate at 0.8 mL/min. The constituent was detected at 340 nm; the spectrum range was from 200 to 600 nm. The data of HPLC analysis is shown in Figure 3.2. Comparison with standards revealed that SQE contained chlorogenic acid, p-coumaric acid and triclin [Gong et al., 2010].

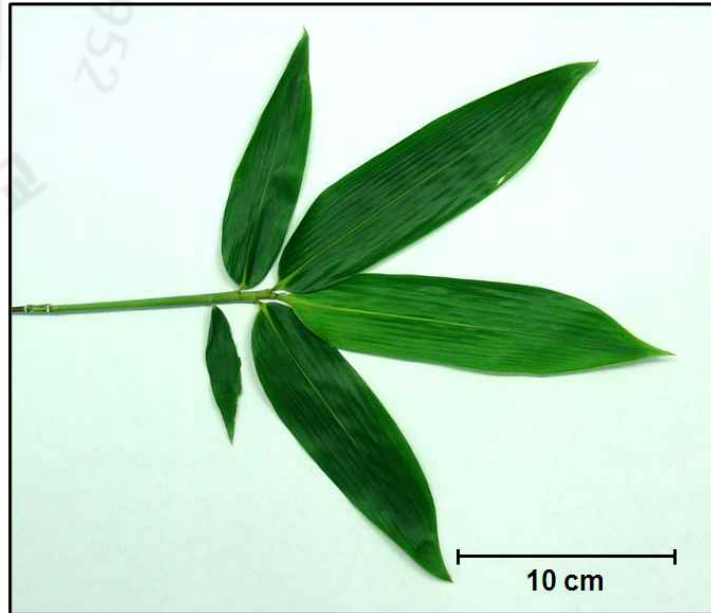


Figure 3.1. Picture of *Sasa quelpaertensis*. The *Sasa quelpaertensis* was collected from Mt. Halla on Jeju island, Republic of Korea.

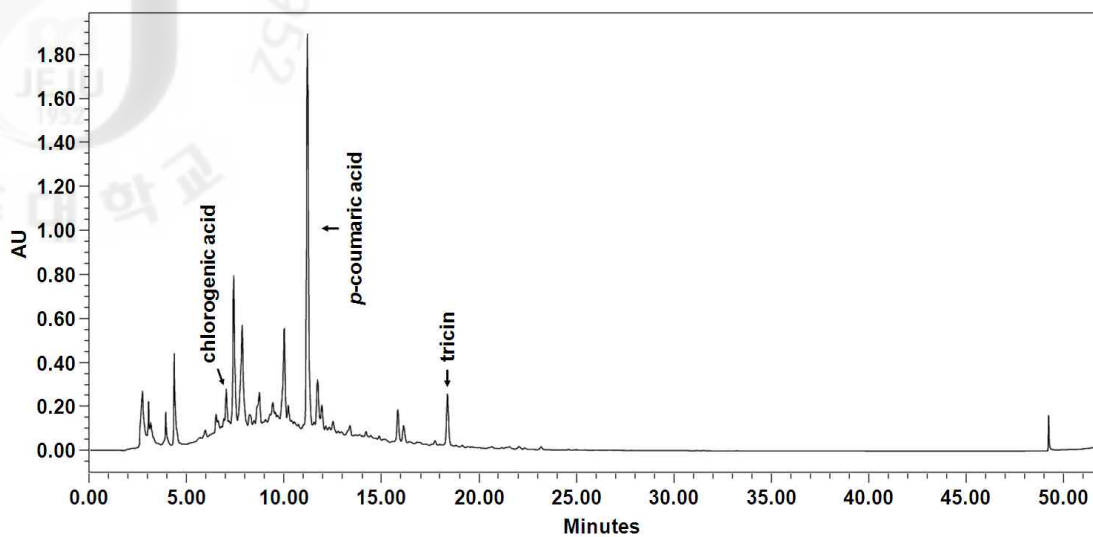


Figure 3.2. HPLC chromatogram of SQE.

### **3.4.3. Animals**

The animal study protocol was approved by the Institutional Animal Care and Use Committee of Jeju National University. After purchase, 30 4-week-old male C57BL/6 mice (Nara Biotech Co., Ltd., Seoul, Korea) were adapted for 1 week to specific temperature ( $22\pm 2^{\circ}\text{C}$ ), humidity ( $50\pm 5\%$ ), and lighting (light 08:00–20:00) conditions. The animals were housed in plastic cages (2 mice/cage) and given free access to drinking water and food. After adaptation, the C57BL/6 mice (now 5 weeks old;  $22.6\pm 1.2$  g) were randomly divided into three groups of 10 mice each. One group (normal diet, ND) was fed a 10% kcal fat diet (D12450B; Research Diets, New Brunswick, NJ, USA; protein: 19.2%, carbohydrate: 67.3%, fat: 4.3%, and others; 3.85 kcal/g), and two groups (high-fat diet, HFD; HFD+SQE) were fed a 60% kcal fat diet (D12492; Research Diets; protein: 26.2%, carbohydrate: 26.3%, fat: 34.9%, and others; 5.24 kcal/g). SQE was dissolved in 0.1% carboxymethyl cellulose (CMC) and administered orally to the animals at a dosage of 150 mg/kg/day for 70 days. The oral administration volume was approximately 100  $\mu\text{L}$ /10 g weight. Mice in the ND and the HFD groups were given 0.1% CMC.

### **3.4.4. Measurement of body weight, food intake, liver weight, epididymal adipose tissue weight, and perirenal adipose tissue weight**

Body weight and food intake were measured once every 5 day throughout the 70 days experimental period. At the end of the feeding period, the mice were anesthetized with diethyl ether after an overnight fast. The liver, epididymal adipose tissue, and perirenal adipose tissue were weighed after rapid removal from the sacrificed mice.

### **3.4.5. Biochemical analysis**

After 70 days, the mice were sacrificed by ether anesthesia overdose. Blood samples were drawn from the abdominal aorta into a vacuum tube and were allowed to stand at room temperature for 30 min for clotting. Serum samples were then collected by centrifugation at  $1,000 \times g$  for 15 min. Total cholesterol (T-CHO), triglyceride (TG), glutamic pyruvic transaminase (GPT), glutamic oxaloacetic transaminase (GOT), and lactate dehydrogenase (LDH) concentrations in serum were assayed using commercial kits (ASANPHARM, Seoul, Korea) and an automatic blood analyzer (Kuadro; BPC Biosed, Rome, Italy).

#### **3.4.6. Histology**

After blood was drained from the livers, the livers and epididymal adipose tissue were fixed in 10% neutral formalin solution for 48 h. The tissue was subsequently dehydrated in a graded ethanol series (75–100%) and embedded in paraffin wax. The embedded tissue was sectioned (8- $\mu\text{m}$ -thick sections), stained with hematoxylin and eosin (H&E), and examined by light microscopy (Olympus BX51; Olympus Optical, Tokyo, Japan), and then photographed at a final magnification of 50 $\times$ , 100 $\times$ , or 200 $\times$ .

#### **3.4.7. Cell culture and differentiation**

3T3-L1 preadipocytes obtained from the American Type Culture Collection (Rockville, MD, USA) were cultured in DMEM containing 1% PS and 10% bovine calf serum (Gibco BRL) at 37°C under a 5% CO<sub>2</sub> atmosphere. To induce differentiation, 2 day post-confluent preadipocytes (designated day 0) were cultured in MDI differentiation medium (DMEM containing 1% PS, 10% FBS, 0.5 mM IBMX, 1  $\mu\text{M}$  dexamethasone, and 5  $\mu$

g/mL insulin) for 2 days. The cells were then cultured for another 2 days in DMEM containing 1% PS, 10% FBS, and 5 µg/mL insulin. Thereafter, the cells were maintained in post-differentiation medium (DMEM containing 1% PS and 10% FBS), with replacement of the medium every 2 days.

#### **3.4.8. Cell viability and cytotoxicity**

The effect of SQE on cell viability and cytotoxicity was determined by MTT and LDH assays. Mature 3T3-L1 adipocytes were cultured in DMEM containing 1% PS, 10% FBS, and SQE for 24 h. MTT (400 µg/mL) was added to each well, and the plates were incubated at 37°C for 4 h. The liquid in the plate was removed, and dimethyl sulfoxide (DMSO) was added to dissolve the MTT-formazan complex. Optical density was measured at 540 nm. The effect of SQE on cell viability was evaluated by comparing the relative absorbance with that of control cultures. The cytotoxic effect of SQE was measured using the LDH Cytotoxicity Detection Kit. The LDH activities in medium and cell lysate were measured to evaluate cytotoxicity according to the manufacturer's protocol (LDH released into medium / maximal LDH release × 100).

#### **3.4.9. Western blot analysis**

Adipose tissue was homogenized in ice-cold buffer containing lysis buffer [1× RIPA (Upstate Biotechnology, Temecula, CA, USA), 1 mM PMSF, 1 mM Na<sub>3</sub>VO<sub>4</sub>, 1 mM NaF, and 1 µg/mL each of aprotinin, pepstatin, and leupeptin]. 3T3-L1 cells were washed with ice-cold PBS, collected, and centrifuged. The cell pellets were resuspended in lysis buffer and incubated on ice for 1 h. The adipose tissue and 3T3-L1 cell debris were then removed by centrifugation and protein concentrations in the lysates were determined using

Bio-Rad Protein Assay Reagent (Bio-Rad Laboratories, Hercules, CA, USA). The adipose tissue and 3T3-L1 cell lysates were then subjected to electrophoresis on 10% polyacrylamide gels containing sodium dodecyl sulfate (SDS) and transferred to polyvinylidene difluoride membranes. The membranes were blocked with a solution of 0.1% Tween-20 in Tris-buffered saline containing 5% bovine serum albumin (BSA) at room temperature for 1 h. After incubation overnight at 4°C with primary antibody, the membranes were incubated with horseradish peroxidase-conjugated secondary antibody at room temperature for 1 h. Immunodetection was carried out using ECL Western blotting detection reagent (Amersham Biosciences, Piscataway, NJ, USA).

#### **3.4.10. RNA preparation and quantitative real-time RT-PCR analysis**

Total RNA was extracted from the adipose tissue and 3T3-L1 adipocytes using the TRIzol reagent, according to the manufacturer's instructions, and then treated with DNase (Wako Pure Chemical Industries, Ltd., Osaka, Japan). cDNA was synthesized from 1 µg of total RNA in a 20 µL reaction using a Maxime RT PreMix Kit (iNtRON Biotechnology, Seongnam, Kyunggi, Korea). The following primers were used in real-time RT-PCR analysis: adiponectin, 5'-GAC CTG GCC ACT TTC TCC TC-3' and 5'-GTC ATC TTC GGC ATG ACT GG-3'; carnitine palmitoyltransferase-1a (CPT-1a), 5'-ACC CTG AGG CAT CTA TTG ACA-3' and 5'-TGA CAT ACT CCC ACA GAT GGC-3'; β-actin, 5'-AGG CTG TGC TGT CCC TGT AT-3' and 5'-ACC CAA GAA GGA AGG CTG GA-3'. Samples were prepared using iQ SYBR Green Supermix (Bio-Rad Laboratories) according to the manufacturer's instructions. Adiponectin, CPT-1a, and β-actin mRNA expression were measured by quantitative real-time RT-PCR using the Chromo4 Real-Time PCR System (Bio-Rad Laboratories). The formation of a single product was

verified by melting curve analysis. The expression levels of adiponectin and CPT-1a were normalized to that of  $\beta$ -actin. Data were analyzed using Opticon Monitor software (ver. 3.1; Bio-Rad Laboratories).

#### 3.4.11. Statistical analysis

Values are expressed as means  $\pm$  S.D. or S.E.. One-way analysis of variance (ANOVA) was used for multiple comparisons. Treatment effects were analyzed by the paired t-test or Duncan's multiple range test using SPSS software (ver. 12.0; SPSS Inc., Chicago, IL, USA). Differences were considered statistically significant at  $p < 0.05$ .



## 3.5. RESULTS

### 3.5.1. Anti-obesity effect of *Sasa quelpaertensis* aqueous extract (SQE)

#### 3.5.1.1. SQE improved high-fat-diet (HFD)-induced obesity

After 70 days on the HFD, the mean body weight and body weight gain in the HFD group were more than 35.2% and 176.1% higher than those in the ND group, indicating that the HFD induced obesity (Figure 3.3, Table 3.1). SQE administration (150 mg/kg/day) significantly decreased body weight and body weight gains in the HFD+SQE group relative to those in the non-SQE-treated HFD group (12.8% and 31.0% lower, respectively). The weights of epididymal and perirenal adipose tissue were also significantly higher in the HFD group (134.9% and 146.0%, respectively) than in the ND group. Epididymal and perirenal adipose tissue weights were significantly lower in the HFD+SQE group (29.7 and 21.1%, respectively) than in the HFD group (Table 3.2). Histological analysis of epididymal adipose tissue confirmed that adipocyte size was markedly increased in the HFD group compared with the ND group after 70 days, whereas adipocyte size was markedly decreased in the HFD+SQE group compared with the HFD group (Figure 3.4).

Food intake did not significantly differ among the HFD groups. However, the serum levels of T-CHO and TG were significantly lower in the HFD+SQE group (11.5% and 39.7%, respectively) than in the HFD group (Table 3.3).

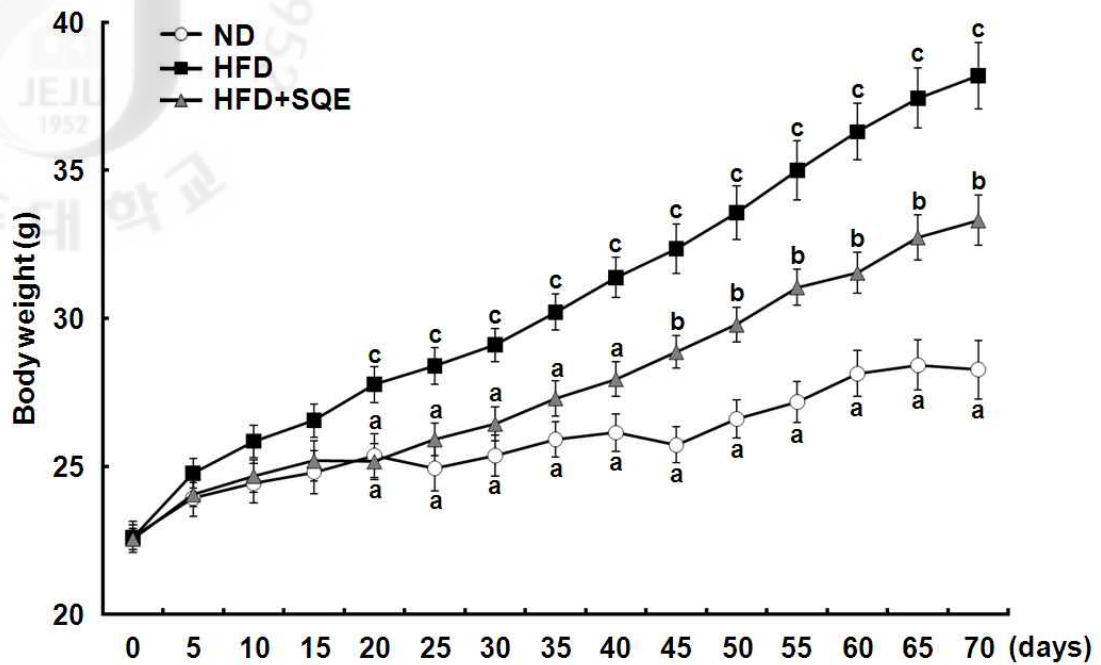


Figure 3.3. Effect of SQE on body weight changes in mice fed a normal diet (ND), high-fat-diet (HFD), or HFD+SQE. Body weights were measured at 5 day intervals for 70 days. Results are shown as means  $\pm$  S.E. ( $n=10$ ). Mean separation was performed using Duncan's multiple range test. <sup>a,b,ac,c</sup>Means not sharing a common superscript are significantly different ( $p<0.05$ ).

Table 3.1. Effects of SQE supplementation on body weight gain in high-fat-diet (HFD)-induced obese experimental group after 70 days.

Group	ND	HFD	HFD+SQE
Initial body weight (g)	22.61±0.53	22.60±0.42	22.55±0.36
Final body weight (g)	28.26±0.99 <sup>a</sup>	38.20±1.12 <sup>c</sup>	33.31±1.12 <sup>b</sup>
Body weight gain (g)	5.65±0.60 <sup>a</sup>	15.60±0.78 <sup>c</sup>	10.76±0.59 <sup>b</sup>
Intake of PBEE (mg/kg of body weight/day)	-	-	150

Values are expressed as means ± S.E. ( $n=10$ ). Values with different letters in each assay are significantly different from each other between the ND, HFD, HFD+SQE groups by Duncan's multiple range test ( $p<0.05$ ).

Table 3.2. Effects of SQE supplementation on epididymal adipose tissue weight and perirenal adipose tissue weight in high-fat-diet (HFD)-induced obese experimental group after 70 days.

Group	ND	HFD	HFD+SQE
Epididymal adipose tissue (g)	0.86±0.05 <sup>a</sup>	2.02±0.12 <sup>c</sup>	1.42±0.06 <sup>b</sup>
Perirenal adipose tissue (g)	0.50±0.06 <sup>a</sup>	1.23±0.07 <sup>c</sup>	0.97±0.06 <sup>b</sup>

Values are expressed as means ± S.E. ( $n=10$ ). Values with different letters in each assay are significantly different from each other between the ND, HFD, HFD+SQE groups by Duncan's multiple range test ( $p<0.05$ ).

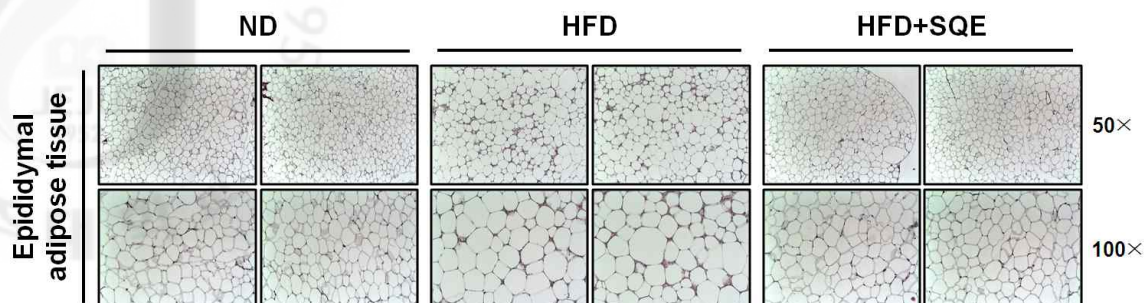


Figure 3.4. Effect of SQE on fatty droplets in epididymal adipose tissue of mice fed a normal diet (ND), high-fat-diet (HFD), or HFD+SQE. Hematoxylin and eosin (H&E)-stained photomicrographs of epididymal adipose sections are shown at 50 $\times$  and 100 $\times$ .

Table 3.3. Effects of SQE supplementation on serum levels of T-CHO, TG, and food intake in high-fat-diet (HFD)-induced obese experimental group after 70 days.

Group	ND	HFD	HFD+SQE
Food intake (g/cage/5 day)	26.57±0.40 <sup>a</sup>	21.19±0.28 <sup>b</sup>	21.04±0.28 <sup>b</sup>
T-CHO (mg/dL)	119.71±4.09 <sup>a</sup>	179.14±3.90 <sup>c</sup>	158.57±2.38 <sup>b</sup>
TG (mg/dL)	92.29±4.86 <sup>a</sup>	138.43±9.15 <sup>b</sup>	83.43±3.03 <sup>a</sup>

Values are expressed as means ± S.E. ( $n=10$ ). Values with different letters in each assay are significantly different from each other between the ND, HFD, HFD+SQE groups by Duncan's multiple range test ( $p<0.05$ ).

*3.5.1.2. SQE reduced damage of liver in high-fat-diet (HFD)-induced obese mice*

We next examined the effect of SQE on the levels of serum GPT, GOT, and LDH in HFD mice. SQE administration significantly reduced the levels of these markers of cell damage. The levels of serum GPT and GOT were significantly lower in the HFD+SQE group (52.1% and 23.4%, respectively) than in the HFD group (Table 3.4). Serum LDH levels were also significantly lower in the HFD+SQE group (42.3%) than in the HFD group (Table 3.4). In addition, liver weight was significantly lower in the HFD+SQE group than in the HFD group.

Figure 3.5 presents photomicrographs of liver tissue samples stained with H&E. The H&E analysis of the liver revealed fatty infiltration in the HFD group compared with the ND group; however, no fatty infiltration was observed in the livers of the HFD+SQE group.

Table 3.4. Effects of SQE supplementation on serum levels of GPT, GOT, and LDH and liver weight in high-fat-diet (HFD)-induced obese experimental group after 70 days.

Group	ND	HFD	HFD+SQE
GPT (IU/L)	8.57±0.85 <sup>a</sup>	17.29±3.03 <sup>b</sup>	8.29±0.65 <sup>b</sup>
GOT (IU/L)	42.29±1.62 <sup>a</sup>	57.43±3.14 <sup>b</sup>	44.00±1.21 <sup>a</sup>
LDH (IU/L)	440.86±80.48 <sup>a</sup>	981.86±117.44 <sup>b</sup>	566.57±26.43 <sup>a</sup>
Liver weight (g)	1.07±0.06 <sup>a</sup>	1.30±0.08 <sup>b</sup>	1.01±0.03 <sup>a</sup>

Values are expressed as means ± S.E. ( $n=10$ ). Values with different letters in each assay are significantly different from each other between the ND, HFD, HFD+SQE groups by Duncan's multiple range test ( $p<0.05$ ).



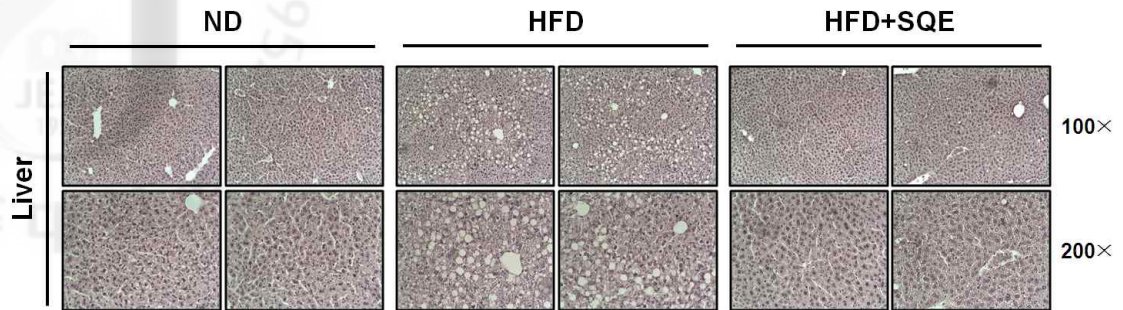


Figure 3.5. Effect of SQE on fatty droplets in the livers of mice fed a normal diet (ND), high-fat-diet (HFD), or HFD+SQE. Hematoxylin and eosin (H&E)-stained photomicrographs of liver tissue sections are shown at 100× and 200×.

*3.5.1.3. SQE restored AMPK phosphorylation and adiponectin expression in epididymal adipose tissue*

Next, we tested protein expressions responsible for fatty acid  $\beta$ -oxidation in the epididymal adipose tissue. As shown in Figure 3.6, protein expressions of phosphorylated forms of AMPK and its immediate substrate (phosphorylated forms of ACC) were higher in the HFD+SQE group than in the HFD group after 70 days. After 70 days of the HFD, the gene expression of adiponectin was lower in the HFD group than in the ND group (Figure 3.7), but was restored in the HFD+SQE group.

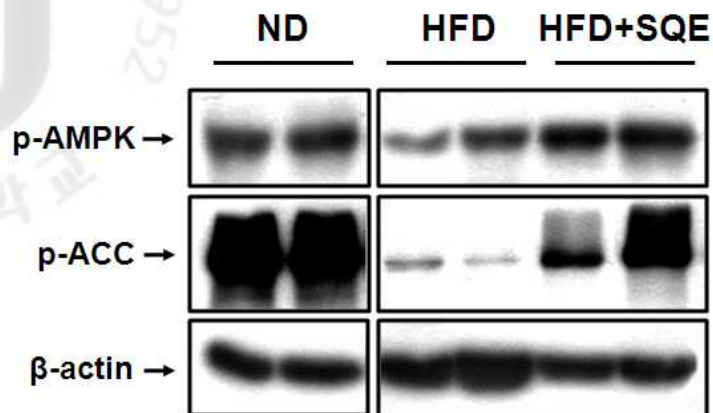


Figure 3.6. Effect of SQE on protein expression in epididymal adipose tissue of mice fed a normal diet (ND), high-fat-diet (HFD), or HFD+SQE. p-AMPK and p-ACC protein expression in epididymal tissue were determined by Western blot analysis. The data shown are representative of three independent experiments.

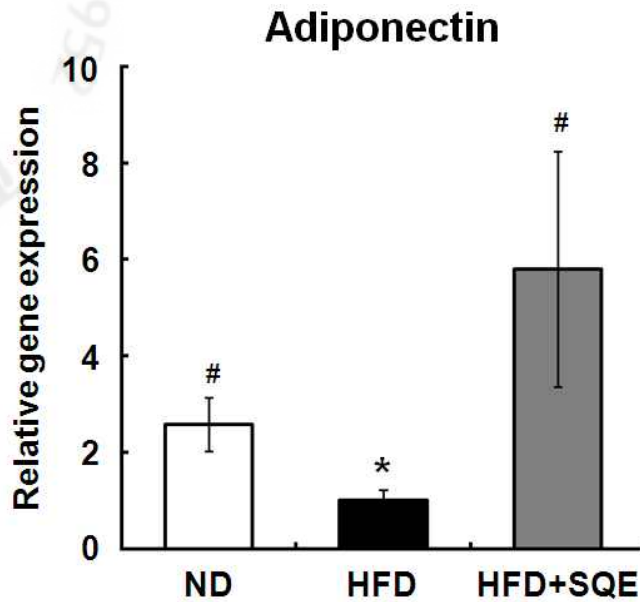


Figure 3.7. Effect of SQE on adiponectin mRNA expression in epididymal adipose tissue of mice fed a normal diet (ND), high-fat-diet (HFD), or HFD+SQE. Real-time RT-PCR analysis of adiponectin mRNA expression in epididymal tissue. All value are presented as means  $\pm$  S.D. ( $n=10$ ;  $*p<0.05$  compared with ND and  $\#p<0.05$  compared with HFD). The data shown are representative of three independent experiments.

#### 3.5.1.4. SQE activated the AMPK pathway in mature 3T3-L1 adipocytes

The effect of SQE on cell viability and cytotoxicity of mature 3T3-L1 adipocytes was first evaluated by MTT and LDH assays. An SQE concentration of 1,000  $\mu\text{g/mL}$  did not affect the viability ( $97.33 \pm 6.08\%$  compared to the control) or cytotoxicity ( $-1.15 \pm 2.85\%$  compared to the control) of the mature 3T3-L1 adipocytes (Figure 3.8). To characterize the effects of SQE on the phosphorylation of AMPK and ACC *in vitro*, we treated mature 3T3-L1 adipocytes with various concentrations of SQE. Consistent with the *in vivo* data, SQE markedly induced phosphorylation of AMPK and ACC in a dose-dependent manner (Figure 3.9). Thus, we investigated the effects downstream of AMPK activation by treating mature 3T3-L1 adipocytes with SQE. SQE increased the mRNA levels of CPT-1a, which is involved in fatty acid oxidation (Figure 3.10).

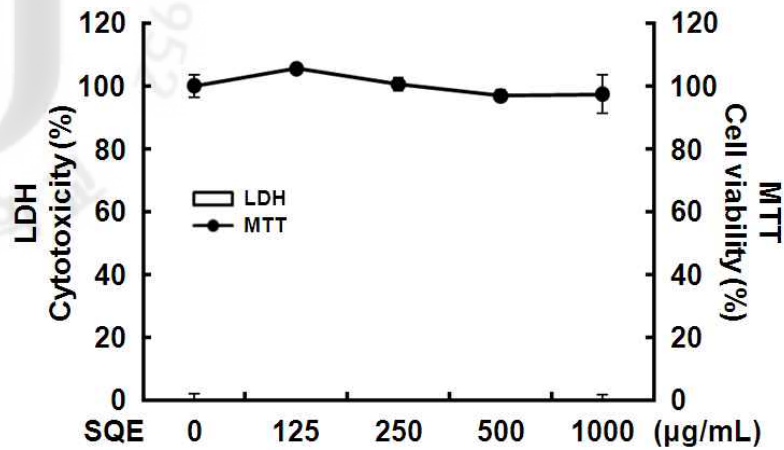
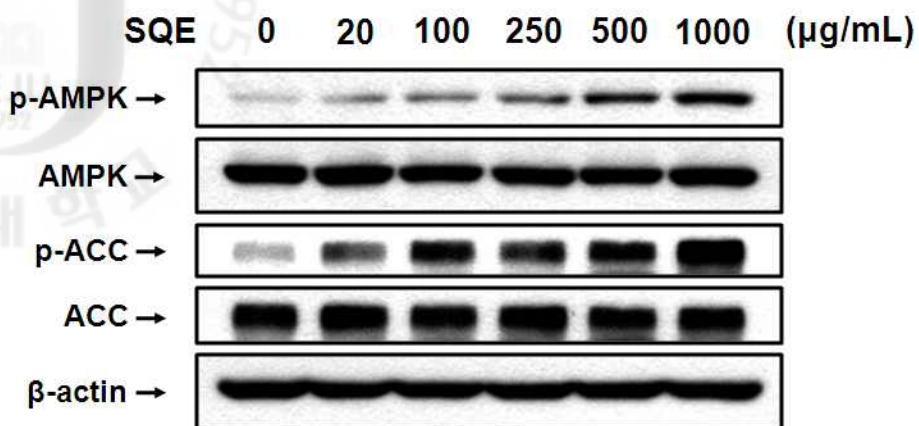
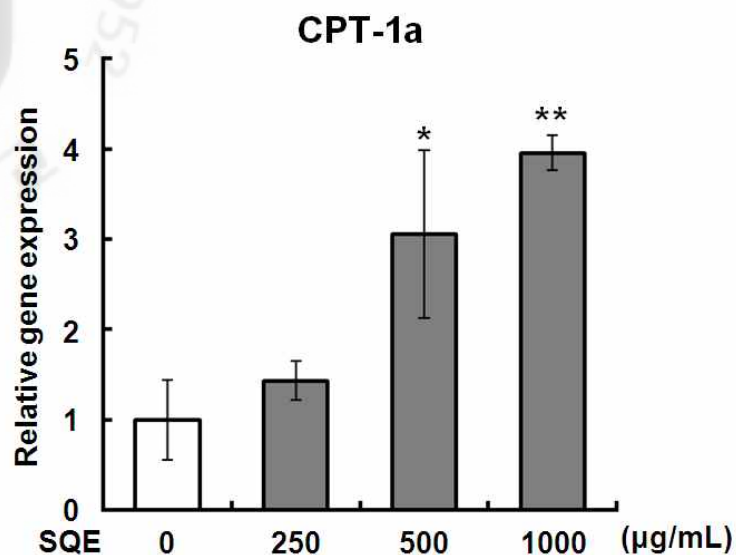


Figure 3.8. Effect of SQE on viability and cytotoxicity of mature 3T3-L1 adipocytes. 3T3-L1 preadipocytes were induced to differentiate as described in the Materials and Methods section. On day 8, viability and cytotoxicity were assessed in MTT and LDH assays. All values are presented as means  $\pm$  S.D. ( $n=3$ ;  $*p<0.05$  compared to no SQE). The data shown are representative of three independent experiments.



**Figure 3.9.** Effect of various SQE concentration on phosphorylation of AMPK and ACC in mature 3T3-L1 adipocytes. 3T3-L1 preadipocytes were induced to differentiate as described in the Materials and Methods section. On day 8, mature 3T3-L1 adipocytes were incubated for 16 h with serum-free DMEM containing 0.2% BSA. The cells were then treated with post-differentiation medium containing various SQE concentrations for 24 h. Western blot analysis of the effect of SQE dose on p-AMPK, AMPK, p-ACC, and ACC expression. The data shown are representative of three independent experiments.



**Figure 3.10. Effect of various SQE concentration on gene expression of CPT-1a in mature 3T3-L1 adipocytes.** 3T3-L1 preadipocytes were induced to differentiate as described in the Materials and Methods section. On day 8, mature 3T3-L1 adipocytes were incubated for 16 h with serum-free DMEM containing 0.2% BSA. The cells were then treated with post-differentiation medium containing various SQE concentrations for 24 h. Real-time RT-PCR of the effect of SQE on CPT-1a gene expression. All values are presented as means  $\pm$  S.D. ( $n=3$ ;  $*p<0.05$  and  $**p<0.001$  compared to no SQE). The data shown are representative of three independent experiments.



## 3.6. DISCUSSION

### 3.6.1. Anti-obesity effect of *Sasa quelpaertensis* aqueous extract (SQE)

Adipose tissue is a dynamic organ that plays an important role in energy balance and changes in mass according to the metabolic requirements of the organism [Harp, 2004]. We examined the effects of SQE on HFD-induced fat accumulation in the adipose tissue of C57BL/6 mice. Body weight gain, adipose tissue weight, and T-CHO and TG serum levels were significantly lower in SQE-treated mice than in the HFD group, with no change in the amount of food intake. Moreover, histological analysis revealed a greater number of large cells in the epididymal adipose tissue of the HFD group, a typical sign of obese adipose tissue. However, the epididymal adipose tissue of the HFD+SQE group exhibited a small number of large cells and fewer pathological signs. Obesity, diabetes, and atherosclerosis have been associated with reduced adiponectin levels [Ahima, 2006]. In the present study, SQE recovered the expression of adiponectin mRNA, which had been elevated in C57BL/6 mice fed with the HFD. These results indicated that SQE might have anti-obesity activities *in vivo* without affecting the amount of food intake.

We also analyzed the effects of SQE on the development of fatty liver, which is strongly associated with obesity [James and Day, 1999]. Upon histological analysis, the livers of the HFD group exhibited the accumulation of numerous fatty droplets, a typical sign of fatty liver. However, the livers of the HFD+SQE group exhibited a much smaller degree of lipid accumulation and fewer pathological signs. Moreover, liver weight was significantly lower in the HFD+SQE group than in the HFD group. Serum GPT, GOT, and LDH levels are clinically and toxicologically important indicators, and rise as a

result of tissue damage caused by toxicants or disease conditions. In the HFD group, the activities of liver function markers, including serum GPT, GOT, and LDH, were significantly elevated relative to those in the ND group and were improved by SQE supplementation. These results indicate that the administration of SQE can dramatically suppress the development of HFD-induced fatty liver.

AMPK is known to play a major role in glucose and lipid metabolism and to control metabolic disorders, such as diabetes, obesity, and cancer [Carling, 2004]. AMPK has emerged as a therapeutic target for metabolic disorders [Zhang et al., 2009]. To detect other specific molecular targets through which SQE exerted inhibitory effects on obesity, we examined the effects on AMPK signaling in epididymal adipose tissue and mature 3T3-L1 adipocytes. AMPK is known to be a metabolic master switch that is activated by intracellular stress conditions, including glucose deficiency, hypoxia, and reactive oxygen species (ROS) activity [Hardie, 2007]. AMPK activation is associated with metabolic organs, including the liver, skeletal muscle, pancreas, and adipose tissue; thus, AMPK has been targeted in the development of drugs to treat metabolic diseases [Zhang et al., 2009]. In the present study, SQE recovered the expression of phosphorylated forms of AMPK, which had been reduced in C57BL/6 mice fed with the HFD. Furthermore, treatment with SQE induced AMPK phosphorylation in a dose-dependent manner, and the activation of this kinase led to the phosphorylation of its substrate, ACC, in mature 3T3-L1 adipocytes. These results suggest that SQE influenced metabolic processes related to the AMPK signaling pathway. AMPK activation increases fatty acid oxidation by reducing malonyl-CoA through the inhibition of ACC, and this process up-regulates CPT-1a expression [Merrill et al., 1997]. CPT-1a regulates long-chain fatty acid transport across the mitochondrial membrane [Hao et al., 2010]. SQE enhanced the expression of CPT-1a mRNA in a

dose-dependent manner in mature 3T3-L1 adipocytes. These results suggest that SQE promoted fatty acid  $\beta$ -oxidation by activating AMPK in HFD-induced obese mice and 3T3-L1 adipocytes.

Several recent studies have described the beneficial health effects of *Sasa* species leaves [Choi et al., 2008; Yang et al., 2010], which contain polysaccharides, lignin, chlorophyllin, and flavonoids that exert strong anti-tumor activity and protective effects on spontaneous mammary tumorigenesis [Suzuki et al., 1968; Yamafuji and Murakami, 1968; Tsunoda et al., 1998; Ren et al., 2004]. However, the bioactive compounds responsible for anti-obesity activity in *Sasa* leaves have not yet been identified. Because SQE contains a mixture of compounds, further research is necessary to clarify the relationship between anti-obesity effects and the active compounds in SQE.

In conclusion, we have shown that the administration of SQE to mice with HFD-induced obesity reduced body weight gain, adipose tissue weight, cell size in adipose tissue, and the accumulation of fatty droplets in the liver. SQE reduced serum TC and TG levels, thereby regulating lipid metabolism. SQE also increased the phosphorylation of AMPK and ACC in epididymal adipose tissue and mature 3T3-L1 adipocytes. Taken together, these results suggest that SQE may protect against HFD-induced obesity through the activation of the AMPK pathway in adipose tissue and the inhibition of fatty droplet accumulation in liver tissue.

## CONCLUSION

This study was carried out to investigate biological activities of selected plant resources distributed in Jeju Island such as *Petalonia binghamiae* (J. Agaradh) Vinogradova (Miyeokse), *Citrus sunki* Hort. ex Tanaka (Jinkyul), and *Sasa queipaertensis* Nakai (Jeju joritdae) and phytochemicals isolated from its.

### **Anti-obesity effect of *Petalonia binghamiae***

First, water soluble extracts of *Petalonia binghamiae* inhibits adipogenesis by down-regulating the adipocyte-specific transcriptional regulator, attenuates the mitotic clonal expansion process. Furthermore, the extracts inhibits glucose uptake in mature 3T3-L1 adipocytes. Moreover, the extracts protect against high-fat-diet-induced obesity through adipocyte differentiation and glucose uptake in mature adipocytes. Second, ethanolic extracts of *Petalonia binghamiae* activates the AMPK signaling pathway, and inhibites the lipogenesis in mature 3T3-L1 adipocytes. Moreover, the extracts improve high-fat-diet-induced obesity by increasing fatty acid  $\beta$ -oxidation and inhibiting lipogenesis in the adipose tissue. Third, fucoxanthin, derived from PBE inhibits adipogenesis when present during the intermediate and late stages of the differentiation period. Moreover, fucoxanthin inhibits glucose uptake in mature 3T3-L1 adipocytes by inhibiting the IRS activation. Taken together, our findings demonstrate that anti-obesity effects of *Petalonia binghamiae* may improve HFD-induced obesity by activity of fucoxanthin.

### **Anti-obesity effect of *Citrus sunki***

Fist, ethanolic extracts of *Citrus sunki* activates the AMPK and PKA signaling pathway in mature 3T3-L1 adipocytes. Moreover, the extracts

improve high-fat-diet-induced obesity by elevated fatty acid  $\beta$ -oxidation and lipolysis in adipose tissue. Second, sinensetin, derived from CSE enhance differentiation of preadipocytes by cAMP/PKA pathway. Also, sinensetin stimulates lipolysis and inhibits glucose uptake by down-regulating the phosphorylation of IRS and Akt in mature 3T3-L1 adipocytes. Furthermore, sinensetin attenuates the lipogenesis by down-regulating the expression of SREBP1c in mature 3T3-L1 adipocytes. Also, sinensetin increased fatty acid  $\beta$ -oxidation in mature 3T3-L1 adipocytes by AMPK activation. Taken together, our findings demonstrate that anti-obesity effects of *Citrus sunki* may improve HFD-induced obesity by activity of sinensetin.

#### **Anti-obesity effect of *Sasa quelpaertensis***

Hot water extracts of *Sasa quelpaertensis* activates the AMPK signaling pathway in mature 3T3-L1 adipocytes. Moreover, the extracts improve against high-fat-diet-induced obesity through the activation of the AMPK pathway in adipose tissue and the inhibition of fatty droplet accumulation in liver tissue.



## REFERENCES

- Ahima RS, Adipose tissue as an endocrine organ, *Obesity* (Silver Spring) Suppl 5 (2006) 242S–249S.
- Ahmad F, Cong LN, Stenson Holst L, Wang LM, Rahn Landström T, Pierce JH, Quon MJ, Degerman E, Manganiello VC, Cyclic nucleotide phosphodiesterase 3B is a downstream target of protein kinase B and may be involved in regulation of effects of protein kinase B on thymidine incorporation in FDCP2 cells, *J. Immunol.* 164 (2000) 4678–4688.
- Ahmadian M, Wang Y, Sul HS, Lipolysis in adipocytes, *Int. J. Biochem. Cell Biol.* 42 (2010) 555–559.
- Akiyama T, Ishida J, Nakagawa S, Ogawara H, Watanabe S, Itoh N, Shibuya M, Fukami Y, Genistein, a specific inhibitor of tyrosine-specific protein kinases, *J. Biol. Chem.* 262 (1987) 5592–5595.
- Arner P, Human fat cell lipolysis: biochemistry, regulation and clinical role. *Best Pract. Res. Clin. Endocrinol. Metab.* 19 (2005) 471–482.
- Bae K, *The Medicinal plants of Korea*. Kyo-Hak Publishing Company, Seoul. (2000).
- Barak Y, Nelson MC, Ong ES, Jones YZ, Ruiz-Lozano P, Chien KR, Koder A, Evans RM, PPAR $\gamma$  is required for placental, cardiac, and adipose tissue development, *Mol. Cell* 4 (1999) 585–595.
- Barnes LA, Opitz JM, Gilbert-Barnes E, Obesity: genetic, molecular, and environmental aspects, *Am. J. Med. Genet. A* 143A (2007) 3016–3034.
- Blumenthal M, Busse WR, Goldberg A, Gruenwald J, Hall T, Riggins CW, Rister RS, *The Complete German Commission E Monographs: Therapeutic*

Guide to Herbal Medicines, American Botanical Council, Austin, 1998.

Bogacka I, Xie H, Bray GA, Smith SR, Pioglitazone induces mitochondrial biogenesis in human subcutaneous adipose tissue in vivo, *Diabetes* 54 (2005) 1392-1399.

Carling D, The AMP-activated protein kinase cascade - a unifying system for energy control, *Trends Biochem. Sci.* 29 (2004) 18-24.

Choi YH, Park S, Hockman S, Zmuda-Trzebiatowska E, Svannelid F, Haluzik M, Gavrilova O, Ahmad F, Pepin L, Napolitano M, Taira M, Sundler F, Stenson Holst L, Degerman E, Manganiello VC, Alterations in regulation of energy homeostasis in cyclic nucleotide phosphodiesterase 3B-null mice. *J. Clin. invest.* 116 (2006) 3240-3251.

Choi SY, Ko HC, Ko SY, Hwang JH, Park JG, Kang SH, Han SH, Yun SH, Kim SJ, Correlation between flavonoid content and the NO production inhibitory activity of peel extracts from various citrus fruits, *Biol. Pharm. Bull.* 30 (2007) 772-778.

Choi YJ, Lim HS, Choi JS, Shin SY, Bae JY, Kang SQ, Kang IJ, Kang YH, Blockage of chronic high glucose-induced endothelial apoptosis by *Sasa borealis* bamboo extract, *Exp. Biol. Med.* 233 (2008) 580-591.

Choo HJ, Kim JH, Kwon OB, Lee CS, Mun JY, Han SS, Yoon YS, Yoon G, Choi KM, Ko YG, Mitochondria are impaired in the adipocytes of type 2 diabetic mice, *Diabetologia.* 49 (2006) 784-791.

Christy RJ, Kaestner KH, Geiman DE, Lane MD, CCAAT/enhancer binding protein gene promoter: binding of nuclear factors during differentiation of 3T3-L1 preadipocytes, *Proc. Natl. Acad. Sci. USA* 88 (1991) 2593-2597.

Darlington GJ, Ross SE, MacDougald OA, The role of C/EBP genes in adipocyte differentiation, *J. Biol. Chem.* 273 (1998) 30057-30060.

Díez JJ, Iglesias P, The role of the novel adipocyte-derived hormone adiponectin in human disease, *Eur. J. Endocrinol.* 148 (2003) 293-300.

Dong Y, Ji G, Cao A, Shi J, Shi H, Xie J, Wu D, Effects of sinensetin on proliferation and apoptosis of human gastric cancer AGS cells, *Zhongguo Zhong Yao Za Zhi* 36 (2011) 790-794.

Elks ML, Manganiello VC, Antilipolytic action of insulin: role of cAMP phosphodiesterase activation, *Endocrinology* 116 (1985) 2119-2121.

Englert G, Bjornland T, Liaaen-Jensen S, 1D and 2D NMR study of some allenic carotenoids of the fucoxanthin series, *Magn. Reson. Chem.* 28 (1990) 519-528.

Enriori PJ, Evans AE, Sinnayah P, Jobst EE, Tonelli-Lemos L, Billes SK, Glavas MM, Grayson BE, Perello M, Nilni EA, Grove KL, Cowley MA, Diet-induced obesity causes severe but reversible leptin resistance in arcuate melanocortin neurons, *Cell Metab.* 5 (2007) 181-194.

Eriksson H, Ridderstråle M, Degerman E, Ekholm D, Smith CJ, Manganiello VC, Belfrage P, Tornqvist H, Evidence for the key role of the adipocyte cGMP-inhibited cAMP phosphodiesterase in the antilipolytic action of insulin, *Biochim. Biophys. Acta.* 1266 (1995) 101-107

Farmer SR, Transcriptional control of adipocyte formation, *Cell Metab.* 4 (2006) 263-273.

Fruhbeck G, Gómez-Ambrosi J, Muruzábal FJ, Burrell MA, The adipocyte: a model for integration of endocrine and metabolic signaling in energy metabolism regulation, *Am. J. Physiol. Endocrinol. Metab.* 280 (2001) E827-847.

Fruhbeck G, Overview of adipose tissue and its role in obesity and metabolic disorders, *Methods Mol. Biol.* 456 (2008) 1-22.



Fryer LG, Parbu-Patel A, Carling D, The anti-diabetic drugs rosiglitazone and metformin stimulate AMP-activated protein kinase through distinct signaling pathways, *J. Biol. Chem.* 277 (2002) 25226-25232.

Galati EM, Monforte MT, Kirjavainen S, Forestieri AM, Trovato A, Tripodo MM, Biological effects of hesperidin, a citrus flavonoid. (Note I): antiinflammatory and analgesic activity, *Farmaco* 40 (1994) 709-712.

Green H, Meuth M, An established pre-adipose cell line and its differentiation in culture, *Cell* 3 (1974) 127-133.

Goldstein JL, Rawson RB, Brown MS, Mutant mammalian cells as tools to delineate the sterol regulatory element-binding protein pathway for feedback regulation of lipid synthesis, *Arch. Biochem. Biophys.* 397 (2002) 139-148.

Gong J, Wu X, Lu B, Zhang Y, Safety evaluation of polyphenol-rich extract from bamboo shavings, *Afr. J. Biotechnol.* 9 (2010) 77-86.

Gonzalez GA, Montminy MR, Cyclic AMP stimulates somatostatin gene transcription by phosphorylation of CREB at serine 133, *Cell* 59 (1989) 675-680.

Gregoire FM, Adipocyte differentiation: from fibroblast to endocrine cell, *Exp. Biol. Med.* 226 (2001) 997-1002.

Gregoire FM, Smas CM, Sul HS, Understanding adipocyte differentiation, *Physiological Rev.* 78 (1998) 783-809.

Guerre-Millo M, Adipose tissue and adipokines: for better or worse, *Diabetes Metab.* 30 (2004) 13-19.

Hamm JK, Park BH, Farmer SR, A role for C/EBP $\beta$  in regulating peroxisome proliferator-activated receptor gamma activity during adipogenesis in

3T3-L1 preadipocytes, *J. Biol. Chem.* 276 (2001) 18464-18471.

Hansen PA, Han DH, Nolte LA, Chen M, Holloszy JO, DHEA protects against visceral obesity and muscle insulin resistance in rats fed a high-fat diet, *Am. J. Physiol.* 273 (1997) 1704-1708.

Hao J, Shen W, Yu G, Jia H, Li X, Feng Z, Wang Y, Wever P, Wertz K, Sharman E, Liu J, Hydroxytyrosol promotes mitochondrial biogenesis and mitochondrial function in 3T3-L1 adipocyte, *J. Nutr. Chem.* 21 (2010) 634-644.

Hardie DH, AMP-activated/SNR1 protein kinases: conserved guardians of cellular energy, *Nat. Rev. Mol. Cell Biol.* 8 (2007) 774-785.

Harmon AW, Harp JB, Differential effects of flavonoids on 3T3-L1 adipogenesis and lipolysis, *Am. J. Physiol. Cell Physiol.* 280 (2001) C807-813.

Harp JB, New insights into inhibitors of adipogenesis, *Curr. Opin. Lipidol.* 15 (2004) 303-307.

Haugan JA, Englert G., Liaaen-Jensen S, Algal carotenoids 50. Alkali lability of fucoxanthin - reactions and products, *Acta Chem. Scand.* 46 (1992) 614-624.

Haslam DW, James WP., Obesity, *Lancet* 366 (2005) 1197-1209.

Holm C, Osterlund T, Laurell H, Contreras JA, Molecular mechanisms regulating hormone-sensitive lipase and lipolysis, *Annu. Rev. Nutr.* 20 (2000) 365-393.

Hotamisligil GS, Shargill NS, Spiegelman BM, Adipose expression of tumor necrosis factor- $\alpha$ : direct role in obesity-linked insulin resistance, *Science* 259 (1993) 87-91.

Huang B, Wang Y, Thousand Formulas and Thousand Herbs of Traditional Chinese Medicine, Heilongjiang Education Press, Harbin, 1993.

Hung PF, Wu BT, Chen HC, Chen YH, Chen CL, Wu MH, Liu HC, Lee MJ, Kao YH, Antimitogenic effect of green tea (-)-epigallocatechin gallate on 3T3-L1 preadipocytes depends on the ERK and Cdk2 pathways, Am. J. Physiol. Cell Physiol. 288 (2005) C1094-1108.

James O, Day C, Non-alcoholic steatohepatitis: another disease of affluence, Lancet 353 (1999) 1634-1636.

Kang SI, Jin YJ, Ko HC, Choi SY, Hwang JH, Whang I, Kim MH, Shin HS, Jeong HB, Kim SJ, *Petalonia* improves glucose homeostasis in streptozotocin-induced diabetic mice, Biochem. Biophys. Res. Commun. 373 (2008) 265-269.

Kanzaki M, Insulin receptor signals regulating GLUT4 translocation and actin dynamics, Endocr. J. 53 (2006) 267-293.

Katagiri K, Arakawa S, Kurahashi R, Hatano Y, Impaired contact hypersensitivity in diet-induced obese mice, J. Dermatol. Sci. 46 (2007) 117-126.

Kessler RC, Davis RB, Foster DF, Van Rompay MI, Walters EE, Wilkey SA, Kaptchuk TJ, Eisenberg DM, Long-term trends in the use of complementary and alternative medical therapies in the United States, Ann. Intern. Med. 135 (2001) 262-268.

Kim EJ, Jung SN, Son KH, Kim SR, Ha TY, Park MG, Jo IG, Park JG, Choe W, Kim SS, Ha J, Antidiabetes and antiobesity effect of cryptotanshinone via activation of AMP-activated protein kinase, Mol. Pharmacol. 72 (2007) 62-72.

Kim JB, Spiegelman BM, ADD1/SREBP1 promotes adipocyte differentiation

and gene expression linked to fatty acid metabolism, *Genes Dev.* 10 (1996) 1096-1107.

Kim JB, Wright HM, Wright M, Spiegelman BM, ADD1/SREBP1 activates PPAR $\gamma$  through the production of endogenous ligand, *Proc. Natl. Acad. Sci. USA* 95 (1998) 4333-4337.

Kim JK, So H, Youn MJ, Kim HJ, Kim Y, Park C, Kim SJ, Ha YA, Chai KY, Kim SM, Kim KY, Park R, *Hibiscus sabdariffa* L. water extract inhibits the adipocyte differentiation through the PI3-K and MAPK pathway, *J. Ethnopharmacol.* 114 (2007) 260-267.

Kim JM, Shunichi S, Kim DJ, Park CB, Takasuka N, Baba-Triyama H, Ota T, Nir Z, Khachik F, Shimidzu N, Tanaka Y, Osawa T, Uraji T, Murakoshi M, Nishino H, Tsuda H, Chemopreventive effects of carotenoids and curcumins on mouse colon carcinogenesis after 1,2-dimethylhydrazine initiation, *Carcinogenesis* 19 (1998) 81-85.

Kitamura T, Kitamura Y, Kuroda S, Hino Y, Ando M, Kotani K, Konishi H, Matsuzaki H, Kikkawa U, Ogawa W, Kasuga M, Insulin-induced phosphorylation and activation of cyclic nucleotide phosphodiesterase 3B by the serine-threonine kinase Akt, *Mol. Cell. Biol.* 19 (1999) 6286-6296.

Ko HC, Jang MG, Kang CH, Lee NH, Kang SI, Lee SR, Park DB, Kim SJ, Preparation of a polymethoxyflavone-rich fraction (PRF) of *Citrus sunki* Hort. ex Tanaka and its antiproliferative effects, *Food Chem.* 123 (2010) 484-488.

Kopelman PG, Obesity as a medical problem, *Nature* 404 (2000) 635-643.

Koutnikova H, Cock TA, Watanabe M, Houten SM, Campy MF, Dierich A, Auwerx J, Compensation by the muscle limits the metabolic consequences of lipodystrophy in PPAR $\gamma$  hypomorphic mice, *Proc. Natl. Acad. Sci. USA*

100 (2003) 14457-14462.

Kuda T, Hishi T, Maekawa S, Antioxidant properties of dried product of 'haba-nori', an edible brown alga, *Petalonia binghamiae* (J. Agaradh) Vinogradova, Food Chem. 98 (2006) 545-550.

Kurowska EM, Manthey JA, Hypolipidemic effects and absorption of citrus polymethoxylated flavones in hamsters with diet-induced hypercholesterolemia, J. Agric. Food Chem. 52 (2004) 2879-2886.

Langin D, Adipose tissue lipolysis as a metabolic pathway to define pharmacological strategies against obesity and the metabolic syndrome, Pharmacol. Res. 53 (2006) 482-491.

Lee CH, Jeong TS, Choi YK, Hyun BH, Oh GT, Kim EH, Kim JR, Han JI, Bok SH, Anti-atherogenic effect of citrus flavonoids, naringin and naringenin, associated with hepatic ACAT and aortic VCAM-1 and MCP-1 in high cholesterol-fed rabbits, Biochem. Bioph. Res. Co., 284 (2001) 681-688.

Lee YS, Cha BY, Saito K, Choi SS, Wang XX, Choi BK, Yonezawa T, Teruya T, Nagai K, Woo JT, Effects of a Citrus depressa Hayata (shiikuwasa) extract on obesity in high-fat diet-induced obese mice, Phytomed. 18 (2011) 648-654.

Londos C, Brasaemle DL, Gruia-Gray J, Servetnick DA, Schultz CJ, Levin DM, Kimmel AR, Perilipin: unique proteins associated with intracellular neutral lipid droplets in adipocytes and steroidogenic cells, Biochem. Soc. Trans. 23 (1995) 611-615.

Maeda H, Hosokawa M, Sashima T, Funayama K, Miyashita K, Fucoxanthin from edible seaweed, *Undaria pinnatifida*, shows antiobesity effect through UCP1 expression in white adipose tissues, Biochem. Biophys. Res.

Commun. 332 (2005) 392-397.

Maeda H, Hosodawa M, Sashima T, Miyashita K, Dietary combination of fucoxanthin and fish oil attenuates the weight gain of white adipose tissue and decreases blood glucose in obese/diabetic KK-Ay mice, J. Agric. Food Chem. 55 (2007) 7701-7706.

Maeda H, Hosokawa M, Sashima T, Takahashi N, Kawada T, Miyashita K, Fucoxanthin and its metabolite, fucoxanthinol, suppress adipocyte differentiation in 3T3-L1 cells, Int. J. Mol. Med. 18 (2006) 147-152.

MacDougald OA, Lane MD, Transcriptional regulation of gene-expression during adipocyte differentiation, Annu. Rev. Biochem. 64 (1995) 345-373.

Martini CN, Plaza MV, Vila Mdel C, PKA-dependent and independent cAMP signaling in 3T3-L1 fibroblasts differentiation, Mol. Cell Endocrinol. 298 (2009) 42-47.

Mauriege P, Pergola GD, Berlan M, Lafontan M, Human fat cell beta-adrenergic receptors: beta agonist-dependent lipolytic responses and characterization of beta-adrenergic binding sites on human fat cell membranes with highly selective beta1-antagonists, J. Lipid Res., 29 (1988) 587-601.

Meex RC, Schrauwen P, Hesselink MK, Modulation of myocellular fat stores: lipid droplet dynamics in health and disease, Am. J. Physiol. Regul. Integr. Comp. Physiol. 297 (2009) R913-R924.

Merrill GF, Kurch EJ, Hardie DG, Winder WW, AICA riboside increased AMP-activated protein kinase, fatty acid oxidation, and glucose uptake in rat muscle, Am. J. Physiol. Endocrinol. Metab. 273 (1997) E1107-E1112.

Mizushima Y, Sugiyama Y, Yoshida H, Hanashima S, Yamazaki T, Kamisuki S, Ohta K, Takemura M, Yamaguchi T, Matsukage A, Yoshida S,

Saneyoshi M, Sugawara F, Sakagauchi K, Galactosyldiacylglycerol, a mammalian DNA polymerase  $\alpha$ -specific inhibitor from a sea alga, *Petalonia binghamiae*, Biol. Pharm. Bull. 24 (2001) 982-987.

Mori K, Ooi T, Hiraoka M, Oka N, Hamada H, Tamuara M, Kusumi T, Fucoxanthin and its metabolites in edible brown algae cultivated in deep seawater, Mar. Drugs 2 (2004) 63-72.

Niehof M, Manns MP, Trautwein C, CREB controls LAP/C/EBP $\beta$  transcription, Mol. Cell. Biol. 17 (1997) 3600-3613

Nogata Y, Sakamoto K, Shiratsuchi H, Ishii T, Yano M, Ohta H, Flavonoid composition of fruit tissues of citrus species, Biosci. Biotech. Bioch. 70 (2006) 178-192.

Ntambi JM, Kim YC, Adipocyte differentiation and gene expression, J. Nutr. 12 (2000) 3122S-3126S.

Okabe S, Takeuchi K, Takagi K, Shibata M, Stimulatory effect of the water extract of bamboo grass (Folin solution) on gastric acid secretion in pylorus-ligated rats, Jap. J. Pharmacol. 25 (1975) 608-609.

Park BH, Qiang L, Farmer SR, phosphorylation of C/EBP $\beta$  at a consensus extracellular signal-regulated kinase/glycogen synthase kinase 3 site is required for the induction of adiponectin gene expression during the differentiation of mouse fibroblasts into adipocytes, Mol. Cell. Biol. 24 (2004) 8671-8680.

Payne VA, Au WS, Lowe CE, Rahman SM, Friedman JE, O'Rahilly S, Rochford JJ, C/EBP transcription factors regulate SREBP1c gene expression during adipogenesis, Biochem. J. 425 (2009) 215-223.

Rangwala SM, Lazar MA, Transcriptional control of adipogenesis, Annu. Rev. Nutr. 20 (2000) 539-559.

- Rasouli N, Kern PA, Adipocytokines and the metabolic complications of obesity, *J. Clin. Endocrinol. Metab.* 93 (2008) S64-S73.
- Rayalam S, Della-Fera MA, Baile CA, Phytochemicals and regulation of the adipocyte cycle, *J. Nutr. Biochem.* 19 (2008) 717-726.
- Ren M, Reilly RT, Sacchi N, Sasa health exerts a protective effect on Her2/NeuN mammary tumorigenesis, *Anticancer Res.* 24 (2004) 2879-2884.
- Rosen ED, Spiegelman BM, Molecular regulation of adipogenesis, *Annu. Rev. Cell Dev. Biol.* 16 (2000) 145-171.
- Rosen, ED, Walkey CJ, Puigserver P, Spiegelman BM, Transcriptional regulation of adipogenesis, *Genes Dev.* 14 (2000) 1293-1307.
- Roza JM, Xian-Liu Z, Guthrie N, Effect of citrus flavonoids and tocotrienols on serum cholesterol levels in hypercholesterolemic subjects, *Altern. Ther. Health Med.* 13 (2007) 44-48.
- Sachindra NM, Sato E, Maeda H, Hosokawa M, Niwano Y, Kohno M, Miyashita K, Radical scavenging and singlet oxygen quenching activity of marine carotenoid fucoxanthin and its metabolites, *J. Agric. Food Chem.* 55 (2007) 8516-8522.
- Saha AK, Avilucea PR, Ye JM, Assifi MM, Kraegen EW, Ruderman NB, Pioglitazone treatment activates AMP-activated protein kinase in rat liver and adipose tissue in vivo, *Biochem. Biophys. Res. Commun.* 314 (2004) 580-585.
- Saito M, Ueno M, Ogino S, Kubo K, Nagata J, Takeuchi M, High dose of *Garcinia cambogia* is effective in suppressing fat accumulation in developing male Zucker obese rats, but highly toxic to the testis, *Food. Chem. Toxicol.* 43 (2005) 411-419.



Satomi Y, Nishino H, Fucoxanthin, a natural carotenoid, induces G<sub>1</sub> arrest and GADD45 gene expression in human cancer cells, *In Vivo* 21 (2007) 305-309.

Shibata M, Yamatake M, Sakamoto M, Kanamori K, Takagi K, Pharmacological studies on bamboo grass (1). Acute toxicity and anti-inflammatory and antiulcerogenic activities of water-soluble fraction (Folin) extracted from *Sasa albomarginata* Makino et Shibata. *Nihon Yakurigaku Zasshi* 71 (1975) 481-485.

Shiratori K, Ohgami K, Ilieva I, Jin XH, Koyama Y, Miyashita K, Yoshida K, Kase S, Ohno S, Effects of fucoxanthin on lipopolysaccharide-induced inflammation *in vitro* and *in vivo*, *Exp. Eye Res.* 81 (2005) 422-428.

Spiegelman BM, Flier JS, Adipogenesis and obesity: rounding out the big picture, *Cell* 87 (1996) 377-389.

Stephane G, Tseng YH, Kahn CR, Developmental origin of fat tracking obesity to its source, *Cell* 131 (2007) 242-256.

Suzuki S, Saito T, Uchiyama M, Akiya S, Studies on the anti-tumor activity of polysaccharides. I. Isolation of hemicelluloses from Yakushima-bamboo and their growth inhibitory activities against sarcoma-180 solid tumor, *Chem. Pharm. Bull.* 16 (1968) 2032-2039.

Tang QQ, Grønberg M, Huang H, Kim JW, Otto TC, A. Pandey, M.D. Lane, Sequential phosphorylation of CCAAT enhancer-binding protein  $\beta$  by MAPK and glycogen synthase kinase 3 $\beta$  is required for adipogenesis, *Proc. Natl. Acad. Sci. USA* 102 (2005) 9766-9771.

Tang QQ, Otto TC, Lane MD, Mitotic clonal expansion: a synchronous process required for adipogenesis, *Proc. Natl. Acad. Sci. USA* 100 (2003) 44-49.

Tang QQ, Otto TC, Lane MD, CCAAT/enhancer-binding protein  $\beta$  is required for mitotic clonal expansion during adipogenesis, Proc. Natl. Acad. Sci. USA 100 (2003) 850-855.

Thompson BR, Lobo S, Bernlohr DA, Fatty acid flux in adipocytes: the in's and out's of fat cell lipid trafficking, Mol. Cell Endocrinol. 318 (2010) 24-33.

Trayhurn P, Beattie JH, Physiological role of adipose tissue: white adipose tissue as an endocrine and secretory organ, Proc. Nutr. Soc. 60 (2001) 329-339.

Tsunoda S, Yamamoto K, Skamoto S, Inoue H, Nagasawa H, Effects of *Sasa* Health, extract of bamboo grass leaves, on spontaneous mammary tumourigenesis in SHN mice, Anticancer Res. 18 (1998) 153-158.

Wichtl M, Bisset NG, Herbal drugs and phytopharmaceuticals, Trans from 2nd German ed, Medpharm Scientific Publisher, Stuttgart, 1994.

Wilson-Fritch L, Nicoloso S, Chouinard M, Lazar MA, Chui PC, Leszyk J, Straubhaar J, Czech MP, Corvera S, Mitochondrial remodeling in adipose tissue associated with obesity and treatment with rosiglitazone, J. Clin. Invest. 114 (2004) 1281-1289.

World Health Organization 2002 World health report: reducing risks. World Health Organization, Geneva, Switzerland, PHL: Promoting Healthy Life2.

Wu-Wong JR, Berg CE, Wang J, Chiou WJ, Fissel B, Endothelin stimulates glucose uptake and GLUT4 translocation via activation of endothelin ETA receptor in 3T3-L1 adipocytes, J. Biol. Chem. 274 (1999) 8103-8110.

Wu ZD, Rosen ED, Brun R, Hauser S, Adelmant G, Troy AE, Mckeeon C, Darlington GJ, Spiegelman BM, Cross-regulation of C/EBP $\alpha$  and PPAR $\gamma$  controls the transcriptional pathway of adipogenesis and insulin

sensitivity, Mol. Cell 3 (1999) 151-158.

Yamafuji K, Murakami H, Antitumor potency of lignin and pyrocatechol and their action on deoxyribonucleic acid, Enzymologia 35 (1968) 139-153.

Yamauchi T, Kamon J, Waki H, Murakami K, Motojima K, Komeda K, Ide T, Kubota N, Terauchi Y, Tobe K, Miki H, Tsuchida A, Akanuma Y, Nagai R, Kimura S, Kadowaki T, The mechanisms by which both heterozygous peroxisome proliferator-activated receptor  $\gamma$  (PPAR $\gamma$ ) deficiency and PPAR $\gamma$  agonist improve insulin resistance, J. Biol. Chem. 276 (2001) 41245-41254.

Yang JH, Lim HS, Heo YR, *Sasa borealis* leaves extract improves insulin resistance by modulating inflammatory cytokine secretion in high fat diet-induced obese C57/BL6J mice, Nutr. Res. Pract. 4 (2010) 99-105.

Youngren JF, Regulation of insulin receptor function, Cell Mol. Life. Sci. 64 (2007) 873-891.

Zhang BB, Zhou G, Li C, AMPK: and emerging drug target for diabetes and the metabolic syndrom, Cell Metab. 9 (2009) 407-416.

Zhang JW, Klemm DJ, Vinson C, Lane MD, Role of CREB in transcriptional regulation of CCAAT/enhancer-binding protein  $\beta$  gene during adipogenesis, J. Biol. Chem. 279 (2004) 4471-4478.

Zimmet P, Alberti KG, Shaw J, Global and societal implications of the diabetes epidemic, Nature 414 (2001) 782-787.

## 배경 및 요약

전 세계적으로 질병과 사망 원인이 되고 있는 비만은 에너지 섭취와 소비 사이의 균형이 깨지면서 발생한다. 비만은 건강이 나빠질 정도로 신체에 지방이 초과된 상태를 말하며, 평균 수명이 감소할 뿐만 아니라 또 다른 건강문제를 야기하게 되므로 21세기의 가장 큰 공중위생 문제들 중 하나로 보고 있다. 일반적으로 비만은 과도한 에너지 섭취, 운동 부족, 유전, 내분비계 이상, 약물, 정신적인 문제들이 그 원인으로 작용한다고 알려져 있다.

지방조직은 다양한 adipokine들을 분비하는 내분비 기관으로서 대사의 항상성을 유지하는데 필수적이며 에너지 항상성에도 중요한 역할을 한다. 지방조직은 지질 형태로 에너지를 저장하고, 에너지가 충분치 않거나 영양물질의 신호에 반응하여 저장된 에너지를 지방산 형태로 방출하여 에너지를 보충한다. 더 나아가, 면역반응, 인슐린 감수성, 식품 섭취에 관여하는 호르몬과 인자들의 분비를 통해 내분비계 기능을 한다. 지방조직에 과도하게 지방이 축적되면 비만을 일으키고 결과적으로 제2형 당뇨병, 고혈압, 심장질환 같은 질환들의 발병을 야기하므로 비만의 예방과 치료는 건강증진에 중요하다.

식이요법과 운동은 비만 치료에 가장 효율적이다. 더욱이 비만 치료는 고지방이나 고당 같은 고에너지의 소비를 감소시키고 식이섬유 섭취를 증가시키는 식이 개선이 중요하다. 고지방식은 일반적인 비만의 발병 원인과 유사하기 때문에 동물모델에서 내장비만 유도에 사용되고 있다. 따라서 내장지방을 효과적으로 감소시키는 식물유래 활성 성분들은 생활습관병을 예방할 수 있다.

중성지방은 포유류의 주요 에너지 저장소인 백색지방조직에 저장된다. 에너지가 과다하면 중성지방은 세포내의 지방구 형태로 저장되고, 에너지가 필요할 때는 지방분해(lipolysis)를 통해 지방구에서 지방산으로 방출된다. 간 조직에서도 VLDL 생성을 위해 중성지방이 합성된다. 그러나 지방조직에서 일어나는 지방분해는 다른 조직으로 에너지를 공급하기 위한 고유한 기능이다. 따라서 지방세포에서 지방분해를 증가시키는 것은 비만 치료를 위한 유용한 표적이 될 수 있다. 하지만 일반적으로 비만환자의 혈액에서 검출되는 고 농도의 지방산은 인슐

린 저항성과 같은 대사질환과 관련되므로 지방분해와 더불어 지방산의 산화 또한 체내의 지방을 감소시키는데 중요하게 작용한다.

현재 비만 치료에 사용되고 있는 합성제제들의 부작용이 알려지고 있어 안전성이 증강된 비만치료제가 요구되고 있다. 최근에는 항비만 활성 또는 지방조직에 직접적인 효과를 나타내는 식물유래 추출물 혹은 생리활성물질들이 식이 보충제로 사용되고 있다. 이에 따라 식물자원으로부터 유용 항비만 소재를 탐색하는 연구들이 급격히 증가하고 있는 추세이다.

본 연구는 제주도에 서식하는 식물자원들로부터 유용한 항비만 소재를 개발하기 위한 기초연구로 수행되었다. 저자는 약 300 여종의 식물 추출물들을 대상으로 3T3-L1 전구지방세포의 분화억제 활성을 탐색하여, 지방분화 억제활성이 우수한 3종 [미역쇠, *Petalonia binghamiae* (J. Agaradh) Vinogradova; 진귤, *Citrus sunki* Hort. ex Tanaka; 제주조릿대, *Sasa quelpaertensis* Nakai]를 선별하였다. 본 연구에서는 미역쇠, 진귤, 제주조릿대의 추출물들과 미역쇠와 진귤에서 분리한 fucoxanthin, sinensetin의 항비만 효과를 보고한다.

## PART 1. 갈조류인 미역쇠(*Petalonia binghamiae*)와 미역쇠에서 분리된 fucoxanthin의 항비만 효과

본 연구는 미역쇠 추출물과 미역쇠에서 분리한 fucoxanthin의 항비만 활성을 조사한 것이다.

첫째, 고지방식이로 유도된 비만 쥐에서 미역쇠 효소 추출물(PBEE)의 항비만 활성을 조사하였다. PBEE는 농도 의존적으로 전구지방세포의 adipogenesis를 억제시켰고, 분화중인 3T3-L1 전구지방세포에서 PPAR $\gamma$ , C/EBP $\alpha$ , aP2의 발현을 감소시켰다. 또한, 지방세포 분화의 mitotic clonal expansion 과정을 억제시켰고, 인슐린으로 자극된 성숙한 3T3-L1 지방세포에서 IRS의 인산화를 감소시킴으로써 포도당의 흡수를 억제시켰다. 그리고 PBEE는 고지방식이로 유도된 비만 쥐에서 항비만 효과를 나타냈다. 이 동물모델에서, 500mg/L의 PBEE가 첨가된 물을 30일간 먹인 결과 체중을 감소시켰고, 지방 저장도 감소되었다. 또한, PBEE는 혈청의 GPT, GOT를 감소시켰고, HDL 콜레스테롤은 증가시켰다. 더욱이, 고

지방식이로 유도된 지방간에 나타나는 간조직의 지방구 축적을 감소시켰다. 종합해보면, PBEE는 배양된 세포에서 adipogenesis를 억제시키고 동물모델에서 비만을 억제시킨다는 것을 알 수 있다.

둘째, 고지방식이로 유도된 생쥐에서 미역쇠 에탄올 추출물(PBE)의 항비만 효과를 조사하였다. PBE는 체중 증가량, 지방조직 무게, 혈청의 중성지방을 감소시켰고, 고지방식이로 유도된 지방간에 나타나는 간조직의 지방구 뿐만 아니라 혈청의 GPT, GOT를 감소시켰다. 중요한 것은, PBE는 부고환 지방조직에서 AMPK와 ACC의 인산화를 증가시켰다는 것이다. 이러한 *in vivo* 결과와 일치하게도, PBE는 성숙한 3T3-L1 지방세포에서 AMPK와 ACC의 인산화를 증가시켰고, SREBP1c 발현은 감소시켰다. 이 결과들은 PBE가 지방산  $\beta$ -산화의 향상과 lipogenesis의 감소를 통해 항비만 효과를 발휘한다는 것을 알 수 있다.

셋째, 3T3-L1 전구지방세포의 세 가지의 분화 단계에서 adipogenesis에 미역쇠에서 유래된 fucoxanthin의 효과를 조사하였다. 3T3-L1 전구지방세포의 분화 과정은 이른 단계 (day 0-2, D0-D2), 중간 단계 (day 2-4, D2-D4), 늦은 단계 (day 4-, D4-)로 나뉜다. Fucoxanthin을 이른 단계(D0-D2)에 처리하였을 때 3T3-L1 지방세포의 분화를 향상시켰다. 또한 PPAR $\gamma$ , C/EBP $\alpha$ , SREBP1c, aP2의 단백질 발현을 증가시켰고, adiponectin의 mRNA 발현 또한 증가시켰다. 하지만, fucoxanthin은 중간 단계(D2-D4)와 늦은 단계(D4-D7) 동안은 PPAR $\gamma$ , C/EBP $\alpha$ , SREBP1c의 단백질 발현을 감소시켰다. 또한, IRS의 인산화의 감소를 통해 성숙한 3T3-L1 지방세포에서 포도당 흡수를 억제시켰다. 더욱이, 성숙한 3T3-L1 지방세포에서 LKB1, AMPK, ACC의 인산화를 증가시켰다. 이 결과들은 fucoxanthin이 3T3-L1의 분화 단계에 따라 다양한 효과를 발휘하며, 포도당 흡수를 억제할 뿐만 아니라 지방산  $\beta$ -산화를 향상시킨다는 것을 알 수 있다.

종합해보면, 고지방식이로 유도된 비만 모델에서 미역쇠 추출물의 항비만 효과는 fucoxanthin의 활성을 통한 효과라 사료된다.

## PART 2. 미성숙 진귤(*Citrus sunki*) 과피와 진귤 과피에서 분리된 sinensetin의 항비만 효과

진굴 과피는 아시아에서 소화 불량, 기관지 천식 같은 많은 질병을 치료하는데 널리 사용했던 전통적인 약제이다. 이에 미성숙 진굴 과피 에탄올 추출물(CSE) 과 진굴 과피에서 유래된 sinensetin의 항비만 활성을 조사하였다.

첫째, 고지방식이로 유도된 C57BL/6 생쥐와 성숙한 3T3-L1 지방세포를 이용하여 CSE의 항비만 효과를 조사하였다. 동물실험에서, CSE는 고지방식이 대조군(HFD)에 비해 체중증가량, 지방조직 무게, 혈청의 콜레스테롤, 중성지방을 유의적으로 감소시켰다. 또한 CSE는 혈청의 GPT, GOT, LDH를 감소시켰다. 더욱이, 고지방식이로 유도된 지방간에 나타나는 간조직의 지방구 축적을 감소시켰다. CSE는 부고환 지방조직에서 지방산  $\beta$ -산화에 관여하는 AMPK와 ACC의 인산화를 증가시켰을 뿐만 아니라 성숙한 3T3-L1 지방세포에서 AMPK, ACC의 인산화를 증가시켰다. 더욱이, 성숙한 지방세포에서 PKA와 HSL의 인산화에 의해 lipolysis를 향상시켰다. 이 결과들은 CSE가 lipolysis와 지방산  $\beta$ -산화의 증가를 통해 항비만 효과를 갖는다는 것을 알 수 있다.

둘째, sinensetin은 감귤류에서 발견되는 폴리메톡시 플라본이다. 3T3-L1 세포에서 폴리메톡시 플라본이 풍부하게 들어있는 *Citrus sunki* 추출물에서 분리한 sinensetin의 지질대사에 관한 효과를 조사하였다. Sinensetin은 3T3-L1 전구지방세포를 IBMX가 포함되지 않은 분화유도 배지에 배양하였을 때 PPAR $\gamma$ , C/EBP $\alpha$ ,  $\beta$ , aP2의 발현을 증가시켰다. Sinensetin은 C/EBP $\beta$ 의 발현에 중요한 역할을 하는 CREB의 활성과 C/EBP $\beta$ 의 활성에 중요한 역할을 하는 ERK의 활성을 증가시켰을 뿐만 아니라, 분화중인 3T3-L1 세포에서 세포질내 cAMP를 증가시킴으로써 PKA의 활성을 증가시켰다. 더욱이, sinensetin은 성숙한 3T3-L1 지방세포에서 cAMP 경로에 의해 자극되는 lipolysis를 자극하였고, SREBP1c의 발현을 감소시켰으며, IRS와 Akt의 활성을 감소시킴으로써 포도당 흡수를 감소시켰다. 또한, 지방산 산화와 관련된 AMPK, ACC 활성화와 CPT-1a의 발현을 증가시킴으로써 지방산 산화를 증가시켰다.

종합해보면, 고지방식이로 유도된 비만 모델에서 미성숙 진굴 과피 추출물의 항비만 효과의 일부는 sinensetin에 기인한다고 사료된다.

### PART 3. 제주조릿대(*Sasa quelpaertensis*) 잎의 항비만 효과

몇몇 조릿대 종들의 잎은 항산화, 항종양, apoptosis, 인슐린 저항성 개선 효과와 같은 약리작용을 발휘한다. 저자는 고지방식으로 유도된 C57BL/6 생쥐와 성숙한 3T3-L1 지방세포를 이용하여 제주조릿대 잎 열수 추출물(SQE)의 항비만 활성을 조사하였다. SQE를 70일간 고지방식이 군에 먹인 결과 대조군(HFD)에 비해 체중증가량, 지방조직 무게, 혈청의 콜레스테롤 및 중성지방을 유의적으로 감소시키는 것을 확인하였다. SQE는 혈청에서 GPT, GOT, LDH를 감소시켰고, 고지방식으로 유도된 지방간에 나타나는 간조직의 지방구 축적을 감소시켰다. 또한, SQE는 부고환 지방조직에서 지방산  $\beta$ -산화에 관여하는 AMPK와 ACC의 인산화를 증가시켰다. 추가적으로, SQE는 성숙한 3T3-L1 지방세포에서 AMPK, ACC의 인산화를 증가시켰다. 이 결과들은 SQE가 지방산  $\beta$ -산화의 증가와 간조직에서 지방구 축적을 감소시킴으로써 항비만 효과를 나타낸다고 사료된다.